7-1-2009

Environmental regulation of carbon isotope discrimination and internal CO2 conductance in C3 leaves

Christopher Bickford

Follow this and additional works at: https://digitalrepository.unm.edu/biol_etds

Recommended Citation

Christopher P. Bickford
Candidate
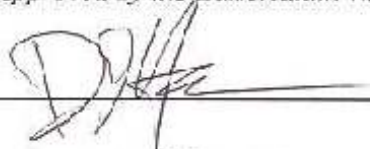
Biology
Department

This dissertation is approved, and it is acceptable in quality
and form for publication:

Approved by the Dissertation Committee:

_____, Chairperson

_____

_____

_____

_____

_____

_____

_____

ENVIRONMENTAL REGULATION OF CARBON ISOTOPE DISCRIMINATION AND INTERNAL CO2 CONDUCTANCE IN C3 LEAVES

BY

CHRISTOPHER PAUL BICKFORD

B.S., Botany, University of Oklahoma, 2001
M.Sc., Forestry, Northern Arizona University, 2005

DISSERTATION

Submitted in Partial Fulfillment of the
Requirements for the Degree of

Doctor of Philosophy
Biology

The University of New Mexico
Albuquerque, New Mexico

August 2009

DEDICATION

In memory of my mother, Karen Jeanne Huff Bickford, who could not be here today.

ACKNOWLEDGMENTS

Many people have aided me in this dissertation process, and I am grateful to all of them. I thank my advisors Dave Hanson and Nate McDowell for their time, patience, and advice over the years. It was a wonderful experience learning about the process of doing science from you both. I thank my family, in particular my father Paul Bickford, and friends for being there through all the ups and downs and supporting me all the way; I wouldn't be where I am today without you. Finally, I wish to express my deepest gratitude to my wonderful wife, Karen Bagne, who has been here through this entire process.

ENVIRONMENTAL REGULATION OF CARBON ISOTOPE
DISCRIMINATION AND INTERNAL CO2 CONDUCTANCE
IN C3 LEAVES

BY

CHRISTOPHER PAUL BICKFORD

ABSTRACT OF DISSERTATION

Submitted in Partial Fulfillment of the
Requirements for the Degree of

Doctor of Philosophy
Biology

The University of New Mexico
Albuquerque, New Mexico

August 2009

Environmental regulation of carbon isotope discrimination and internal CO_2 conductance in C_3 leaves

by

Christopher Paul Bickford

B.Sc., Botany, University of Oklahoma, 2001

M.Sc., Forestry, Northern Arizona University, 2005

Ph.D, Biology, University of New Mexico, 2009

ABSTRACT

Stable carbon isotopes are powerful tools for elucidating leaf- and ecosystem-level processes, and recent technological developments provide new opportunities to assess the isotopic flux during leaf gas exchange. In these studies I used a tunable diode laser spectroscope coupled to a infra-red gas analyzer to measure the isotopic composition of leaf gas exchange at high frequency in both field and greenhouse settings and assess environmental regulation of carbon isotope discrimination (Δ) and internal conductance of CO_2 to sites of carboxylation (g_i). I measured Δ and g_i across diurnal and seasonal periods in field-grown *Juniperus monosperma* trees and used these data to 1) assess the diurnal variation in Δ in response to environmental

drivers, 2) test predictions from existing models of Δ, 3) test the linearity of the relationship between Δ and the ratio of intercellular to ambient CO_2 partial pressure (p_i/p_a), 4) test the hypothesis that g_i varies at diurnal timescales and 5) test the influence of g_i in Δ models. Results show photosynthetic photon flux density, soil water availability, and vapor pressure deficit were significant environmental drivers of diurnal Δ patterns, and that existing models generally produced model predictions of Δ within 1-3‰ of observed values. Linear models adequately described significant relationships between observed Δ and p_i/p_a, but second order models better described the relationship under some conditions. g_i varied diurnally and ranged between 0.03-2.0 μmol m^{-2} s^{-1} Pa^{-1}. Accounting for this variation improved model predictions of Δ compared with a model that omits g_i, and parameterizing g_i based on dynamic variables such as time of day produced the greatest improvement in predictions. These findings demonstrate the need for model improvements to better predict Δ under field conditions.

Greenhouse studies were conducted to address the influence of soil water deficit (SWD) and leaf water potential (Ψ_w) on g_i. Plants with isohydric tendencies were droughted and g_i assessed using slope-based isotopic methods. Results showed no significant difference in Ψ_w or g_i between droughted and control plants and suggest Ψ_w may buffer the g_i response to SWD.

Table of Contents

List of Figures

List of Tables

Chapter 1

Introduction

Stable carbon isotope analyses have a long history in plant biology that includes differentiation of photosynthetic pathways (Smith & Epstein 1971), development of physiological theory of carbon isotope fractionation (O'Leary 1981; Farquhar *et al*. 1982), crop improvement (Farquhar & Richards 1984), ecological studies (Ehleringer 1993; Brooks *et al*. 1997), ecosystem process studies (Bowling *et al*. 2002; McDowell *et al*. 2004), and biosphere-atmosphere interactions (Yakir 2003; Randerson *et al*. 2006). The biophysical discrimination against the $^{13}C^{16}O_2$ isotopologue during photosynthesis (Δ) is the consequence of numerous fractionation factors, most of which are relatively well understood but include important exceptions. These fractionation factors are points along the CO_2 photosynthetic pathway from the atmosphere to sites of carboxylation where different diffusion and carboxylation rates of the $^{12}CO_2$ and $^{13}CO_2$ isotopologues result in accumulations of $^{13}CO_2$ in gas, liquid, or solid samples which differ from the composition of atmospheric air (Farquhar, Ehleringer & Hubick 1989; Brugnoli & Farquhar 2000; Bowling *et al*. 2008). The role of many factors underlying Δ in leaf gas exchange are well understood and include the fractionations associated with CO_2 diffusion through the leaf boundary layer and stomata (Craig 1953), CO_2 entry into solution (Mook, Bommerson & Staverman 1974), diffusion through solution (O'Leary 1984), and carboxylation due to enzymatic activity (Roeske & O'Leary 1984). Early studies suggested isotopic fractionations associated with day respiration (e), photorespiration (f) and g_i were minimal or non-existent (Farquhar *et al*. 1982), but mounting evidence strongly suggests e, f, and g_i all have large roles in Δ.

Mechanistic models are used to predict Δ across a variety of temporal and spatial scales, but direct comparisons of their performance against empirical data are rare. Two related models are currently used to describe Δ: a comprehensive model that incorporates fractionation factors associated with the entire diffusion pathway of CO_2, carboxylation and decarboxylation (Δ_{comp}; Farquhar, O'Leary & Berry 1982; Farquhar & Richards 1984), and a simplified version of Δ_{comp} that omits many of the diffusion related fractionation factors and all decarboxylation components (Δ_{simple}; Farquhar et al. 1982). Variation in Δ_{simple} is driven by variation in the ratio of CO_2 partial pressure in the intercellular spaces and in the atmosphere (p_i/p_a) interacting with key model parameters (Farquhar, O'Leary & Berry 1982). These key drivers of Δ_{simple} include 1) the carboxylation term, b, that represents net fractionation associated with phosphoenolpyruvate (PEP) carboxylase and Ribulose-1,5-bisphosphate carboxylase/oxygenase (Rubisco), and 2) the fractionation associated with diffusion in air and through stomata (a; 4.4‰) (Farquhar et al. 1989). b is typically estimated at ~27‰ in Δ_{simple}, or ~2‰ lower than early measurements of the full Rubisco fractionation (~29‰; Roeske & O'Leary 1984), to account for omitted fractionation factors (Farquhar & Richards 1984). Recent work suggests net Rubisco fractionation may be between 25-30‰ (Tcherkez & Farquhar 2005) and b may be as low as 27.4‰ in tobacco (*Nicotiana tabacum*; McNevin et al. 2007) and 26‰ in *Senecio* (Lanigan et al. 2008). Δ_{comp} incorporates the factors discussed above plus fractionation associated with CO_2 diffusion, including g_i, and decarboxylation activity. g_i is dynamic and may be an important driver of Δ by reducing the diffusion rate from stomatal cavities to the chloroplast (Flexas et al. 2008), but tests of the influence of g_i in predicting Δ are few (Cai et al. 2008). A major

focus of this study was to examine the diurnal patterns of Δ and g_i under field conditions and use these data to test Δ_{simple} and Δ_{comp} against a high frequency dataset representative of seasonal shifts in physiological activity in a semi-arid ecosystem.

Isotopic fractionation associated with the decarboxylation activities of day respiration and photorespiration (Δ_{ef}) has a demonstrable effect on Δ. Direct measurements of e are not currently possible, and consequently the isotopic fractionation associated with dark respiration (e_d) is often used as a surrogate estimator for e, though recent evidence demonstrates day and dark respiration involve different biochemical pathways (Tcherkez et $al.$ 2008). Several environmental variables have been shown to influence e_d, including drought (Duranceau et $al.$ 1999; Ghashghaie et $al.$ 2001; Ghashghaie et $al.$ 2003), temperature (Tcherkez et $al.$ 2003) and irradiance (Barbour et $al.$ 2007). Studies have demonstrated a large range of f values ($\sim$ 3-8‰), but the role of environmental regulation is largely confined to temperature effects on photorespiration (Brooks & Farquhar 1985; Gillon & Griffiths 1997). Recently, Tcherkez (2006) reported the primary regulating enzyme of photorespiration, glycine decarboxylase, has a large role in f and proposed that f is approximately +10‰, a finding reinforced in recent empirical work showing f equal to 11.6‰ in $Senecio$ (Lanigan et $al.$ 2008). Both e and f are parameterized within the comprehensive model of carbon isotope discrimination (Δ_{comp}; Farquhar et $al.$ 1982; Farquhar & Richards 1984) in conjunction with their respective respiratory fluxes, day respiration (R_d) and photorespiration (O). Within Δ_{comp} the interaction between e, R_d, f, and O is summarized in a decarboxylation term (Δ_{ef}) that is subtracted from the carboxylation component. The interactive contribution of e and R_d has a negative sign, but results in positive forcing on predicted Δ. Concurrent f and O

3

activities have a positive isotopic signature, and consequently have a negative forcing effect in Δ_{comp}. To some extent these negative and positive influences nullify one another in the cumulative respiratory isotopic signature, but if one process dominates under a set of environmental conditions then positive or negative forcing of the overall Δ signature may occur. One research foci of this study was to examine the patterns of Δ_{ef} under field conditions and in a controlled experimental setting to assess diurnal variation in the field and in response to water stress.

Temperature and water stress have been shown to impact diffusion of CO_2 across cell walls and through cellular membranes to sites of carboxylation (g_i). Temperature has been shown to regulate g_i within the biologically significant range of 10° to 40°C in tobacco (Bernacchi *et al*. 2002), a finding supported in more recent work using different species (Warren & Dryer 2006; Yamori *et al*. 2006). Water stress reduces g_i, as demonstrated experimentally in *Pseudotsuga* seedlings (Warren, Livingston & Turpin 2004) and *Olea* (Diaz-Espejo, Nicolas & Fernandez 2007) and in a comprehensive field study using *Quercus* and *Fraxinus* (Grassi & Magnani 2005). However, the physiological signal linking leaf water deficit and shifts in g_i remains elusive. The strong regulatory effect of lamina water balance on leaf processes such as stomatal conductance (Buckley 2005) warrants exploration of leaf water potential (ψ_w) as a regulator of g_i. Reports of strong linkages between aquaporin function and g_i (Flexas *et al*. 2006; Miyazawa *et al*. 2008; Uehlein *et al*. 2008) provide a possible mechanism for explain rapid variation in g_i in response to a multitude of environmental factors, as has been demonstrated in response to CO_2 concentration (Flexas *et al*. 2007). In this study I explore if linkages exist between

g_i and Ψ_w by assessing g_i in droughted isohydric plants, where leaves maintain relatively

constant diurnal Ψ_w in response to soil water deficit.

References

Barbour MM, McDowell NG, Tcherkez G, Bickford CP, Hanson DT. **2007.** A new measurement technique reveals rapid post-illumination changes in the carbon isotope composition of leaf-respired CO_2. *Plant, Cell and Environment* **30:** 469-482.

Bernacchi CJ, Portis AR, Nakano H, von Caemmerer S, Long SP. **2002.** Temperature response of mesophyll conductance. Implications for the determination of rubisco enzyme kinetics and for limitations to photosynthesis in vivo. *Plant Physiology* **130:** 1992-1998.

Bowling DR, McDowell NG, Bond BJ, Law BE, Ehleringer J.R. 2002 ^{13}C content of ecosystem respiration is linked to precipitation and vapor pressure deficit. *Oecologia* **13:** 113-124.

Bowling DR, Pataki DE, Randerson JT. **2008.** Carbon isotope in terrestrial ecosystem pools and CO_2 fluxes. *New Phytologist* **178**: 24-40.

Brooks A, Farquhar GD. **1985.** Effect of temperature on the CO_2/O_2 specificity of ribulose-1,5-bisphosphate carboxylase/oxygenase and the rate of respiration in the light. *Planta* **165:** 397-406.

Brooks JR, Flanagan LB, Buchmann N, Ehleringer JR. **1997.** Carbon isotope composition of boreal plants: functional grouping of life forms. *Oecologia* **110:** 301-311.

Brugnoli E, Farquhar GD. **2000.** Photosynthetic fractionation of carbon isotopes. In: Leegood RC, Sharkey TD, von Caemmerer S, eds. *Photosynthesis: Physiology and Metabolism* . The Netherlands: Kluwer Academic, 399-434.

Buckley TN 2005. The control of stomata by water balance. *New Phytologist Tansley Review* **168**: 275-291.

Cai T, Flanagan LB, Jassal RS, Black TA. **2008.** Modelling environmental controls on ecosystem photosynthesis and the carbon isotope composition of ecosystem-respired CO_2 in a coastal Douglas-fir forest. *Plant, Cell and Environment* **31**: 435-453.

Diaz-Espejo A, Nicolas E, Fernandez JE . **2007.** Seasonal evolution of diffusional limitations and photosynthetic capacity in olive under drought. *Plant, Cell and Environment* **30:** 922-933.

Duranceau M, Ghashghaie J, Badeck F, Deleens E, Cornic G. **1999.** $\delta^{13}C$ of CO_2

respired in the dark in relation to $\delta^{13}C$ of leaf carbohydrates in *Phaseolus vulgaris* L. under progressive drought. *Plant, Cell and Environment* **22:** 515-523.

Ehleringer JR. **1993.** Variation in leaf carbon isotope discrimination in *Encelia farinosa*: implications for growth, competition, and drought survival. *Oecologia* **95:** 340-346.

Farquhar GD, Ehleringer JR, Hubick KT. **1989.** Carbon isotope discrimination and photosynthesis. *Annual Review of Plant Physiology and Plant Molecular Biology* **40:** 503-537.

Farquhar GD, Richards RA. **1984.** Isotopic composition of plant carbon correlates with water-use efficiency of wheat genotypes. *Australian Journal of Plant Physiology* **11:** 539-552.

Farquhar GD, O'Leary MH, Berry JA. **1982.** On the relationship between carbon isotope discrimination and the intercellular carbon dioxide concentration in leaves. *Australian Journal of Plant Physiology* **9:** 121-137.

Flexas J, Ribas-Carbo M, Hanson DT, Bota J, Otto B, Cifre J, McDowell N, Medrano H, Kaldenhoff R. **2006.** Tobacco aquaporin NtAQP1 is involved in mesophyll conductance to CO_2 in vivo. *Plant Journal* **48:** 427-439.

Flexas J, Diaz-Espejo A, Galmčs J , Kaldenhoff R, Medrano H, Ribas-Carbo M. **2007.** Rapid variations of mesophyll conductance in response to changes in CO_2 concentration around leaves. *Plant, Cell and Environment* **30:** 1284-1298.

Flexas J, Ribas-Carbo M, Diaz-Espejo A, Galmes J, Medrano H. **2008.** Mesophyll conductance to CO_2: current knowledge and future prospects. *Plant, Cell and Environment* **31**: 602-621.

Ghashghaie J, Duranceau M, Badeck F-W, Cornic G, Adeline M-T, Deleens E . **2001.** $\delta^{13}C$ of CO_2 respired in the dark in relation to $\delta^{13}C$ of leaf metabolites: comparison between *Nicotiana sylvestris* and *Helianthus annuus* under drought. *Plant, Cell and Environment* **24:** 505-515.

Ghashghaie J, Badeck FW, Lanigan G, Nogues S, Tcherkez G, Deleens E, Cornic G, Griffiths H. **2003.** Carbon isotope fractionation during dark respiration and photorespiration in C_3 plants. *Phytochemistry Reviews* **2:** 145-161.

Gillon JS, Griffiths H. **1997.** The influence of (photo)respiration on carbon isotope discrimination in plants. *Plant, Cell and Environment* **20:** 1217-1230.

Lanigan GJ, Betson N, Griffiths H, Seibt U. **2008.** Carbon isotope fractionation during photorespiration and carboxylation in Senecio. *Plant Physiology* **148:** 2013-2020.

McDowell NG, Bowling DR, Schauer A, Irvine J, Bond BJ, Law BE, Ehleringer JR. **2004.** Associations between carbon isotope ratios of ecosystem respiration, water availability, and canopy conductance. *Global Change Biology* **10:** 1767-1784.

McNevin DB, Badger MR, Whitney SM, von Caemmerer S, Tcherkez GGB, Farquhar GD. 2007. Differences in carbon isotope discrimination of three variants of D-Ribulose-1,5-bisphosphate carboxylase/oxygenase reflect differences in their catalytic mechanisms. *Journal of Biological Chemistry* **282:** 36068-36076.

Mook W.G., Bommerson J.C., Staverman W.H. 1974. Carbon isotope fractionations between dissolved bicarbonate and gaseous carbon dioxide. *Earth and Planetary Science Letters* **22:** 169-176.

O'Leary MH. **1981.** Carbon isotope fractionation in plants. *Phytochemistry* **20:** 553-567.

O'Leary M.H. 1984. Measurement of the isotopic fractionation associated with diffusion of carbon dioxide in aqueous solution. *Journal of Physical Chemistry* **88:** 823-825.

Randerson JT, Masiello CA, Still CJ, Rahn T, Poorter H, Field CB. **2006.** Is carbon within the global terrestrial biosphere becoming more oxidized? Implications for trends in atmospheric O-2. *Global Change Biology* **12:** 260-271.

Roeske CA, O'Leary MH. **1984.** Carbon isotope effects on the enzyme-catalyzed carboxylation of ribulose bisphosphate . *Biochemistry* **23:** 6275-6284.

Smith BN, Epstein S. **1971.** Two categories of $^{13}C/^{12}C$ ratios for higher plants. *Plant Physiology* **47:** 380-384.

Tcherkez Guillaume. **2006.** How large is the carbon isotope fractionation of the photorespiratory enzyme glycine decarboxylase? *Functional Plant Biology* **33:** 911-920.

Tcherkez G, Bligny R, Gout E, Mahe A, Hodges M, Cornic G. **2008.** Respiratory metabolism of illuminated leaves depends on CO_2 and O_2 conditions. *Proceedings of the National Academy of Science* **105:** 797-802.

Tcherkez G, Farquhar GD. **2005.** Carbon isotope effect predictions for enzymes involved in the primary carbon metabolism of plant leaves. *Functional Plant Biology* **32:** 277-291.

Tcherkez G, Nogues S, Bleton J, Cornic G, Badeck F, Ghashghaie J. **2003.** Metabolic origin of carbon isotope composition of leaf dark-respired CO_2 in French bean. *Plant Physiology* **131:** 237-244.

Uehlein N, Otto B, Hanson DT, Fischer M, McDowell N, Kaldenhoff R. **2008.** Function of *Nicotiana tabacum* aquaporins as chloroplast gas pores challenges the concept of membrane CO_2 permeability. *The Plant Cell* **20:** 648-657.

Warren C.R., Dreyer E. 2006. Temperature response of photosynthesis and internal conductance to CO_2: results from two independent approaches. *Journal of Experimental Botany* **12:** 3057-3067.

Yakir D. 2003. The stable isotope composition of atmospheric CO_2. *In: Treatise on*

Geochemistry. Vol. **4** (Ed. R.L. Rudnick), pp. 175-212. Elsevier Press. San Diego.

Yamori W, Noguchi K, Hanba YT, Terashima I. **2006.** Effects of internal conductance on the temperature dependence of the photosynthetic rate in spinach leaves from contrasting growth temperatures. *Plant Cell Physiology* **47:** 1069-1080.

Chapter 2

This is the pre-peer reviewed version of the following article: High frequency field measurements of diurnal carbon isotope discrimination and internal conductance in a semi-arid species, *Juniperus monosperma*. *Plant, Cell and Environment* doi: 10.1111/j.1365-3040.2009.01959.x, which has been published in final form at

http://www3.interscience.wiley.com/journal/119880240/issue

High frequency field measurements of diurnal carbon isotope discrimination and internal conductance in a semi-arid species, *Juniperus monosperma*

CHRISTOPHER P. BICKFORD[1], NATE G. MCDOWELL[2], ERIK B. ERHARDT[3], DAVID T. HANSON[1]

[1]*University of New Mexico, Department of Biology, MSC03-2020, Albuquerque, NM 87131;* [2]*Earth and Environmental Sciences Division, MS-J495, Los Alamos National Laboratory, Los Alamos, NM 87544 USA;* [3]*University of New Mexico, Department of Mathematics and Statistics, MSC03-2150, Albuquerque, NM 87131*

Running title: Diurnal Δ and g_i

Abstract

We present field observations of carbon isotope discrimination (Δ) and internal

conductance of CO_2 (g_i) collected using tunable diode laser spectroscopy (*TDL*). Δ

ranged from 12.0‰–27.4‰ over diurnal periods with daily means of 16.3 ± 0.2‰ during

drought to 19.0 ± 0.5‰ during monsoon conditions. We observed a large range in g_i,

from 0.04–8.53 µmol m^{-2} s^{-1} Pa^{-1} among measured leaves, but most g_i estimates were less

than 4.0 µmol m^{-2} s^{-1} Pa^{-1}. We tested the comprehensive Farquhar, O'Leary & Berry

(1982) model of Δ (Δ_{comp}), a simplified form of Δ_{comp} (Δ_{simple}), and recently suggested

amendments ($\Delta_{revised}$; Wingate *et al.* 2007). Sensitivity analyses demonstrated that

varying g_i had a substantial effect on Δ_{comp}, resulting in mean differences between

observed Δ (Δ_{obs}) and Δ_{comp} ranging from 0.04‰ to 9.6‰. First order regressions

adequately described the relationship between Δ and the ratio of substomatal to

atmospheric CO_2 partial pressure (p_i/p_a) on all three days, but second order models better

described the relationship in July and August. The three tested models each predicted Δ_{obs}

best on different days. In June Δ_{simple} outperformed Δ_{comp} and $\Delta_{revised}$, but incorporating g_i

and all non-photosynthetic fractionations improved model predictions in July and August.

Keywords: mesophyll conductance, carbon isotopes, *Juniperus monosperma*, Farquhar

model, decarboxylation activity, p_i/p_a, transfer conductance

Introduction

Stable carbon isotope analyses have a long history in plant biology that includes

differentiation of photosynthetic pathways (Smith & Epstein 1971), development of

physiological theory of carbon isotope fractionation (O'Leary 1981; Farquhar *et al*.

1982), crop improvement (Farquhar & Richards 1984), ecological studies (Ehleringer

1993; Brooks *et al*. 1997), ecosystem process studies (Bowling *et al*. 2002, McDowell *et

al*. 2004), and biosphere-atmosphere interactions (Yakir 2003; Randerson *et al*. 2006).

The biological and physical discrimination against the $^{13}C^{16}O_2$ isotopologue during

diffusion and carboxylation is a strong regulator of the isotopic signature of ecosystem

exchange with the atmosphere as it largely determines the ^{13}C composition of the

substrate pool which supplies respiratory activity (Barbour *et al*. 2005; Knohl *et al*. 2005;

Bowling, Pataki & Randerson 2008). The transfer of this signature throughout the

ecosystem provides a useful signal to partition components of ecosystem carbon

exchange and aid in carbon cycle modeling (Ciais *et al*. 1995; Tu & Dawson 2005;

McDowell *et al.* 2008a).

     A substantial body of literature describing a linear relationship between leaf

carbon isotope discrimination (Δ) and the ratio of internal to atmospheric CO_2 partial

pressure (p_i/p_a) has accumulated in the last three decades (Farquhar *et al*. 1982b;

Brugnoli *et al*. 1988; Farquhar, Ehleringer & Hubick 1989; Ehleringer, Phillips &

Comstock 1992; Brugnoli & Farquhar 2000). The p_i/p_a ratio is useful because it

succinctly describes the dominant physical and biochemical constraints to photosynthesis.

Similarly, the linear relationship between Δ and p_i/p_a observed in previous studies

emphasizes the importance of stomatal conductance and biochemistry in Δ. The full

model of Δ developed by Farquhar *et al*. (1982) also accounts for other factors such as internal conductance of CO_2 from stomatal cavities to sites of carboxylation (g_i) and apparent isotopic fractionations associated with the decarboxylation processes of day respiration and photorespiration (Δ_{ef}), as well as other diffusion related fractionations. Recent evidence suggests that g_i and Δ_{ef} are sensitive to environmental factors that vary diurnally (Bernacchi *et al*. 2002; Ghashghaie *et al*. 2003; Warren, Livingston & Turpin 2004), but their role in the variation in Δ observed in a field setting remains poorly understood.

Temperature and water stress have been shown to impact g_i. Bernacchi *et al*. (2002) found temperature regulated g_i within the biologically significant range of 10° to 40°C in tobacco, a finding supported in work presented by Yamori *et al*. (2006) and Warren & Dreyer (2006) using different species. Water stress also reduces g_i, as demonstrated experimentally in *Pseudotsuga* seedlings (Warren *et al*. 2004) and *Olea* (Diaz-Espejo, Antonio & Fernandez 2007) and in a comprehensive field study using *Quercus* and *Fraxinus* (Grassi & Magnani 2005). Recently, a strong linkage between aquaporin function and g_i was established (Flexas *et al*. 2006; Uehlein *et al*. 2008), providing a possible mechanism for rapid variation in g_i in response to a multitude of environmental factors, as has been demonstrated in response to CO_2 concentration (Flexas *et al*. 2007). While seasonal changes in g_i have been documented in a field setting (Grassi & Magnani 2005; Diaz-Espejo *et al*. 2007) diurnal variation in g_i has not yet been reported.

The influence of environmental factors on Δ_{ef} is less well known. Temperature and light have been shown to influence day respiration and photorespiration, both of

which affect CO_2 evolution within a leaf (Brooks & Farquhar 1985; Kozaki & Takeba 1996; Atkin *et al.* 2000; Atkin *et al.* 2005). The apparent fractionation associated with day respiration (*e*) and photorespiration (*f*) are each the result of biochemical reactions that may be subject to environmental control (Ghashghaie *et al.* 2003). A consistent enrichment of 6‰ in the dark respired $^{13}C/^{12}C$ ratio ($\delta^{13}C_{resp}$) of CO_2 compared to sucrose of droughted and control *Phaseolus* leaves has been observed (Duranceau *et al.* 1999). Such respiratory enrichment has been shown to depend on species and on plant water status (Ghashghaie *et al.* 2001), temperature (Tcherkez *et al.* 2003), and light exposure (Barbour *et al.* 2007a). Estimates of *e* have largely been inferred from studies of dark respiration, but recent evidence suggests these dark respiration fractionations may not be representative of day respiratory fractionation (Tcherkez *et al.* 2008). Field observations of the diurnal patterns of the cumulative fractionation associated with respiratory and photorespiratory processes, estimated here in Δ_{ef}, may allow us to better understand the influence of environmental factors on this component of Δ.

In recent years advances in optical systems utilizing tunable diode laser spectroscopy (*TDL*) have simplified high frequency measurements of the abundance of individual isotopologues $^{13}C^{16}O_2$, $^{12}C^{16}O_2$, and $^{12}C^{18}O^{16}O$ in ecosystem studies (Bowling *et al.* 2003; Griffis *et al.* 2004; McDowell *et al.* 2008a) and leaf-scale studies in greenhouse settings (Barbour *et al.* 2007a,b). Similar *TDL* leaf-scale measurements can now be attempted in a field setting. The objectives of this study were to 1) examine the temporal variation in Δ, $\delta^{13}C_{resp}$, g_i, and Δ_{ef} under ambient field conditions, 2) test the hypothesis that g_i varies across the day, 3) test the hypothesis that Δ varies linearly in response to shifts in p_i/p_a under field conditions, 4) test the influence of g_i in a

comprehensive leaf model of Δ, and 5) test the predictive capabilities of three models: the comprehensive Farquhar *et al*. (1982) model of Δ (Δ_{comp}), a recently suggested amendment to Δ_{comp} ($\Delta_{revised}$; Wingate *et al*. 2007) and the simplified form of the comprehensive model (Δ_{simple}). We used a combined *TDL*-infra-red gas analyzer (*IRGA*) system to obtain high frequency field measurements of leaf gas exchange synchronized with online isotopic measurements, similar to those used in previous greenhouse studies (Barbour *et al*. 2007a). Previous work has demonstrated substantial diurnal variation in leaf discrimination in diverse field settings including tropical forest (Harwood *et al*. 1998) and mesic conifer forest (Wingate *et al*. 2007). We report ~ 20 Δ measurements/hour over diurnal periods during both dry and wet seasons from a semi-arid woodland.

Methods

The field site was located on Mesita Del Buey in Los Alamos, New Mexico USA (latitude 35° 50' N, longitude 106° 16'W; elevation 2140 m) in a piñon-juniper woodland (*Pinus edulis* Engelm. and *Juniperus monosperma* Engelm. Sarg., respectively) dominated primarily by juniper and understory grasses and forbs (Breshears 2008; McDowell *et al*. 2008b). This semi-arid region typically has a bi-modal precipitation regime, with substantial winter snowfall (October–April), followed by a dry period (May–June), and monsoonal precipitation from July through early September (Breshears 2008). Precipitation at our site in 2006 totaled 119 mm in winter and 224 mm in summer. Soils on the site are Typic Haplustalfs and Typic Ustochrepts (Davenport, Wilcox & Breshears 1996).

Leaf gas exchange measurements

We measured diurnal (06:00–19:00 MST) leaf gas exchange from the bottom third of the canopy on two juniper trees on 12 June 2006, two different juniper trees on 11 July 2006, and a single juniper on 14 August 2006. We coupled a *TDL* (TGA100A, Campbell Scientific Inc.) to a portable photosynthesis system (LI-COR 6400, LI-COR Biosciences) fitted with a conifer chamber (LI-COR 6400-05) to quantify the concentration of CO_2 and its isotopologues $^{13}C^{16}O_2$ and $^{12}C^{16}O_2$ in gas entering and exiting the leaf chamber, herein referred to as the reference and sample gas streams (i.e. Barbour *et al*. 2007a). We supplied atmospheric air via a 50 L buffer volume to the LI-Cor 6400, which recorded the CO_2 and water vapor concentration of the reference and sample gas every 10 seconds. These same gas streams were dried to a constant low humidity and plumbed directly into the *TDL* using ultra-low porosity tubing (Synflex type 1300 ¼" diameter, Saint Gobrain Performance Plastics) wherein the *TDL* measured the CO_2 isotopologues $^{13}C^{16}O^{16}O$ and $^{12}C^{16}O^{16}O$ at a rate of 500Hz. These 500Hz data were then averaged down to 10Hz, and all means were calculated from the 10Hz data. Our 3 minute *TDL* measurement cycle consisted of two reference tanks and the reference and sample gas streams, each measured for 45 s, from which we calculated means of isotopologue concentrations over the last 15 s of each inlet cycle. We combined these *TDL* data with *IRGA* generated data after incorporating the 33 second lag between the two instruments.

We used a LI-COR conifer chamber to maximize leaf area and allow natural light interception on the scale-like juniper foliage, regulating the chamber flow rate between 250 and 500 μmol s^{-1} to maintain a sufficient CO_2 drawdown and control chamber

humidity. We attempted to maintain CO_2 drawdown ≥ 40 μmol CO_2 mol^{-1} air within the leaf chamber. Under moderate conditions chamber temperature was unregulated, but under conditions of high ambient air temperature ($> 35°C$) and solar radiation the *IRGA* block temperature control was engaged to control leaf temperature below $35°C$, as measured by energy balance. On 12 June, we collected data from six leaf areas diurnally and from two leaf areas at night. On 11 July, we collected data from five leaf areas diurnally and two leaf areas during dark measurements. In both June and July each leaf area was measured for 30 minutes to an hour and individual leaves were typically measured more than once each day. Finally, on 14 August we collected all data from one leaf area diurnally during a seven hour period, and one leaf area during dark measurements. The isotopic signature of nocturnal respiration ($\delta^{13}C_{resp}$) was measured immediately following daylight measurements and beginning when ambient photosynthetic photon flux density (PPFD) fell below 30 μmol photons m^{-2} s^{-1} and foliage exhibited net CO_2 efflux. To achieve a true dark measurement, we applied a heavy shade cloth over the leaf chamber to reduce PPFD to zero and waited for stable chamber conditions (e.g. leaf temperature, respiration rate), which occurred within 5 minutes after the shade cloth was applied. We also determined the carboxylation capacity of these juniper trees on 22 June and 23 July 2007 using assimilation (A) responses to changes in sub-stomatal CO_2 concentration (A/p_i). We collected these data using a LI-COR 6400 fitted with a chamber light source (LI-COR 6400-02B). We measured predawn and mid-day xylem water potential (ψ_w) on five to ten nearby juniper trees on each measurement day using a Scholander-type pressure bomb (PMS Instruments Co., Corvallis, OR, USA; McDowell *et al.* 2008b).

The working standard (WS) calibration tanks used during our diurnal measurements were calibrated against World Meteorological Organization (WMO) certified standard tanks (541.67 μmol CO_2 mol^{-1} air, $\delta^{13}C = -16.16‰$ and 350.34 μmol CO_2 mol^{-1} air, $\delta^{13}C = -8.39‰$) within 24 hours of each measurement campaign. The inter-tank calibration between WMO and working standard tanks typically required 2 hours to complete. Molar mixing ratios of $^{12}CO_2:^{13}CO_2$ in the WS tanks used in the June campaign were $354.04 \pm 0.27:3.82 \pm 0.003$ μmol CO_2 mol^{-1} air (mean ± standard error; n = 11 inter-tank calibrations) and $563.85 \pm 0.27:6.09 \pm 0.003$ μmol CO_2 mol^{-1} air (n = 11). Molar mixing ratios of $^{12}CO_2:^{13}CO_2$ in the WS tanks used in the July and August campaigns were $340.46 \pm 0.29:3.67 \pm 0.003$ μmol CO_2 mol^{-1} air (n = 10) and $518.71 \pm 0.08:5.60 \pm 0.001$ μmol CO_2 mol^{-1} air (n = 6). The WMO certified tanks were filled and $\delta^{13}C$ calibrated at the Stable Isotope Lab (SIL) of the Institute for Arctic and Alpine Research, a cooperating agency of the Climate Monitoring division of the National Oceanic and Atmospheric Administration's Earth Research Laboratory. Measurement variation in the $\delta^{13}C$ of a known tank in the *TDL* measurement mode we used exhibited a standard deviation of 0.06‰ across an hour and 0.20‰ across the day. To account for diurnal instrument drift the *TDL* measured the high and low WS tanks during each three minute cycle and we calculated the deviation between the measured values and the known values to determine a gain and offset for each isotopologue in each tank being measured (Bowling *et al*. 2003). These gain and offset values were then applied to all data. The *TDL* measures the absolute concentration of each isotopologue, so the range of $^{12}CO_2$ and $^{13}CO_2$ in each WS tank should span the measurement range. During the three measurement days our measurements occasionally exceeded the lower end of the total

17

[CO$_2$] in our WS tanks (maximum deviation: 45.7 μmol/mol). To test that the calibration was valid below the lower tank, we used a WMO traceable standard tank (total [CO$_2$] = 142.86 μmol/mol, δ^{13}C = −7.96‰) and an additional unknown tank that had a target total [CO$_2$] of 250 μmol/mol. We measured these two tanks and two WS tanks (344.88 μmol/mol, −8.16‰ and 548.16 μmol/mol, −16.42‰) in series. We calculated the total [CO$_2$] and isotope ratio of the unknown tank by calculating the gain and offset values in two ways: 1) using the span between the 142.86 μmol/mol tank and the 344.86 μmol/mol tank and 2) using the span between the 344.86 μmol/mol tank and the 548.16 μmol/mol tank measurements. The unknown tank was calculated to have a total [CO$_2$] of 247.44 μmol/mol and a δ^{13}C of −20.45‰ using the lower calibration span (#1) and a total [CO$_2$] of 247.43 μmol/mol and a δ^{13}C of −20.45‰ using the higher calibration span (#2), a net difference of 0.01 μmol/mol and 0.00‰. We also determined the [CO$_2$] and δ^{13}C of the 142.86 μmol/mol WMO tank using gain and offset values calculated using the higher calibration span (#2). The result was a total [CO$_2$] of 142.66 μmol/mol and a δ^{13}C of −7.88‰, a net difference of 0.20 μmol/mol and 0.08‰ from SIL certified values. Based on this assessment, we conclude our *TDL* has a linear response that extends beyond the lowest CO$_2$ range we measured in this study.

The *IRGA* was calibrated the morning of each measurement day, and the reference and sample gas analyzers of the *IRGA* were frequently matched to the same gas stream, while disconnected from the *TDL* inlet tubes. After reconnecting the *TDL* inlet tubes with the *IRGA*, the system was leak tested by gently blowing around the chamber, all connections, and the pressure equilibrating vent tube located on the sample line to the *TDL*. The *TDL* was also used to measure the reference and sample gas streams with an

empty leaf chamber and differences were lower than instrument precision (data not shown).

Δ & $\delta^{13}C_{resp}$ calculations

We calculated Δ_{obs} in the chamber following Evans *et al.* (1986):

$$\Delta_{obs} = \frac{\xi(\delta_o - \delta_e)}{1 + \delta_o - \xi(\delta_o - \delta_e)}$$ (1)

where $\xi = c_e/(c_e - c_o)$ is the ratio of the reference CO_2 concentration entering the chamber (c_e) relative to the sample CO_2 concentration outgoing from the chamber (c_o), and δ_e and δ_o are the $\delta^{13}C$ of the reference and sample gas, respectively. All variables incorporated in Δ_{obs} and $\delta^{13}C_{resp}$ (below) are derived from *TDL* measurements of $[^{12}CO_2]$ and $[^{13}CO_2]$, removing inter-instrument variability. Mixing ratios of total $[CO_2]$ were calculated following Barbour *et al.* (2007a). Because the *TDL* measures the concentration of each isotopologue δ_o and δ_e are calculated from the ratio of the molar abundance of each isotopologue and then presented in ratio to the Vienna Pee Dee belemnite (VPDB) standard, that is $\delta = R_s/R_{VPDB} - 1$, where δ represents either δ_o or δ_e, and R_s and R_{VPDB} represent the carbon isotope ratio of the sample and VPDB standard, respectively. We determined $\delta^{13}C_{resp}$ following Barbour *et al.* (2007a):

$$\delta^{13}C_{resp} = \frac{\delta_o - \delta_e(1-p)}{p}$$ (2)

where p equals $(c_o - c_e)/c_o$. We estimated the $\delta^{13}C$ of assimilated sugars ($\delta^{13}C_s$) based on Farquhar *et al.* (1989) where $\delta^{13}C_s = (\delta_e - \Delta_{obs})/(\Delta_{obs} + 1)$. All other reported gas

exchange values are calculated by the LI-6400 software following methods of Farquhar, Caemmerer & Berry (1980), after correcting for leaf area. We determined projected leaf area using a calibrated leaf area meter (LI-3100, LI-COR Biosciences) and all gas exchange calculations are reported on a projected leaf area basis.

Model parameterization

We incorporated our data into the comprehensive model of leaf Δ (Farquhar *et al*. 1982; Farquhar & Richards 1984):

$$\Delta_{comp} = a_b \frac{p_a - p_s}{p_a} + a \frac{p_s - p_i}{p_a} + (b_s + a_w) \frac{p_i - p_c}{p_a} + b \frac{p_c}{p_a} - \frac{\frac{eR_d}{k} + f\Gamma^*}{p_a} \quad (3)$$

where a_b, a, a_w, b_s, and b are the fractionation factors associated with CO_2 diffusion through the leaf boundary layer (2.9‰), stomata (4.4‰), water (0.7‰), fractionation attributed with CO_2 entering solution (1.1‰), and the net fractionation attributed to phosphoenolpyruvate carboxylase and ribulose-1,5-bisphosphate carboxylase/oxygenase activity (estimated at 29‰; Roeske & O'Leary 1984), respectively. The variables p_a, p_s, p_i, and p_c represent the partial pressure (Pa) of CO_2 in the atmosphere surrounding the leaf, at the leaf surface, in the intercellular spaces, and at the sites of carboxylation, respectively. The variables Γ^*, R_d, k, f, and e represent the CO_2 compensation point (Pa) in the absence of day respiration, day respiration rate (μmol m^{-2} s^{-1}), carboxylation efficiency (μmol m^{-2} s^{-1} Pa^{-1}), and fractionations associated with photorespiration and day respiration (‰; see Table 1 for values), respectively. We calculated p_a, p_s, and p_i by incorporating mole fraction measurements of [CO_2] with atmospheric pressure in Los Alamos (mean = 79 kPa), and estimated p_c following Farquhar & Sharkey (1982):

$$p_c = p_i - A / g_i \qquad\qquad (4)$$

where g_i is internal conductance to CO_2 (μmol m^{-2} s^{-1} Pa^{-1}). We chose a moderate g_i of

1.5 μmol m^{-2} s^{-1} Pa^{-1} based on the range of g_i values observed over the study period.

Prevailing theory suggests Γ^* is highly conserved among C_3 species and previous work

has demonstrated strong temperature dependence of the CO_2 photo-compensation point

(Jordan & Ogren 1984; Brooks & Farquhar 1985), on which we based our calculations of

diurnal Γ^*. Our Γ^* calculations accounted for the reduced atmospheric pressure in Los

Alamos and we confirmed our estimates of Γ^* with those calculated using the Sharkey *et

al.* (2007) A/p_i estimating utility (Table 1). Strictly k, the carboxylation efficiency, is A/p_c;

we used the initial slope of A/p_i response curves (n = 10) as a surrogate estimate and

confirmed these slope-based results with calculations presented in Ku & Edwards (1977)

and Wingate *et al.* (2007) (Table 1). Much work has demonstrated an inhibitory effect of

light on respiration rate, even at irradiance as low as 12 μmol m^{-2} s^{-1} (Atkin *et al.* 2000;

Tcherkez *et al.* 2005; Tcherkez *et al.* 2008). To facilitate estimation of R_d we measured

nocturnal respiration rate (PPFD = 0) on all three days for approximately 120 minutes

after cessation of daytime measurements (see **Results**) and used these data to calculate an

estimated R_d value for each day where $R_d = 0.5R$ (Tcherkez *et al.* 2005) and R equals

steady-state respiration rate 30–120 minutes post-illumination (Table 1). We

parameterized the decarboxylation component of Δ_{comp} using constant f (8‰) (Rooney

1988; Tcherkez 2006) and e (-6‰) (Ghashghaie *et al.* 2003) values. Parameterizing e

based on $\delta^{13}C_{resp}$ (typically estimated at -6‰) may be problematic due to shifts in

respiratory biochemistry under illuminated conditions (Tcherkez *et al.* 2008). We

assessed the magnitude of uncertainty introduced at high and low A when varying e by

comparing $(R_d/A)*(p_c/p_a)$ multiplied by values of $e = -6‰$ and $-1‰$ and calculating the

resulting variation in the Δ_{ef} term (see Eq. 10 below).

We also ran model simulations following the recent revisions to the

comprehensive model (eq. 4) put forward by Wingate $et\ al.$ (2007):

$$\Delta_{\text{revised}} = a_b \frac{p_a - p_s}{p_a} + a \frac{p_s - p_i}{p_a} + (b_s + a_w) \frac{p_i - p_c}{p_a} + b \frac{p_c}{p_a} - \frac{\frac{(e + e^*)R_d}{k} + f\Gamma^*}{p_a} \quad (5)$$

where e^* represents apparent fractionation for day respiration expressing the difference

between the isotopic composition of the respiratory substrate and photosynthetic

assimilates at a given time (Table 1). We calculated an e^* value for each three minute

isotopic measurement using the following equation:

$$e^* = \delta^{13}p_a - \Delta_{\text{simple}} - \delta^{13}C_{\text{mean}} \quad (6)$$

where $\delta^{13}p_a$ is the carbon isotope ratio of atmospheric air in the leaf chamber and $\delta^{13}C_{\text{mean}}$

equals the mean calculated from the $\delta^{13}C_{\text{resp}}$ measurements for each measurement date

(see **Results**). In Δ_{revised} we used a constant $e, f, R_d, g_i,$ and k and a temperature dependent

Γ^* (Table 1). We estimated g_i in Δ_{revised} and Δ_{comp} as 1.5 μmol m^{-2} s^{-1} Pa^{-1} based on

observed morning values. Lastly, we modeled Δ for comparison to Δ_{obs} using the most

simplified form of the Farquhar $et\ al.$ (1982) model (Δ_{simple}), which eliminates boundary

layer, g_i, and decarboxylation contributions to CO_2 flux and their associated fractionation

factors:

$$\Delta_{\text{simple}} = a + (b - a) \cdot \frac{p_i}{p_a} \quad (7)$$

where $b = 27‰$ (Gessler et al. 2008). All modeling was performed in Microsoft Excel XP Professional (Microsoft Corp., USA).

Estimation of g_i and Δ_{ef}

We estimated g_i following the slope-based approach (g_{is}) in Evans et al. (1986):

$$g_{is} = (b - b_s - a_w)/r_i \qquad (8)$$

where r_i is the internal resistance to CO_2 transfer estimated as the slope of predicted ^{13}C discrimination minus Δ_{obs} versus A/p_a. In this application predicted discrimination (Δ_i) was determined using equation 3 calculated with infinite g_i, i.e. $p_i = p_c$. In this study variation in A/p_a was the result of natural variation in the leaf environment. We calculated slopes for each time period where new leaf material was enclosed in the leaf chamber and tested each slope using simple linear regression. All negative slopes were rejected because negative slopes result in negative g_{is} estimates. All regression analyses were performed using JMP 5.0.1 (SAS Institute Inc., Cary, NC). We used significant (P $\leq$ 0.10) slope values to estimate g_{is} for each foliage measurement, and determined the viability of each g_{is} estimate by comparing them to A across the entire measurement period. If the g_{is} estimate was too low to facilitate observed A during any portion of the measurement period we deemed that estimate to be erroneous. Finally, based on theory developed by Evans et al. (1986) and Caemmerer & Evans (1991) we used the y-intercept of significant g_{is} plots to estimate Δ_{ef}.

We also estimated g_i using the point based method (g_{ip}; Evans et al. 1986):

$$g_{ip} = \frac{(b - b_s - a_w)A/p_a}{(\Delta_{pred} - \Delta_{obs}) - \Delta_{ef}} \qquad (9)$$

where Δ_{pred} represents a simplified predictive model of leaf Δ:

$$\Delta_{pred} = a_b \frac{p_a - p_s}{p_a} + a \frac{p_s - p_i}{p_a} + b \frac{p_i}{p_a} \qquad (10)$$

and Δ_{ef} is calculated as:

$$\Delta_{ef} = \frac{\frac{eR_d}{k} + f\Gamma^*}{p_a} \qquad (11)$$

where all factors are the same as described in Δ_{comp} (Eq. 3).

g_i sensitivity analysis

We assessed the sensitivity of Δ_{comp} to changes in g_i by holding all parameters listed in Table 1 constant and varying the g_i value used to calculate p_c over each day. We used g_i values ranging from 0.5–2.5 µmol m^{-2} s^{-1} Pa^{-1} and applied each value uniformly across each measurement day.

Statistical analysis

We estimated the error in Δ_{obs} and $\delta^{13}C_{resp}$ by implementing the parametric bootstrap (Davison & Hinkley 1997); we describe the procedure for Δ_{obs}, but $\delta^{13}C_{resp}$ can be substituted in the description. For each measurement cycle we used the sample mean and standard errors (SE) of the concentrations of $^{12}CO_2$ and $^{13}CO_2$ for the high WS tank, low WS tank, reference gas, and sample gas to define eight normal distributions. We drew eight random deviates of $[^{12}CO_2]$ and $[^{13}CO_2]$ from these distributions, calculated a bootstrap replicate of Δ_{obs}, and repeated this 10,000 times to provide a bootstrap sampling distribution of Δ_{obs}. This insured the variance measured with each isotopologue was propagated into each calculation of c_e, c_o, ξ, δ_e, and δ_o and, therefore, into Δ_{obs} and

$\delta^{13}C_{resp}$. The SE of the bootstrap replicates provides an estimate of the SE of Δ_{obs}. We observed that the bootstrap sampling distributions of Δ_{obs} were roughly normal, so the estimated SE characterizes the variation in Δ_{obs}. All bootstrap analyses were performed in R (R Development Core Team 2008).

For both g_{is} and g_{ip} the g_i estimate is a reciprocal transformation of a normally distributed random variable. While the standard errors describe the normal distributions well they are not easily interpretable for the skewed distributions associated with g_{is} and g_{ip}. g_{is} is the reciprocal of r_i, estimated using the normally distributed regression slope (Table 3). For the slope-based g_i, we calculated r_i and $r_i \pm 1SE$ and transformed these three values to the g_i scale (eq. 8) to generate g_i and an estimate of its error. Similarly, for the point-based g_i, we calculated the roughly normally distributed bootstrap mean $\Delta_{obs} \pm$ 1SE and transformed these to the g_i scale (eq. 9). For these data, one SE on the r_i or Δ_{obs} scales is asymmetric on the g_i scale with the upper SE being roughly twice the lower SE.

To assess model performance we first used least squares regression analysis of predicted and observed values but found the residual analysis of data in all months and models exhibited a non-random distribution. Additionally, both the slope and intercept terms were significantly different from one and zero, respectively, and substantially different from one another, making model comparisons difficult to evaluate. We then modified the computation of the residuals so that all models conformed to a slope of one and intercept of zero (i.e. residuals = model prediction − observed data) and calculated the standard deviation (SD) of the residuals. These SD values represented the square root of the sum of the variance and squared model bias, or root mean square error (RMSE),

for each month and model, and facilitated direct comparison of the predictive

performance between models within each month.

Results

Diurnal Δ_{obs}

Juniper Δ_{obs} averaged (mean ± SE) 16.3 ± 0.2‰ in June, 17.2 ± 0.2‰ in July, and 19.0 ±

0.5‰ in August (P ≤ 0.0002 between each). Leaf Δ_{obs} tended to be highest in the early

morning in all three months, followed by mid-morning variability and a decline through

much of the afternoon (Figure. 1). The seasonal Δ_{obs} trend tracked the transition from low

(June) to high (August) soil, leaf, and atmospheric water content (Table 2, Fig. 2D-F).

Similarly, the diurnal trend towards lower Δ_{obs} observed in the afternoon reflects the

transition from relatively high morning leaf ψ_w to lower mid-day ψ_w (Table 2). On July

and August measurement days the variation in leaf Δ_{obs} reflects the stability of the light

environment, with relatively stable PPFD in July concurrent with stable Δ_{obs} and a

heterogeneous light environment in August resulting in fluctuating Δ_{obs} (Fig. 2). On 14

August we lack reliable isotopic data after 13:00 due to low ambient light (PPFD < 100

μmol m^{-2} s^{-1}) preventing A rates high enough to sustain reliable isotopic measurements.

We found a weak but significant correlation between leaf vapor pressure deficit (*VPD*)

and Δ_{obs} (r^2 = 0.20, P < 0.0001; F = 110.22; Fig. 3), PPFD and Δ_{obs} (r^2 = 0.20, P < 0.0001;

F = 114.11), and A and Δ_{obs} (r^2 = 0.11, P < 0.0001; F = 54.97; Fig. 3) using data pooled

across all three days. Excluding the seven very high Δ_{obs} values in the early August

morning, there was a significant relationship between stomatal conductance (g_s) and Δ_{obs}

(r^2 = 0.03, P < 0.0001; F = 16.60; Fig. 3).

Nocturnal δ¹³C_resp

Nocturnal $\delta^{13}C_{resp}$

The isotopic composition of nocturnal respiration was similar in June (mean = −22.6 ±
0.2‰) and July (mean = −22.7 ± 0.2‰; P = 0.70) (Fig. 4) while respiration rates were
dissimilar (2.6 ± 0.04 and 4.8 ± 0.1 $\mu mol\ m^{-2}\ s^{-1}$, respectively; P < 0.0001). In August
mean $\delta^{13}C_{resp}$ was more depleted (mean = −23.5 ± 0.1‰) than values measured in June (P
< 0.0001) and July (P < 0.0001), while respiration rate (mean = 3.7 ± 0.004 $\mu mol\ m^{-2}\ s^{-1}$)
was higher than observed in June (P < 0.0001) and lower than observed in July (P <
0.0001). These $\delta^{13}C_{resp}$ values were enriched compared with estimates of the composition
of recently assimilated sugars, which were −24.66 ± 0.20‰ in June, −25.19 ± 0.17‰ in
July, and −25.97 ± 0.30‰ in August. The step change in $\delta^{13}C_{resp}$ observed approximately
50 minutes post-illumination in June and July was due to cessation of measurement on
one group of foliage and the movement to new foliage.

Temporal variation in g_i and Δ_{ef}

We tested 32 slopes and found seventeen were significant across the three days. These
produced fourteen viable g_{is} and Δ_{ef} estimates based on comparisons to *A*, including two
in June, six in July, and six in August (Fig. 5; Table 3). We also found three slopes in the
August morning which failed our criteria for having a significant slope (P ≤ 0.1), but
whose estimates of g_{is} fit the observed trend and are included in Figure 5 (Table 3). Other
g_{is} estimates failed to support observed *A* or displayed negative slope relationships
between $\Delta_i - \Delta_{obs}$ and A/p_a and were excluded from the analysis. Estimates of g_{ip}
produced non-viable values when Δ_{obs} was larger than Δ_{pred} in bootstrap resamples,

resulting in negative g_{ip} estimates. These 98 negative values, representing 22% of all g_{ip} estimates, were excluded from the analysis.

Internal conductance calculated from slope-based measurements ranged from 0.04–2.14 µmol m^{-2} s^{-1} Pa^{-1} (mean ± SE = 1.06 ± 0.17 µmol m^{-2} s^{-1} Pa^{-1}) across the three days. The 14 August g_{is} measurements were obtained from one leaf area across the morning and early afternoon and demonstrated an increase in g_{is} from 0.04–2.14 µmol m^{-2} s^{-1} Pa^{-1} (Figure 5C). We observed a lower range of variability in July g_{is}, with afternoon values ranging between 0.92 and 1.3 µmol m^{-2} s^{-1} Pa^{-1}. We did not find a significant relationship between leaf temperature (T_l) and g_{is} ($r^2 = 0.003$, P = 0.87; F = 0.028). Estimates of g_{ip} ranged between 0.05–8.53 µmol m^{-2} s^{-1} Pa^{-1} (mean ± SE = 1.89 ± 0.07 µmol m^{-2} s^{-1} Pa^{-1}) across the three measurement days (Figure 5). Sensitivity analysis demonstrated a significant increase (P < 0.0001) in g_{ip} estimates when varying $e = -6$‰ and $f = 8$‰ (mean ± SE = 1.60 ± 0.04 µmol m^{-2} s^{-1} Pa^{-1}) to $e = -1$‰ and $f = 11$‰ (3.31 ± 0.14 µmol m^{-2} s^{-1} Pa^{-1}). There was a small but significant relationship between g_{ip} and T_l ($r^2 = 0.03$, P = 0.0003; F = 13.168).

Δ_{ef} also exhibited diurnal variation, ranging between −22.2 and +1.34‰. In August we observed a low Δ_{ef} value of −21.3‰ in the early morning, later morning values that were not significantly different from zero (P ≤ 0.10), and afternoon values near −2.5‰ (Table 3). The morning value in July was not significantly different from zero, whereas the afternoon Δ_{ef} values were between −4.9‰ and −3.5‰. Our single significant Δ_{ef} value in June was −10.56 ± 5.3‰. The non-zero values of Δ_{ef} occur at early morning, mid-day, or late afternoon, when fluxes are small and errors are likely to be greatest (Table 3).

*Δ*ₒbₛ and *pᵢ/pₐ*

Δ_{obs} and p_i/p_a

First order linear relationships between Δ_{obs} and p_i/p_a were significant in June ($r^2 = 0.25$,

$P < 0.0001$; $F = 58.31$; Figure 7A), July ($r^2 = 0.51$, $P < 0.0001$; $F = 182.61$) and August

($r^2 = 0.72$, $P < 0.0001$; $F = 248.99$); however, second order polynomials described the

relationships with greater predictive power in July ($r^2 = 0.64$, $P < 0.0001$; $F = 151.90$) and

August ($r^2 = 0.88$, $P < 0.0001$; $F = 334.27$; Fig. 6B,C). The curvilinear relationship

between Δ_{obs} and p_i/p_a was most pronounced in the p_i/p_a range between 0.75 and 0.85.

gᵢ sensitivity analysis

g_i sensitivity analysis

Incorporation of variable g_i into Δ_{comp} over diurnal periods produced variation in

predictions of Δ_{comp}. Sensitivity analysis demonstrated using low g_i (0.5 µmol m^{-2} s^{-1} Pa^{-1})

in Δ_{comp} resulted in a mean 6.9‰ underestimate of Δ_{obs} while relatively high g_i (2.5 µmol

m^{-2} s^{-1} Pa^{-1}) resulted in a 0.70‰ overestimate of Δ_{obs} (Table 4). Pairwise comparisons of

the residuals ($\Delta_{obs}-\Delta_{comp}$) resulting from Δ_{comp} predictions incorporating a g_i value of 0.5

µmol m^{-2} s^{-1} Pa^{-1} were significantly different from residuals produced when using g_i

values of 1.0, 1.5, 2.0, and 2.5 µmol m^{-2} s^{-1} Pa^{-1} in Δ_{comp} ($P \leq 0.05$; Tukey's HSD) within

and across all three days. Similarly, all other g_i inputs into Δ_{comp} (1.0, 1.5, 2.0, and 2.5

µmol m^{-2} s^{-1} Pa^{-1}) produced significantly different residuals from one another within each

day and across all three days (Table 4). The RMSE, a measure of the variance and

squared bias associated with the residuals, largely followed the trend observed in the

pairwise residual comparisons and was lower when residual differences were smaller;

this demonstrates the importance of an accurate estimate of g_i for model fit. Internal

conductance values of 1.5 and 2.0 µmol m^{-2} s^{-1} Pa^{-1} produced the best predictions, as determined by lowest pairwise residual differences and RMSE, when applied uniformly across each measurement day (Table 4).

Model predictions: Δ_{comp}, $\Delta_{revised}$, and Δ_{simple}

Model performance varied across the three measurement days (Figure 7). Assessing the error between model predictions and Δ_{obs} in each month showed Δ_{simple} had the lowest RMSE, 2.11‰, in June, Δ_{comp} had the lowest error in July (RMSE = 1.50‰), and $\Delta_{revised}$ exhibited the lowest error in August (RMSE = 3.15‰; Table 5). Substituting $b = 25$‰ into Δ_{simple} reduced model prediction bias (mean = 0.31 ± 0.12‰) but resulted in higher RMSE (mean = 2.65‰ versus 2.42‰ for $b = 27$‰) on all three days compared to using $b = 27$‰. The estimated model prediction bias between Δ_{comp}, $\Delta_{revised,}$ and Δ_{simple} and observed discrimination across all three dates was (mean ± SE) −0.62 ± 0.18‰, −0.28 ± 0.19‰, and 1.63 ± 0.18‰, respectively. However, error assessment revealed the apparent close simulations suggested by the small model prediction bias between modeled and observed values masked substantial variance in all models' predictions of Δ_{obs} (Table 5). At high A, defined here as > 4.0 µmol m^{-2} s^{-1}, uncertainty introduced into Δ_{ef} by utilizing $e = −6$‰ versus −1‰ was equal to 2.21 ± 0.01‰ while at low A, defined here as < 2.0 µmol m^{-2} s^{-1}, the same uncertainty increased to 9.40 ± 1.51‰ (Table 6).

Discussion

The objectives of this study were to 1) examine the temporal variation in Δ, $\delta^{13}C_{resp}$, g_i, and Δ_{ef} under ambient field conditions, 2) test the hypothesis that g_i varies across the day,

3) test the hypothesis that Δ varies linearly in response to shifts in p_i/p_a under field conditions, 4) test the influence of g_i in a comprehensive leaf model of Δ, and 5) test the predictive capabilities of three models: the comprehensive Farquhar *et al.* (1982) model of Δ (Δ_{comp}), a recently suggested amendment to Δ_{comp} ($\Delta_{revised}$; Wingate *et al.* 2007) and the simplified form of the comprehensive model (Δ_{simple}). We observed a large range of variation in Δ, g_i, and Δ_{ef} over diurnal time periods and across the season. Seasonally, $\delta^{13}C_{resp}$ decreased as water availability increased. We found that g_i varied across the day in August and that g_i exerted substantial influence on Δ predictions. We found Δ_{obs} varied in a linear fashion in response to p_i/p_a in June, but second order expressions better described the relationship in July and August. Finally, we found all models reasonably predicted Δ_{obs}, but Δ_{simple} best predicted Δ_{obs} in June, Δ_{comp} best predicted Δ_{obs} in July, and $\Delta_{revised}$ best predicted Δ_{obs} in August.

Diurnal Δ_{obs} & nocturnal $\delta^{13}C_{resp}$

Diurnal Δ_{obs} in our juniper woodland varied between 12.0‰ and 27.4‰, which was similar in trend and magnitude to Δ observed in a tropical forest (Harwood *et al.* 1998) and a mesic *Picea* stand (Wingate *et al.* 2007) (Fig. 1). Variation in Δ_{obs} was generally related to environmental drivers such as PPFD and *VPD* (Figs. 1,2,3). The diurnal trend towards decreasing Δ_{obs} observed in June and July correlates with increasing leaf-to-atmosphere *VPD* observed both days, though low leaf ψ_w and high air temperature likely contributed to low discrimination in June compared to July and August. In August, *VPD* was relatively low and cloudy conditions caused large variation in Δ_{obs}. Cumulatively, these sensitivities to *VPD* and PPFD were similar to those seen in modeled canopy Δ

(Baldocchi & Bowling 2003; Chen & Chen 2007). We also observed several high, but transient, discrimination values in all three months including mid-day values of 31.4‰ in June and 36.9‰ in July, and observations ranging from 29.7–44.9‰ in the early morning in August. These Δ_{obs} values were associated with greater uncertainty, but were similar to values observed in *Piper* and *Picea* (Harwood *et al.* 1998; Wingate *et al.* 2007).

Nocturnal $\delta^{13}C_{resp}$ for the juniper trees in our study ranged from ~ −24 to −22‰ and was moderately enriched compared to most observations in the literature (Bowling *et al.* 2002; Hymus *et al.* 2005; Prater, Mortazavi & Chanton 2005). $\delta^{13}C_{resp}$ values were similar in June and July, and were more enriched in ^{13}C compared to August (Fig. 4). The consistent 2-3‰ enrichment of $\delta^{13}C_{resp}$ compared to estimates of recently assimilated carbohydrate is consistent with previous reports (Duranceau *et al.* 1999; Ghashghaie *et al.* 2001) and may reflect respiratory fractionation, possibly combined with diverse respiratory substrate utilization (Tcherkez *et al.* 2003). This $\delta^{13}C_{resp}$ pattern is consistent with the temporal transition period from drought in June through the onset of summer monsoon in July to the strong monsoon in August.

Temporal variation in g_i & Δ_{ef}

We observed a diurnal increase in g_i occurring in one leaf area across the August morning and early afternoon, and a range of variation in g_i across the three months (Fig. 5). The physiological drivers of this variation in g_i are unknown, but likely involved changes in protein activity facilitating the transfer of CO_2 across cell or chloroplast membranes (Flexas *et al.* 2006; Hanba *et al.* 2006; Uehlein *et al.* 2008). Previous work has demonstrated variability in g_i in response to environmental variables such as temperature

32

(Bernacchi $et\ al$. 2002; Warren & Dryer 2006; Yamori $et\ al$. 2006) and water availability

(Warren $et\ al$. 2004; Grassi & Magnani 2005; Galmés $et\ al$. 2007; Diaz-Espejo $et\ al$.

2007), both of which fluctuate in a field setting. We did not find a significant correlation

between T_l and g_{is} but did find a significant relationship between T_l and g_{ip}. It is possible

that variable irradiance over each measurement period may have confounded any

temperature effect on g_{is}, but the higher temporal frequency of g_{ip} was closer to the

frequency T_l was changing diurnally. Juniper displays anisohydric leaf hydraulic behavior

and concurrent ψ_w measurements (Table 2) demonstrated a seasonal increase and diurnal

decrease in xylem ψ_w. The seasonal ψ_w pattern paralleled our seasonal g_i measurements,

suggesting a linkage between leaf water status and the g_i patterns we observed, but are

confounded by the increase in both g_{is} and g_{ip} in the August morning when ψ_w was

decreasing. Notably, there was a distinct decrease in g_{is} in the upward morning trend that

coincides with extended cloud cover (mean PPFD = 266 ± 46 μmol m^{-2} s^{-1}). We speculate

the large and prolonged drop in incident light played a regulatory role in the lower g_i,

similar to observations of other environmental regulators of g_i in controlled studies

(Delfine $et\ al$. 1999; Bernacchi $et\ al$. 2002; Flexas $et\ al$. 2007). The July data exhibit

modest variation in diurnal g_i, but may reflect natural variation among branches. Given

that our measurements were collected under ambient environmental conditions an

accurate assessment of the factors driving the variation in g_i we observed is not possible

and should be addressed in controlled studies.

The variation in g_{is} is potentially problematic for the slope-based method because

it assumes g_i is constant over the period the slope data are collected. While rapid

variation in g_i has been demonstrated in response to [CO_2] (Flexas $et\ al$. 2007), the rate

and magnitude of diurnal shifts in g_i under field conditions has not been previously reported. Our 30–45 min g_{is} measurement periods may have spanned too long and allowed time for g_i to change in response to the environment. However, aside from periods where Δ_{obs} was highly variable, such as the July mid-day period, g_{ip} values were generally stable around each g_{is} value and show variation was low enough to provide valid g_{is} estimates. Slope-based estimates of g_i tended to underestimate g_{ip} in June and July, but both trended together in August (Figure 5). g_{ip} is sensitive to the parameterization of e and f, and errors in estimating these values may have resulted in over- or under-estimation of g_{ip}.

Most of our g_i estimates agree with values reported in other woody species (Lloyd et al. 1992; De Lucia, Whitehead & Clearwater 2003; Warren et al. 2003; Ethier et al. 2006) but we also found low g_{is} estimates in the early morning and relatively high g_{ip} estimates when Δ_{obs} was highly variable. We found a low g_{is} estimate (0.03 μmol m^{-2} s^{-1} Pa^{-1}) in the August early morning transition period from respiration to net A, where net CO_2 drawdown was between 6-10 μmol mol^{-1}, uncertainty in Δ_{obs} was higher, and measurements may have been more strongly influenced by the isotopic signature of CO_2 evolved during concurrent day respiratory processes. Though low, model simulations demonstrated the 0.03 μmol m^{-2} s^{-1} Pa^{-1} conductance estimate was high enough to allow observed A across the measurement period. Estimates from g_{ip} during this period show consistently negative estimates of g_i (data not shown). High and variable g_{ip} estimates ranged between 4–8 μmol m^{-2} s^{-1} Pa^{-1} during the mid-day period in July, driven by higher uncertainty in Δ_{obs} over this period.

Our measurements of Δ_{ef} suggest that fractionations attributed to decarboxylation activity may not be negligible at dawn and in the afternoon when rates of either respiration or photorespiration may be high (Table 3). Our early morning August measurement occurred during a time of low A/p_a and generated a very negative Δ_{ef} value. If respiration had not fully deactivated to its daytime rate, then it may have had an unusually large impact during that time period (Gillon & Griffiths 1997). By mid-morning in July and August A and g_s had reached a plateau and Δ_{ef} was not significantly different from zero. However, in the June and July afternoons high temperature and PPFD created conditions conducive to higher photorespiration rates that may have contributed to greater variation in afternoon Δ_{ef} values. Further, compared to other C_3 species juniper exhibits high R, from which we estimated R_d, and thus the respiratory component of Δ_{ef} would have a larger impact on net Δ than would be expected for other species. Carefully controlled studies partitioning different components of the net flux will be necessary to elucidate the contribution of each component.

Δ_{obs} and p_i/p_a

We observed significant first order linear relationships between Δ and p_i/p_a in all months, but found second order models better described the curvilinear relationship between Δ and p_i/p_a in July and August (Fig. 6). We propose that the curvilinear relationship is related to the increasing dominance of respiration and associated isotopic signatures on leaf exchanged CO_2 at high p_i/p_a values. Previous work and theory have demonstrated a linear relationship between Δ and p_i/p_a in C_3 plants (Farquhar *et al*. 1982b; Evans *et al*. 1986; Brugnoli *et al*. 1988; Farquhar *et al*. 1989), but unlike our study these data were

collected in controlled settings under steady-state conditions. In both July and August the curvilinear trend between Δ and p_i/p_a was driven by high Δ values. These high Δ values correspond with conditions conducive to high respiratory and photorespiratory flux, notably the early morning and mid-day periods, and may reflect the isotopic signature of a highly enriched substrate (Tcherkez *et al.* 2005).

g_i sensitivity analysis

Incorporating variable internal CO_2 conductance into Δ_{comp} demonstrated g_i exerted substantial influence on predictions of diurnal discrimination. Average observed g_i was near 1.5 μmol m^{-2} s^{-1} Pa^{-1} and our sensitivity analysis showed that relatively low (0.5 μmol m^{-2} s^{-1} Pa^{-1}) and high (2.5 μmol m^{-2} s^{-1} Pa^{-1}) values resulted in large deviations between model predictions and Δ_{obs} (Table 4). However, we have shown that g_i can vary in a leaf over several hours and it is likely incorporating this diurnal variability into leaf and ecosystem models would improve discrimination predictions (McDowell *et al.* 2008a). Future studies should focus on assessing the diurnal variability in g_i independently and testing whether variable diurnal g_i significantly improves the accuracy and precision of predictions of Δ in leaf models.

Model predictions: Δ_{comp}, $\Delta_{revised}$, and Δ_{simple}

Our study supports the use of the more comprehensive models, Δ_{comp} and $\Delta_{revised}$, that incorporate fractionations associated with the diffusion pathway and decarboxylation activity, to describe leaf Δ in our semi-arid system. The limitations of these models are that they require assumptions of the true value of fractionation during carboxylation and

decarboxylation, in addition to an accurate estimate of g_i. Our sensitivity analysis showed that variation in e at low A resulted in ~9‰ variation in Δ_{ef}, emphasizing the importance of e in plants like juniper that exhibit relatively high R compared to A. Our estimate of e was based on the dark respiration fractionation, and we may have over- or under-estimated the true value of e or R_d and introduced model error. However, we have shown both models produced similar errors in their predictions of Δ.

The importance of decarboxylation activity in juniper Δ is reflected both in the e^* values we calculated and the Δ_{ef} estimates obtained from g_i plots. We calculated e^* values ranging from -12.5‰ to $+1.2$‰, values that suggest the isotopic disequilibria between recent photosynthate and the respiratory substrate being utilized was, at times, substantial. Further, our Δ_{ef} estimates were mostly between -6.9‰ and 0‰, whereas previous observations were close to 0‰ (Evans *et al*. 1986). It is also possible that other factors, such as stomatal patchiness, may not be fully captured in our estimates of p_i, which could alter the p_i/p_a ratio important to all of the Δ models (Farquhar 1989).

Despite lacking decarboxylation and g_i components Δ_{simple} outperformed the more comprehensive models in June. Further, Δ_{simple} exhibited modest error in predicting Δ_{obs} compared to Δ_{comp} and $\Delta_{revised}$ in July and August but consistently overestimated Δ_{obs}, predicting Δ values whose mean difference were > 1.0‰ above Δ_{obs} in all three months. This may represent a larger systematic bias than exists in the other models, though utilizing a lower b value reduced model bias while moderately increasing error. However, all of the models exhibited non-trivial RMSE, ranging from 1.5–3.2‰, suggesting that a significant amount of variability remains to be captured. Future field studies should aim to independently estimate the variability in diurnal Δ_{ef} and g_i to ascertain their impacts on

diurnal leaf isotopic exchange. Similarly, future controlled studies should partition the net flux to assess g_i and Δ_{ef}, as well the regulatory influence of environmental variables such as temperature and PPFD on these components of carbon discrimination.

Conclusions

Our study demonstrates the diurnal variation in Δ in our semi-arid conifer ecosystem was of similar trend and magnitude to that observed in ecosystems as diverse as tropical forest and mesic conifer forest. Additionally, we demonstrated that Δ varies rapidly in response to shifts in environmental conditions and that the comprehensive Farquhar *et al*. (1982) model and its descendents are capable of capturing a wide range of diurnal variation in leaf Δ. Our observations are consistent with previous results showing low Δ during conditions of low soil water availability and elevated *VPD* and PPFD, and higher Δ when soil water was more abundant, PPFD was variable, and *VPD* was low. We observed a linear relationship between Δ and p_i/p_a in June, but found a strong curvilinear relationship in July and August. Future studies might be strengthened by testing this relationship in other species over a wide range of p_i/p_a and environmental conditions. Our findings support the inclusion of g_i and decarboxylation activity to attain the most accurate and precise predictions of Δ from leaf models, and evolving technologies such as *TDL* make these improvements more easily achievable. Lastly, the magnitude of diurnal variation in g_i of other C_3 species needs to be quantified, as do the environmental and physiological drivers of this variation, so that g_i can be more accurately parameterized in future ecosystem process models.

Acknowledgements

References

Atkin O.K., Bruhn D., Hurry V.M., Tjoelker M.G. (2005) The hot and the cold: unravelling the variable response of plant respiration to temperature. *Functional Plant Biology* **32**, 87-105.

Atkin O.K., Evans J.R., Ball M.C., Lambers H., & Pons T.L. (2000) Leaf respiration of snow gum in the light and dark. Interactions between temperature and irradiance. *Plant Physiology* **122**, 915-923.

Baldocchi D.D. & Bowling D.R. (2003) Modelling the discrimination of $^{13}CO_2$ above and within a temperate broad-leaved forest canopy on hourly to seasonal time scales. *Plant, Cell and Environment* **26**, 231-244.

Barbour M.M, Hunt J.E., Dungan R.J., Turnbull M.H., Brailsford G.W., Farquhar G.D., Whitehead D. (2005) Variation in the degree of coupling between $\delta^{13}C$ of phloem sap and ecosystem respiration in two *Nothofagus* forests. *New Phytologist* **166**, 497-512.

Barbour M.M., Farquhar G.D., Hanson D.T., Bickford C.P., Powers H., & McDowell N.G. (2007b) A new measurement technique reveals temporal variation in $\delta^{18}O$ of leaf-respired CO_2. *Plant, Cell and Environment* **30**, 456-468.

Barbour M.M., McDowell N.G., Tcherkez G., Bickford C.P., & Hanson D.T. (2007a) A new measurement technique reveals rapid post-illumination changes in the carbon isotope composition of leaf-respired CO_2. *Plant, Cell and Environment* **30**, 469-482.

Bernacchi C.J., Portis A.R., Nakano H., von Caemmerer S., & Long S.P. (2002) Temperature response of mesophyll conductance. Implications for the determination of rubisco enzyme kinetics and for limitations to photosynthesis in vivo. *Plant Physiology* **130**, 1992-1998.

Bowling D.R., McDowell N.G., Bond B.J., Law B.E., & Ehleringer J.R. (2002) ^{13}C content of ecosystem respiration is linked to precipitation and vapor pressure deficit. *Oecologia* **131**, 113-124.

Bowling D.R., Pataki D.E., & J.T. Randerson (2008) Carbon isotopes in terrestrial ecosystem pools and CO_2 fluxes. *New Phytologist Tansley Review* **178**, 24-40.

Bowling D.R., Sargent S.D., Tanner B.D., & Ehleringer J.R. (2003) Tunable diode laser absorption spectroscopy for stable isotope studies of ecosystem-atmosphere CO_2 exchange. *Agricultural and Forest Meteorology* **118**, 1-19.

Breshears D.D. (2008) Structure and function of woodland mosaics: consequences of patch-scale heterogeneity and connectivity along the grassland-forest continuum. In *Western North American Juniperus Woodlands- A Dynamic Vegetation Type*. (Ed O. W. Van Auken.) pp. 58-92. Springer.

Brooks A. & Farquhar G.D. (1985) Effect of temperature on the CO_2/O_2 specificity of ribulose-1,5-bisphosphate carboxylase/oxygenase and the rate of respiration in the light. *Planta* **165**, 397-406.

Brooks J.R., Flanagan L.B., Buchmann N., & Ehleringer J.R. (1997) Carbon isotope composition of boreal plants: functional grouping of life forms. *Oecologia* **110**, 301-311.

Brugnoli E., Hubick K.T., von Caemmerer S., Wong, S.C., Farquhar G.D. (1988) Correlation between the carbon isotope discrimination in leaf starch and sugars of C_3 plants and the ratio of intercellular and atmospheric partial pressures of carbon dioxide. *Plant Physiology* **88**, 1418-1424.

Brugnoli E. & Farquhar G.D. (2000) Photosynthetic fractionation of carbon isotopes. In *Photosynthesis: Physiology and Metabolism*. (Eds R.C. Leegood, T.D. Sharkey, and S. von Caemmerer.) pp. 399-434. Kluwer Academic, The Netherlands.

von Caemmerer S. & Evans J.R. (1991) Determination of the average partial pressure of CO_2 in the chloroplasts from leaves of several C_3 plants. *Australian Journal of Plant Physiology* **18**, 287-305.

Chen B. & Chen J.M. (2007) Diurnal, seasonal and interannual variability of carbon isotope discrimination at the canopy level in response to environmental factors in a boreal forest ecosystem. *Plant, Cell and Environment* **30**, 1223-1239.

Ciais P., Tans P.P., Trolier M., White J.W.C., & Francey R.J. (1995) A large northern hemisphere terrestrial CO_2 sink indicated by the ^{13}C/^{12}C ratio of atmospheric CO_2. *Science* **269**, 1098-1102.

Davenport D.W., Wilcox B.P., & Breshears D.D. (1996) Soil morphology of canopy and inter-canopy sites in a pinon-juniper woodland. *Soil Science Society of America Journal* **60**, 1881-1887.

Davison A.C., Hinkley D.V. (1997) Bootstrap methods and their application. Cambridge University Press, New York, NY, USA.

Delfine S., Alvino A., Villani M.C., & Loreto F. (1999) Restrictions to carbon dioxide conductance and photosynthesis in spinach leaves recovering from salt stress. *Plant Physiology* **119**, 1101-1106.

De Lucia E.H., Whitehead D., & Clearwater M.J. (2003) The relative limitation of photosynthesis by mesophyll conductance in co-occurring species in a temperate rainforest dominated by a conifer *Dacrydium cupressinum. Functional Plant Biology* **30**, 1197-1204.

Diaz-Espejo A., Nicolas E., & Fernandez J.E. (2007) Seasonal evolution of diffusional limitations and photosynthetic capacity in olive under drought. *Plant, Cell and Environment* **30**, 922-933.

Duranceau M., Ghashghaie J., Badeck F., Deleens E., & Cornic G. (1999) $\delta^{13}C$ of CO_2 respired in the dark in relation to $\delta^{13}C$ of leaf carbohydrates in *Phaseolus vulgaris* L. under progressive drought. *Plant, Cell and Environment* **22**, 515-523.

Ehleringer J.R. (1993) Variation in leaf carbon isotope discrimination in *Encelia farinosa*: implications for growth, competition, and drought survival. *Oecologia* **95**, 340-346.

Ehleringer J.R., Phillips S.L., & Comstock J.P. (1992) Seasonal-variation in the carbon isotopic composition of desert plants. *Functional Ecology* **6**, 396-404.

Ethier G.J., Livingston N.J., Harrison D.L., Black T.A., Moran J.A. (2006) Low stomatal and internal conductance to CO_2 versus Rubisco deactivation as determinants of the photosynthetic decline of ageing evergreen leaves. *Plant, Cell and Environment* **29**, 2168-2184.

Evans J.R., Sharkey T.D., Berry J.A., & Farquhar G.D. (1986) Carbon isotope discrimination measured concurrently with gas exchange to investigate CO_2 diffusion in leaves of higher plants. *Australian Journal of Plant Physiology* **13**, 281-292.

Farquhar G.D. (1989) Models of integrated photosynthesis of cells and leaves. *Philosophical Transactions of the Royal Society of London. Series B, Biological Sciences* **323**, 357-367.

Farquhar G.D., Ball M.C., von Caemmerer S., & Roksandic Z. (1982b) Effect of salinity and humidity on $\delta^{13}C$ value of halophytes—Evidence for diffusional isotope fractionation determined by the ratio of intercellular/atmospheric partial pressure of CO_2 under different environmental conditions. *Oecologia* **52**, 121-124.

Farquhar G.D., von Caemmerer S., & Berry J.A. (1980) A biochemical model of photosynthetic CO_2 assimilation in leaves of C_3 species. *Planta* **149**, 78-90.

Farquhar G.D., Ehleringer J.R., & Hubick K.T. (1989) Carbon isotope discrimination and photosynthesis. *Annual Review of Plant Physiology and Plant Molecular Biology* **40**, 503-537.

Farquhar G. D., O'Leary M.H., & Berry J.A. (1982) On the relationship between carbon isotope discrimination and the intercellular carbon dioxide concentration in leaves. *Australian Journal of Plant Physiology* **9**, 121-137.

Farquhar G.D. & Richards R.A. (1984) Isotopic composition of plant carbon correlates with water-use efficiency of wheat genotypes. *Australian Journal of Plant Physiology* **11**, 539-552.

Farquhar G.D. & Sharkey T.D. (1982) Stomatal conductance and photosynthesis. *Annual Review of Plant Physiology* **33**, 317-345.

Flexas J., Diaz-Espejo A., Galmés J., Kaldenhoff R., Medrano H., & Ribas-Carbo M. (2007) Rapid variations of mesophyll conductance in response to changes in CO_2 concentration around leaves. *Plant, Cell and Environment* **30**, 1284-1298.

Flexas J., Ribas-Carbo M., Hanson D.T., Bota J., Otto B., Cifre J., McDowell N., Medrano H., & Kaldenhoff R. (2006) Tobacco aquaporin NtAQP1 is involved in mesophyll conductance to CO_2 in vivo. *Plant Journal* **48**, 427-439.

Galmés J., Medrano H., Flexas J. (2007) Photosynthetic limitations in response to water stress and recovery in Mediterranean plants with different growth forms. *New Phytologist* **175**, 81-93.

Gessler A., Tcherkez G., Peuke A.D., Ghashghaie J., Farquhar G.D. (2008) Experimental evidence for diel variations of the carbon isotope composition in leaf, stem and phloem sap organic matter in *Ricinus communis*. *Plant, Cell and Environment* **31**, 941-953 doi: 10.1111/j.1365-3040.2008.01806.x

Ghashghaie J., Badeck F.W., Lanigan G., Nogues S., Tcherkez G., Deleens E., Cornic G., & Griffiths H. (2003) Carbon isotope fractionation during dark respiration and photorespiration in C_3 plants. *Phytochemistry Reviews* **2**, 145-161.

Ghashghaie J., Duranceau M., Badeck F.-W., Cornic G., Adeline M.-T. & Deleens E. (2001) $\delta^{13}C$ of CO_2 respired in the dark in relation to $\delta^{13}C$ of leaf metabolites: comparison between *Nicotiana sylvestris* and *Helianthus annuus* under drought. *Plant, Cell and Environment* **24**, 505-515.

Gillon J.S. & Griffiths H. (1997) The influence of (photo)respiration on carbon isotope discrimination in plants. *Plant, Cell and Environment* **20**, 1217-1230.

Grassi G. & Magnani F. (2005) Stomatal, mesophyll conductance and biochemical limitations to photosynthesis as affected by drought and leaf ontogeny in ash and oak trees. *Plant, Cell and Environment* **28**, 834-849.

Griffis T.J., Baker J.M., Sargent S.D., Tanner B.D., Zhang J. (2004) Measuring field-scale isotopic CO_2 fluxes with tunable diode laser absorption spectroscopy and micrometeorological techniques. *Agricultural and Forest Meteorology* **124**, 15-29.

Hanba Y., Shibasaka M., Hayashi Y, Hayakawa T., Kasamo K., Terashima I., Katuhara M. (2006) Overexpression of the barley aquaporin HvPIP2;1 increases internal CO_2 conductance and CO_2 assimilation in the leaves of transgenic rice plants. *Plant and Cell Physiology* **47**, suppl. S24-S24.

Harwood K.G., Gillon J.S., Griffiths H., & Broadmeadows M.S.J. (1998) Diurnal variation of $\Delta^{13}CO_2$, $\Delta C^{18}O^{16}O$ and evaporative site enrichment of $\delta H_2^{18}O$ in *Piper aduncum* under field conditions in Trinidad. *Plant, Cell and Environment* **21**, 269-283.

Hymus G.J., Maseyk K., Valentini R., & Yakir D. (2005) Large daily variation in ^{13}C-enrichment of leaf-respired CO_2 in two *Quercus* forest canopies. *New Phytologist* **167**, 377-384.

Jordan D.B. & Ogren W.L. (1984) The CO_2/O_2 specificity of ribulose 1,5 bisphosphate carboxylase/oxygenase. Dependence on ribulosebisphosphate concentration, pH, and temperature. *Planta* **161**, 308-313.

Knohl A., Werner R.A., Brand W.A., Buchmann N. (2005) Short-term variations in ecosystem $\delta^{13}C$ of ecosystem respiration reveals link between assimilation and respiration in a deciduous forest. *Oecologia* **142**, 72-80.

Kozaki A., Takeba G. (1996) Photorespiration protects C3 plants from photooxidation. *Nature* **384,** 557-560.

Ku S.-B. & Edwards G.E. (1977) Oxygen inhibition of photosynthesis II. Kinetic characteristics as affected by temperature. *Plant Physiology* **59**, 991-999.

Lloyd J., Syvertsen J.P., Kriedemann P.E., Farquhar G.D. (1992) Low conductances for CO_2 diffusion from stomata to the sites of carboxylation in leaves of woody species. *Plant, Cell and Environment* **15**, 873-899.

McDowell, N., Baldocchi D., Barbour, M., Bickford C., Cuntz M., Hanson D., Knohl A., Powers H., Rahn T., Randerson J., Riley W., Still C., Tu K., Walcroft A. (2008a) Measuring and modeling the stable isotope composition of biosphere-atmosphere CO_2 exchange: where are we and where are we going? *EOS* **89**, 94-95.

McDowell N.G., Bowling D.R., Schauer A., Irvine J., Bond B.J., Law B.E., & Ehleringer J.R. (2004) Associations between carbon isotope ratios of ecosystem respiration, water availability, and canopy conductance. *Global Change Biology* **10**, 1767-1784.

McDowell N.G., Pockman W.T., Allen C., Breshears D.D., Cobb N., Kolb T., Plaut J., Sperry J., West A., Williams D., & Yepez E.A. (2008b) Mechanisms of plant survival and mortality during drought: Why do some plants survive while others succumb to

drought? *New Phytologist Tansley Review* **178**, 719-739.

O'Leary M.H. (1981) Carbon isotope fractionation in plants. *Phytochemistry* **20**, 553-567.

Prater J.L., Mortazavi B., Chanton J.P. (2005) Diurnal variation of the $\delta^{13}C$ of pine needle respired CO_2 evolved in darkness. *Plant, Cell and Environment* **29**, 202-211.

R Core Development Team (2008). R: A language and environment for statistical computing. R Foundation for Statistical Computing, Vienna, Austria. ISBN 3-900051-07-0, URL http://www.R-project.org.

Randerson J.T., Masiello C.A., Still C.J., Rahn T., Poorter H., & Field C.B. (2006) Is carbon within the global terrestrial biosphere becoming more oxidized? Implications for trends in atmospheric O-2. *Global Change Biology* **12**, 260-271.

Roeske C.A. & O'Leary M.H. (1984) Carbon isotope effects on the enzyme-catalyzed carboxylation of ribulose bisphosphate. *Biochemistry* **23**, 6275-6284.

Rooney M.A. (1988) Short-term carbon isotopic fractionation in plants. Ph.D thesis. University of Wisconsin-Madison.

Sharkey T.D., Bernacchi C.J., Farquhar G.D., Singsaas E.L. (2007) In Practice: Fitting photosynthetic response curves for C_3 leaves. *Plant, Cell and Environment* **30**, 1035-1040.

Smith B.N. & Epstein S. (1971) Two categories of $^{13}C/^{12}C$ ratios for higher plants. *Plant Physiology* **47**, 380-384.

Tcherkez G. (2006) How large is the carbon isotope fractionation of the photorespiratory enzyme glycine decarboxylase? *Functional Plant Biology* **33**, 911-920.

Tcherkez G. Bligny R., Gout E., Mahé A., Hodges M., Cornic G. (2008) Respiratory metabolism of illuminated leaves depends on CO_2 and O_2 conditions. *Proceedings of the National Academy of Sciences* **105**, 797-802.

Tcherkez G., Cornic G., Bligny R., Gout E., Ghashghaie J. (2005) In vivo respiratory metabolism of illuminated leaves. *Plant Physiology* **138**, 1596-1606.

Tcherkez G., Nogues S., Bleton J., Cornic G., Badeck F. & Ghashghaie J. (2003) Metabolic origin of carbon isotope composition of leaf dark-respired CO_2 in French Bean. *Plant Physiology* **131**, 237-244.

Tu K. & Dawson T. (2005) Partitioning ecosystem respiration using stable carbon isotope analyses of CO_2. In *Stable isotopes and Biosphere-Atmosphere Interactions: Processes and Biological Controls*. (Eds L.B. Flanagan, J.R. Ehleringer, and D.E. Pataki.) pp. 125-148. Elsevier Academic Press, Great Britain.

Uehlein N., Otto B., Hanson D.T., Fischer M., McDowell N., Kaldenhoff R. (2008)

Function of *Nicotiana tabacum* aquaporins as chloroplast gas challenges the concept of membrane CO_2 permeability. *The Plant Cell* **20**, 648-657.

Warren C.R., Ethier G.J., Livingston N.J., Grant N.J., Turpin D.H., Harrison D.L., & Black T.A. (2003) Transfer conductance in second growth Douglas-fir (*Pseudotsuga menziesii* (Mirb.)Franco) canopies. *Plant, Cell and Environment* **26**, 1215-1227.

Warren C.R. & Dreyer E. (2006) Temperature response of photosynthesis and internal conductance to CO_2: results from two independent approaches. *Journal of Experimental Botany* **12**, 3057-3067.

Warren C.R., Livingston N.J., & Turpin D.H. (2004) Water stress decreases the transfer conductance of Douglas-fir (*Pseudotsuga menziesii*) seedlings. *Tree Physiology* **24**, 971-979.

Wingate L., Seibt U., Moncrieff J.B., Jarvis P.G., & Lloyd J. (2007) Variations in ^{13}C discrimination during CO_2 exchange by *Picea sitchensis* branches in the field. *Plant, Cell and Environment* **30**, 600-616.

Yakir D. (2003) The stable isotope composition of atmospheric CO_2. *In: Treatise on Geochemistry*. Vol. **4**, pp. 175-212. Elsevier Press.

Yamori W., Noguchi K., Hanba Y.T., & Terashima I. (2006) Effects of internal conductance on the temperature dependence of the photosynthetic rate in spinach leaves from contrasting growth temperatures. *Plant Cell Physiology* **47**, 1069-1080

Tables

Table 1. Parameters used in model simulations of observed discrimination using the comprehensive model (Δ_{comp}) and the revised model ($\Delta_{revised}$). The fractionation factors associated with day respiration, *e*, and photorespiration, *f*, were assumed based on literature values while all the other terms are derived from our data.

Day	k	R_d	Γ*	e	f	g_i	$\Delta_{revised}$ only e*
			Parameters				
12 June	0.38	1.23	2.86 - 5.23	-6	8	1.5	-11.5 to -1.6
11 July	0.40	2.2	3.17 - 5.17	-6	8	1.5	-12.5 to -0.9
14 August	0.40	1.83	2.43 - 4.29	-6	8	1.5	-10.5 to 1.2

Table 2. Mean xylem water potential with standard error (SE) on all three measurement

days. Mid-day values from McDowell *et al*. (2008b).

	Predawn ψ_w (MPa)	SE	Mid-day ψ_w (MPa)	SE
June	-2.47	0.14	-2.93	0.85
July	-0.67	0.03	-1.99	0.03
August	-0.58	0.04	-1.58	0.44

Table 3. Slope and intercept statistics from linear regressions used to calculate g_{is} and estimate Δ_{ef}. Cut-off values for the test of slope significance within each regression was P ≤ 0.10, but three marginal slopes are also represented (*). Most intercepts were not significantly different from zero, but significant intercepts (P ≤ 0.10) deviated substantially from zero.

campaign	Time	slope	SE	P	Δ_{ef}	SE	P	r^2
12-Jun	7:00	22.05	11.13	0.06	-2.19	1.74	0.22	0.18
	13:00	108.63	46.77	0.05	-10.56	5.35	0.08	0.40
11-Jul	9:00	54.81	22.07	0.05	-12.03	6.4	0.11	0.51
	12:00	20.4	10.49	0.09	-3.83	2.29	0.14	0.35
	13:00	27.58	10.55	0.03	-3.58	2.13	0.14	0.49
	14:00	27.32	7.72	0.02	-4.91	2.03	0.06	0.71
	15:00	21.44	7.65	0.01	-3.53	1.79	0.07	0.34
	16:00	29.31	12.35	0.05	-3.12	2.54	0.25	0.41
14-Aug	6:00	757.31	312.02	0.07	-21.31	5.87	0.02	0.60
	7:00	87.24	23.82	0.008	-1.28	1.52	0.42	0.66
	8:00*	22.81	15.53	0.18	-0.41	2.94	0.89	0.21
	9:00	20.21	4.39	0.0002	0.15	0.63	0.8	0.54
	10:00*	15.23	8.47	0.11	1.39	1.52	0.39	0.29
	11:00	43.04	7.68	0.0005	-3.33	0.89	0.006	0.80
	12:00*	13.17	8.86	0.18	-2.11	2.77	0.47	0.22
	13:00	12.69	3.83	0.01	-1.54	1.19	0.23	0.58

Table 4. Results from a sensitivity analysis utilizing variable g_i values within Δ_{comp} and applied across each measurement day. $\Delta_{obs}-\Delta_{comp}$ represents the pairwise residual difference (‰) between observed discrimination (Δ_{obs}) and model predictions (Δ_{comp}). Δ_{comp} predictions using each of the g_i values produced residuals significantly different from one another within each day and across days. As determined by lowest root mean square error (RMSE; ‰) and pairwise residual difference, g_i of 1.5 and 2.0 µmol m^{-2} s^{-1} Pa^{-1} performed best in predicting Δ_{obs}.

g_i	June $\Delta_{obs}-\Delta_{comp}$	$n = 177$ RMSE	July $\Delta_{obs}-\Delta_{comp}$	$n = 176$ RMSE	August $\Delta_{obs}-\Delta_{comp}$	$n = 97$ RMSE
0.5	4.77	2.24	9.61	2.24	6.56	4.95
1.0	1.02	1.85	3.58	1.55	2.06	3.06
1.5	-0.22	1.77	1.57	1.51	0.55	2.66
2.0	-0.85	1.74	0.57	1.53	-0.20	2.54
2.5	-1.22	2.13	-0.04	1.56	-0.84	3.13

Table 5. Comparison of model performance in predicting Δ_{obs}. Means represent the difference between model predictions and Δ_{obs} and RMSE, the root mean square error. Δ_{simple} consistently overestimated Δ_{obs} but showed lower error in predicting Δ_{obs} in June compared to Δ_{comp} and $\Delta_{revised}$. Δ_{comp} exhibited the lowest error in July, while $\Delta_{revised}$ exhibited lower error and mean difference between predicted and observed values in August compared to Δ_{simple} and Δ_{comp}.

	June	$n = 177$	July	$n = 176$	August	$n = 97$
	bias ‰	RMSE ‰	bias ‰	RMSE ‰	bias ‰	RMSE ‰
Δ_{simple}	2.23	**2.11**	1.32	1.80	1.12	3.48
Δ_{comp}	0.28	2.30	-1.58	**1.50**	-0.55	3.19
$\Delta_{revised}$	0.79	2.39	-0.68	1.61	0.34	**3.15**

Table 6. Results from a sensitivity analysis assessing the variation in Δ_{ef}, the decarboxylation term in Δ_{comp}, when parameterized with $e = -6‰$ and $e = -1‰$. The uncertainty introduced into the decarboxylation term at low to high net photosynthetic rate (A) when varying e from $-6‰$ to $-1‰$ is represented in Δ_{ef} (‰). This demonstrates Δ_{ef} is very sensitive to variation in e at low A; in this study < 4% of all measurements were at $A < 2.0$ µmol m^{-2} s^{-1}.

A (µmol m^{-2} s^{-1})	Δ_{ef} (‰)	SE
< 2.00	9.40	1.51
2.00-3.99	2.64	0.04
4.00-9.15	2.21	0.01

Figure Legends

Figure 1. Diurnal variation in carbon isotope discrimination ($\bullet$; Δ_{obs}) on 12 June, 11 July, and 14 August. Error bars represent one standard error. Note change of y-axis scaling in panels.

Figure 2. Environmental parameters on each measurement day. Panels A-C depict incident photosynthetic photon flux density (PPFD) trends across each measurement day. Panels D-F show leaf temperature, as measured by energy balance ($\square$) and vapor pressure deficit (VPD; $\blacktriangledown$) across each measurement day.

Figure 3. The relationship between observed discrimination (Δ_{obs}) and net photosynthetic rate (A; **A**), leaf-to-atmosphere vapor pressure deficit (VPD; **B**), and stomatal conductance (g_s; **C**). Δ_{obs} exhibited a significant correlation with pooled leaf A ($r^2 = 0.11$, $P < 0.0001$) and VPD ($r^2 = 0.20$, $P < 0.0001$). Excluding seven high August morning values, Δ_{obs} exhibited a significant relationship with g_s ($r^2 = 0.03$, $P < 0.0001$).

Figure 4. The ratio of $^{13}CO_2$ to $^{12}CO_2$ in post-illumination nocturnal respiration ($\bullet$; $\delta^{13}C_{resp}$) on the evening of 12 June (**A**), 11 July (**B**) and 14 August (**C**). $\delta^{13}C_{resp}$ was similar in June and July ($P = 0.70$) but August was more significantly more ^{13}C depleted than in June ($P < 0.0001$) and July ($P < 0.0001$). Error bars represent one standard error.

Figure 5. Diurnal variation in internal conductance of CO_2 estimated using sloped-based methods ($\blacksquare$; g_{is}) and point-based methods ($\circ$; g_{ip}) on 12 June (**A**), 11 July (**B**), and 14

August (**C**). Internal conductance values derived from non-significant slopes ($P \geq 0.10$) on 14 August are also represented (■); all g_i estimates from 14 August were measured on one leaf area. Error bars represent one SE and are presented with grey (g_{ip}) and black (g_{is}) lines.

Figure 6. The relationship between observed discrimination (Δ_{obs}) and p_i/p_a. First order linear relationships were observed in June (**A**; $r^2 = 0.25$, $P < 0.0001$), July (**B**; $r^2 = 0.51$, $P < 0.0001$), and August (**C**; $r^2 = 0.72$, $P < 0.0001$) though 2nd order polynomial relationships better described the data in July ($r^2 = 0.64$, $P < 0.0001$) and August ($r^2 = 0.88$, $P < 0.0001$).

Figure 7. The relationship between observed discrimination (Δ_{obs}) and discrimination values predicted using $\Delta_{revised}$ (▲), Δ_{comp} (○), and Δ_{simple} (■) relative to the 1:1 Δ_{obs} line (solid line). Note: axes are unequal among panels to enhance resolution. $\Delta_{revised}$ and Δ_{comp} utilized a $b = 29‰$, while Δ_{simple} was fit with a $b = 27‰$; other parameters are listed in Table 1. Δ_{simple} exhibited the lowest overall error in predicting Δ_{obs} in June, Δ_{comp} exhibited the lowest error in July and $\Delta_{revised}$ exhibited the lowest error in August.

Figure 1.

54
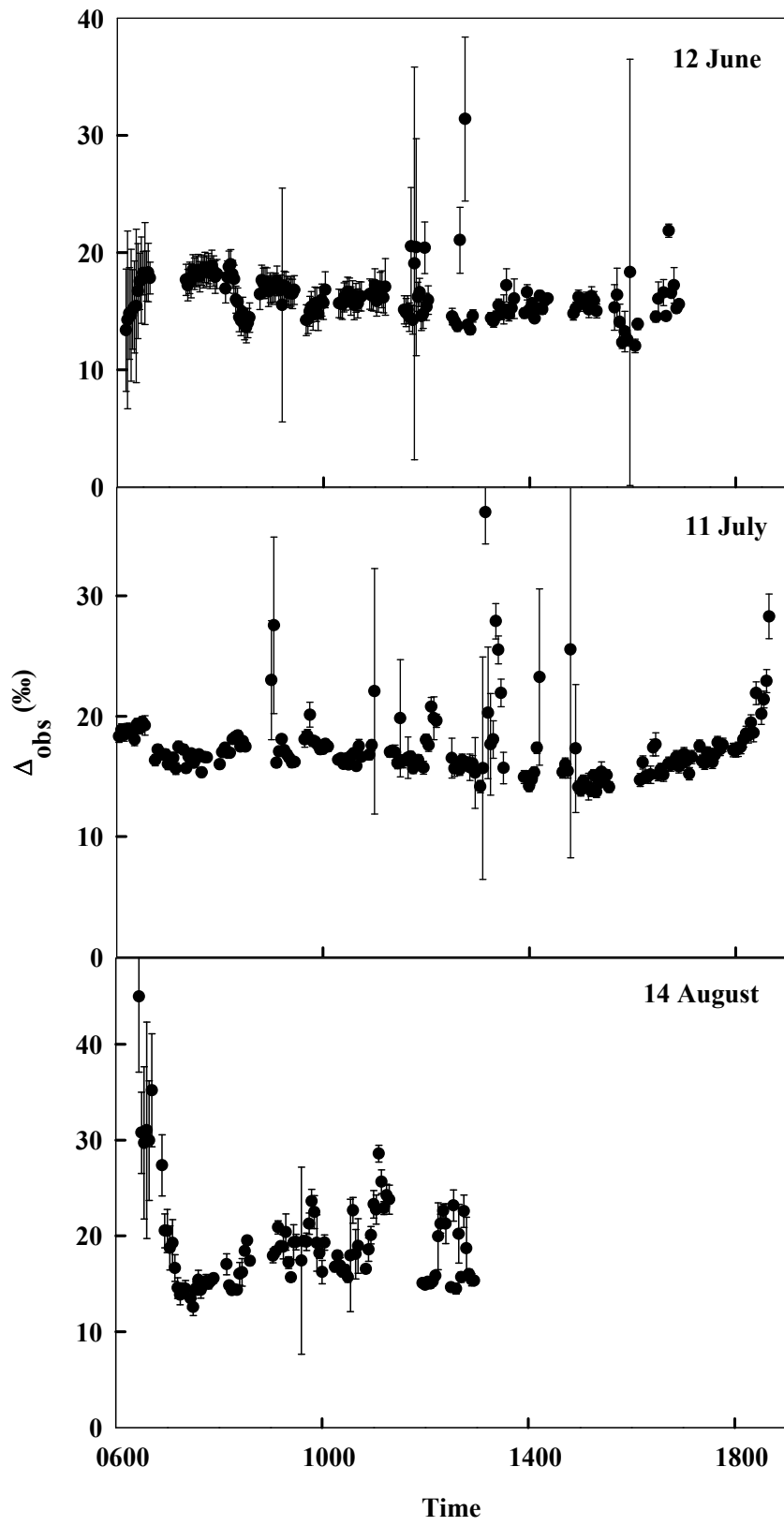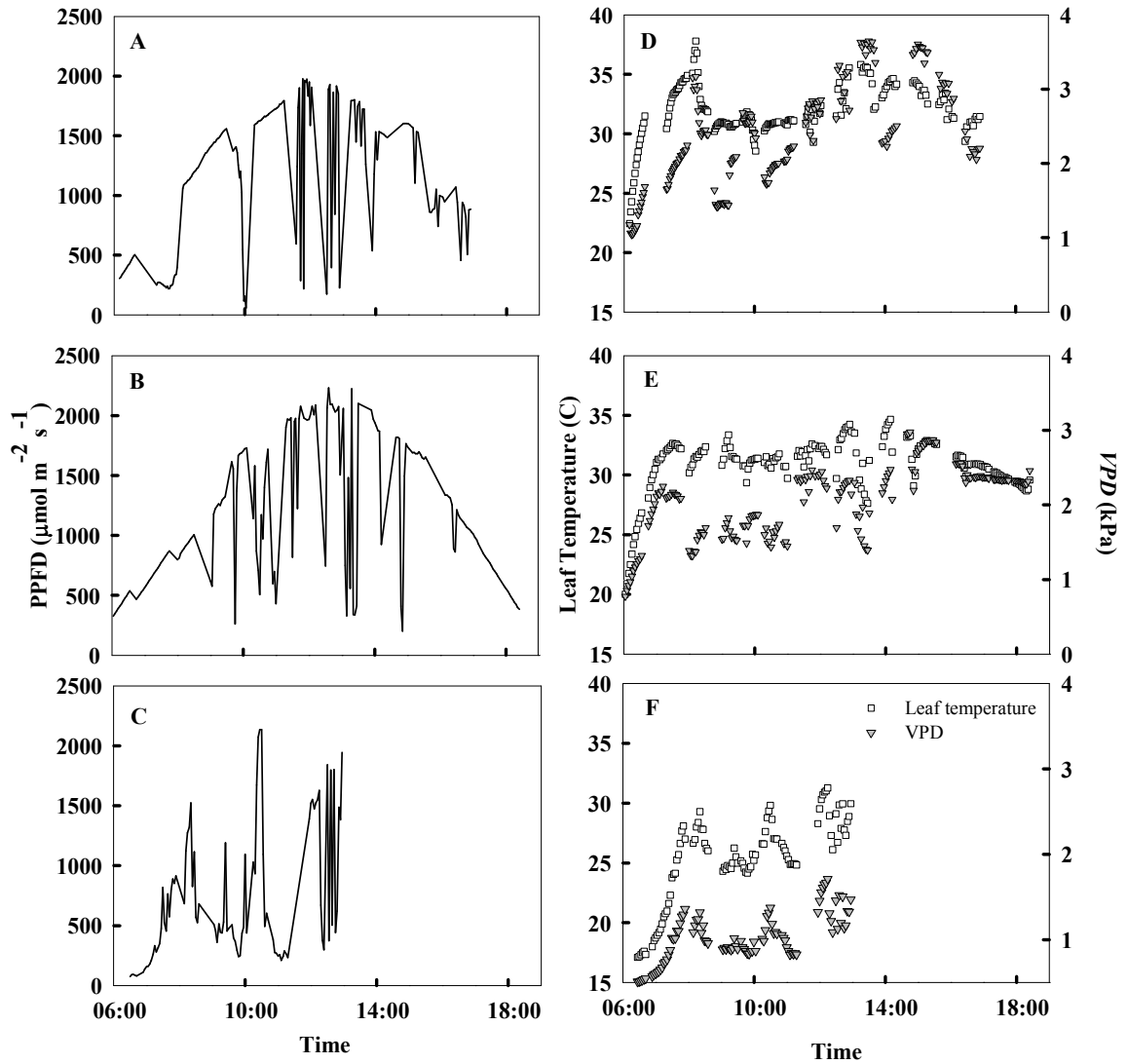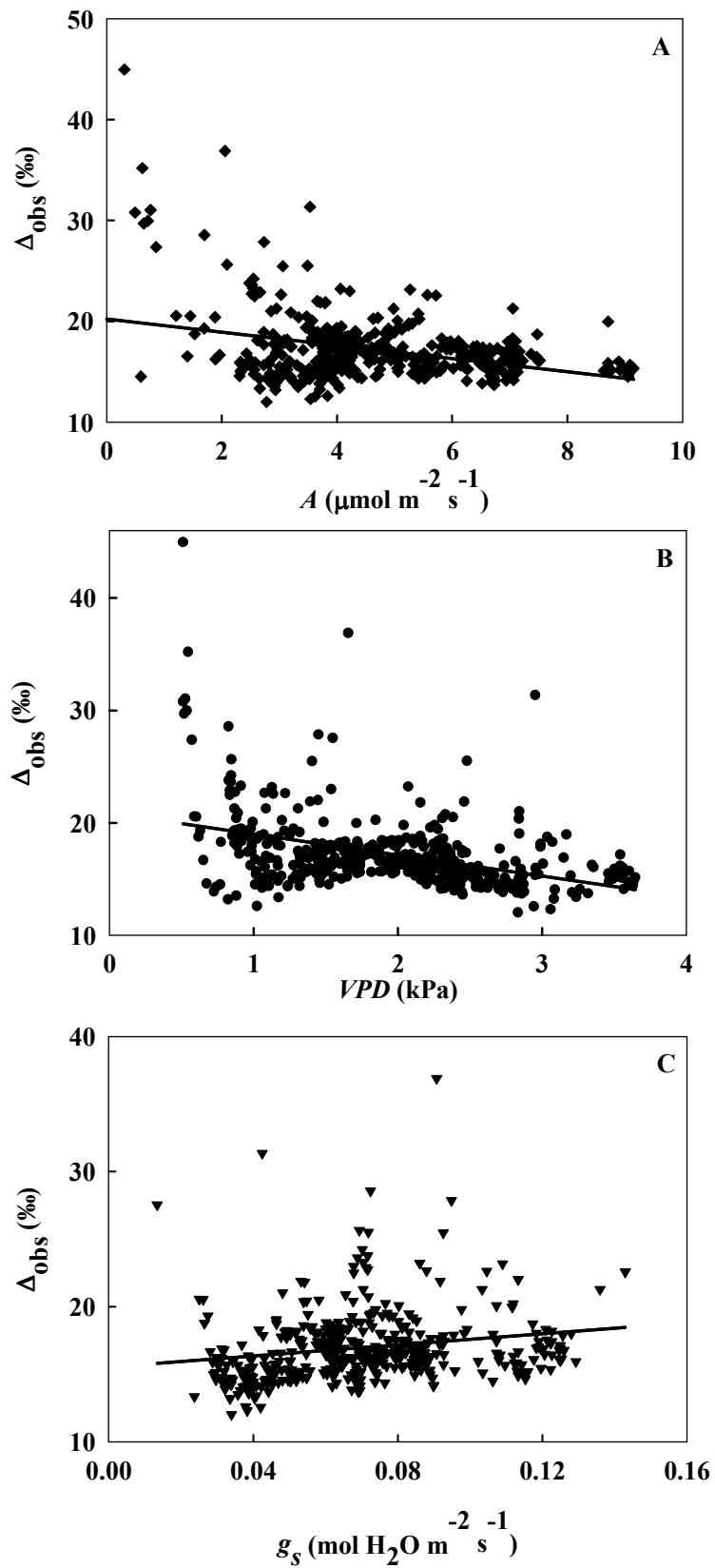
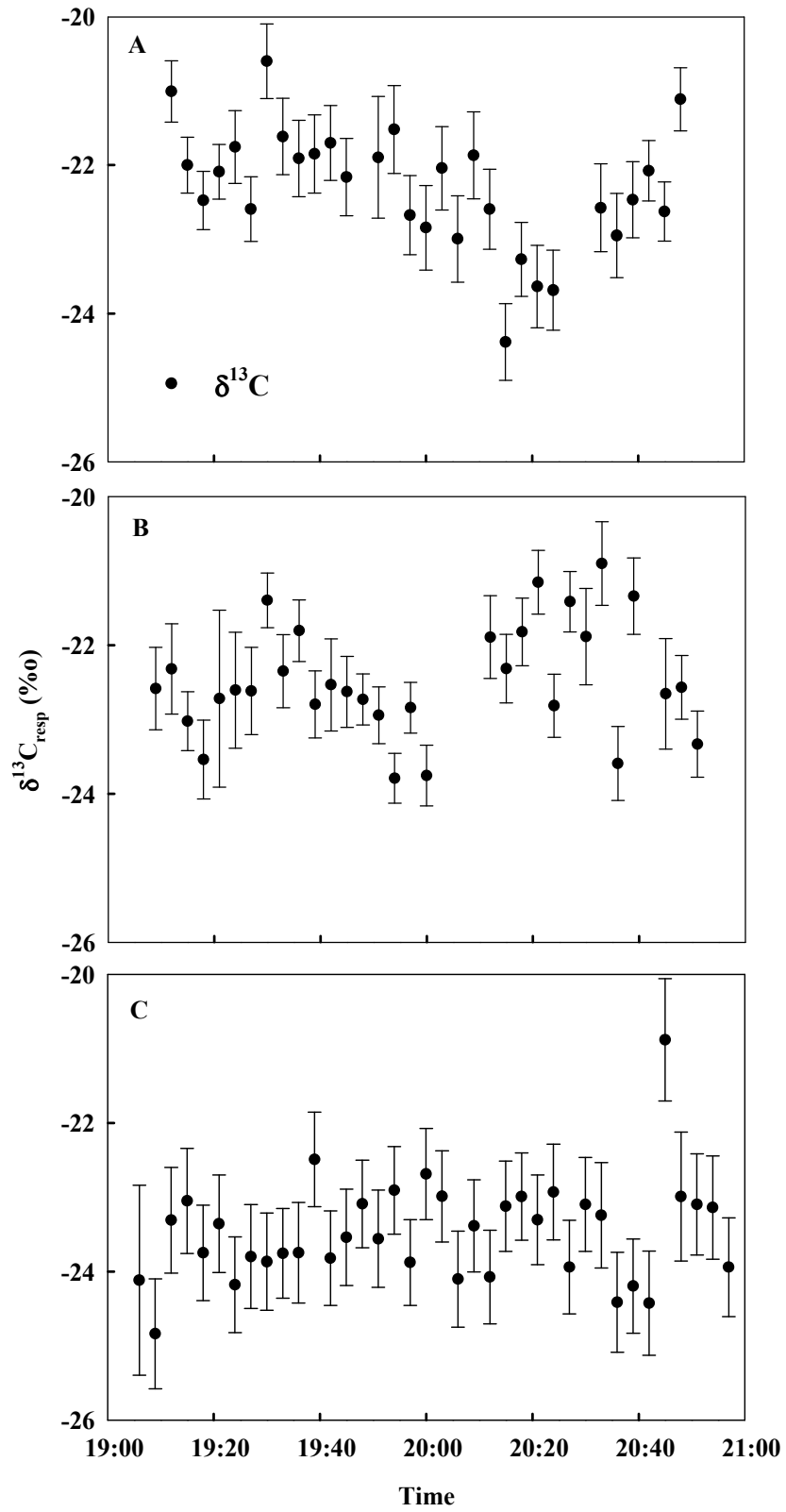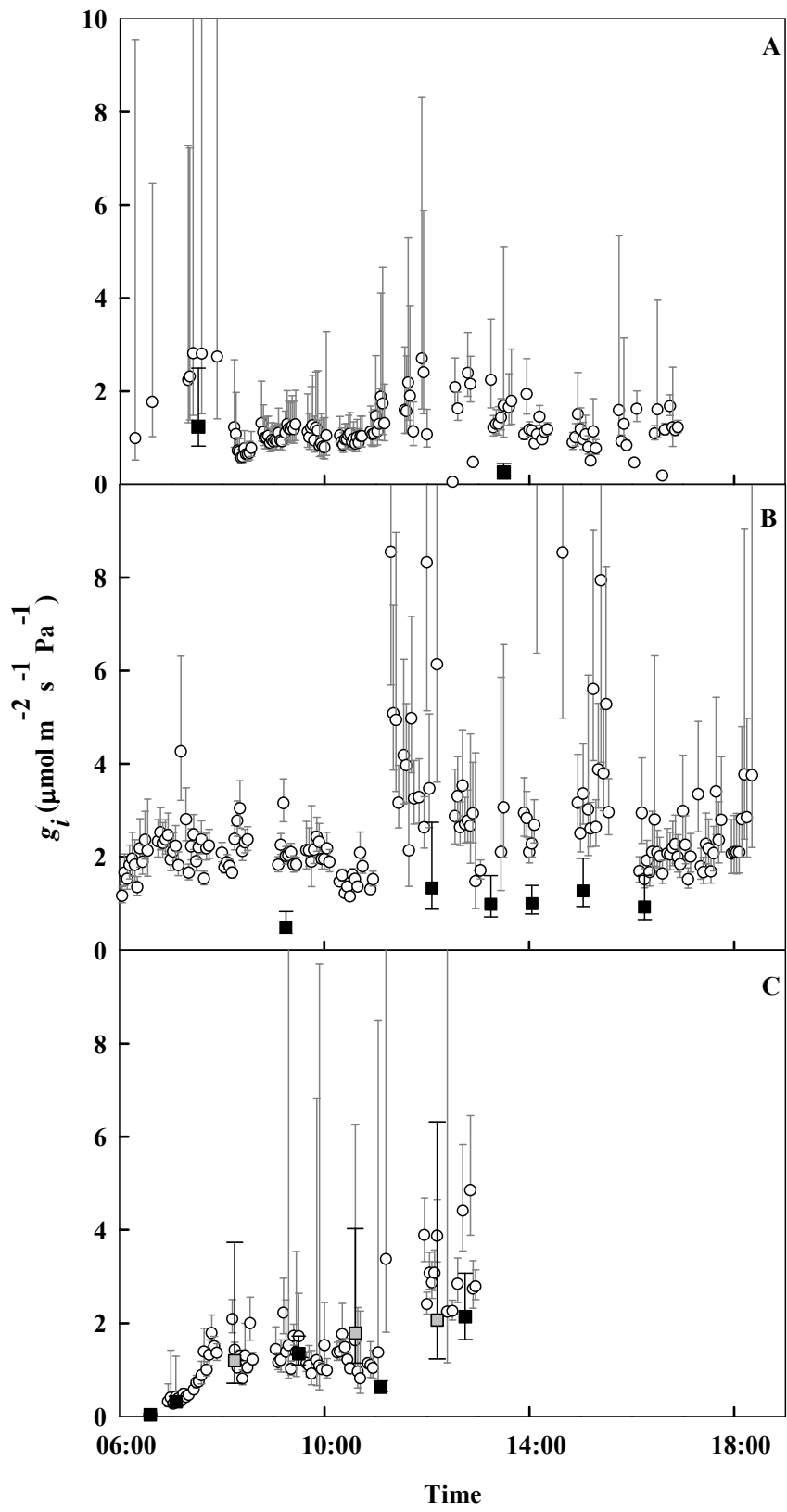**Figure 2.**

Figure 3.
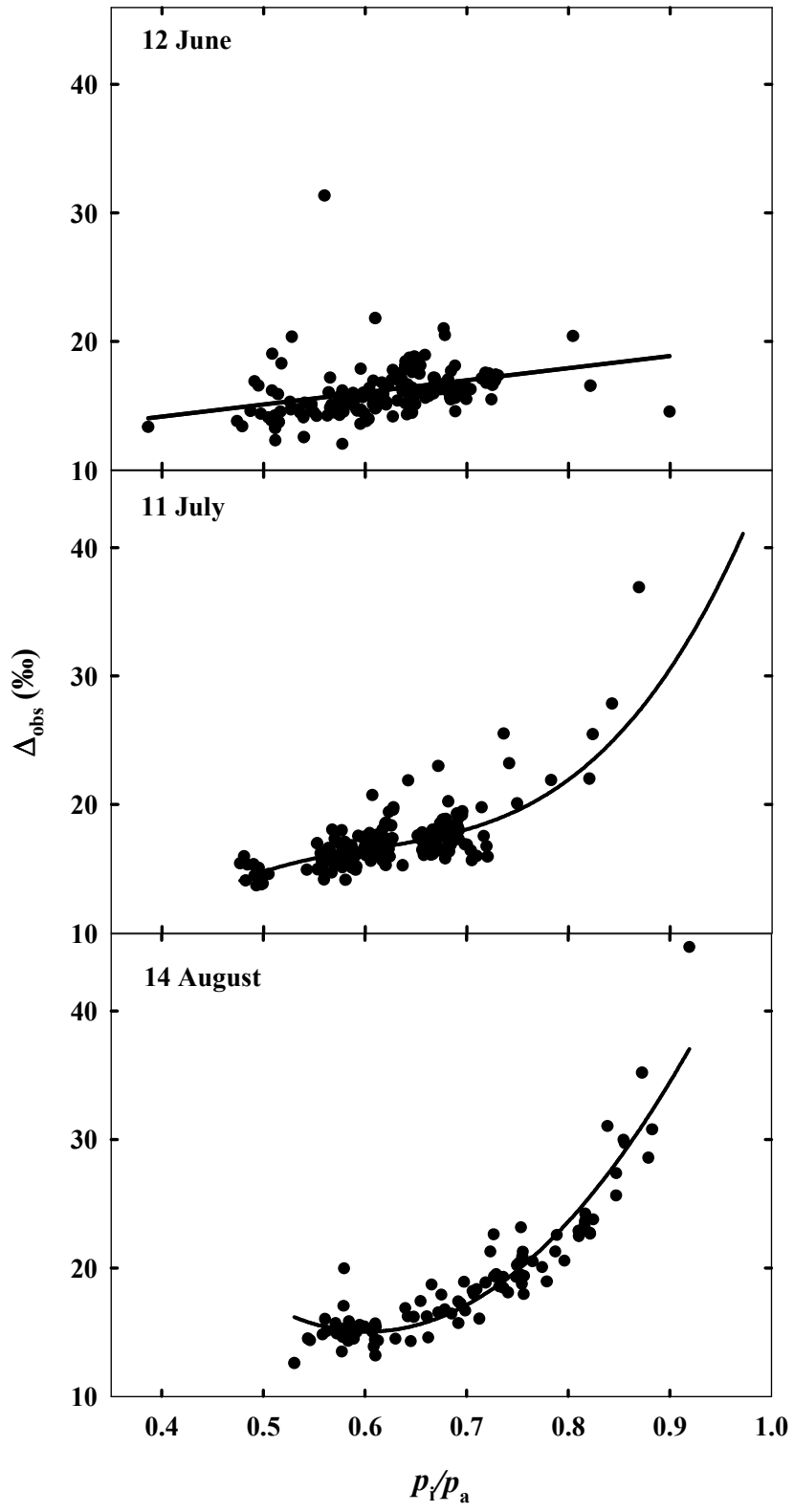
Figure 4.
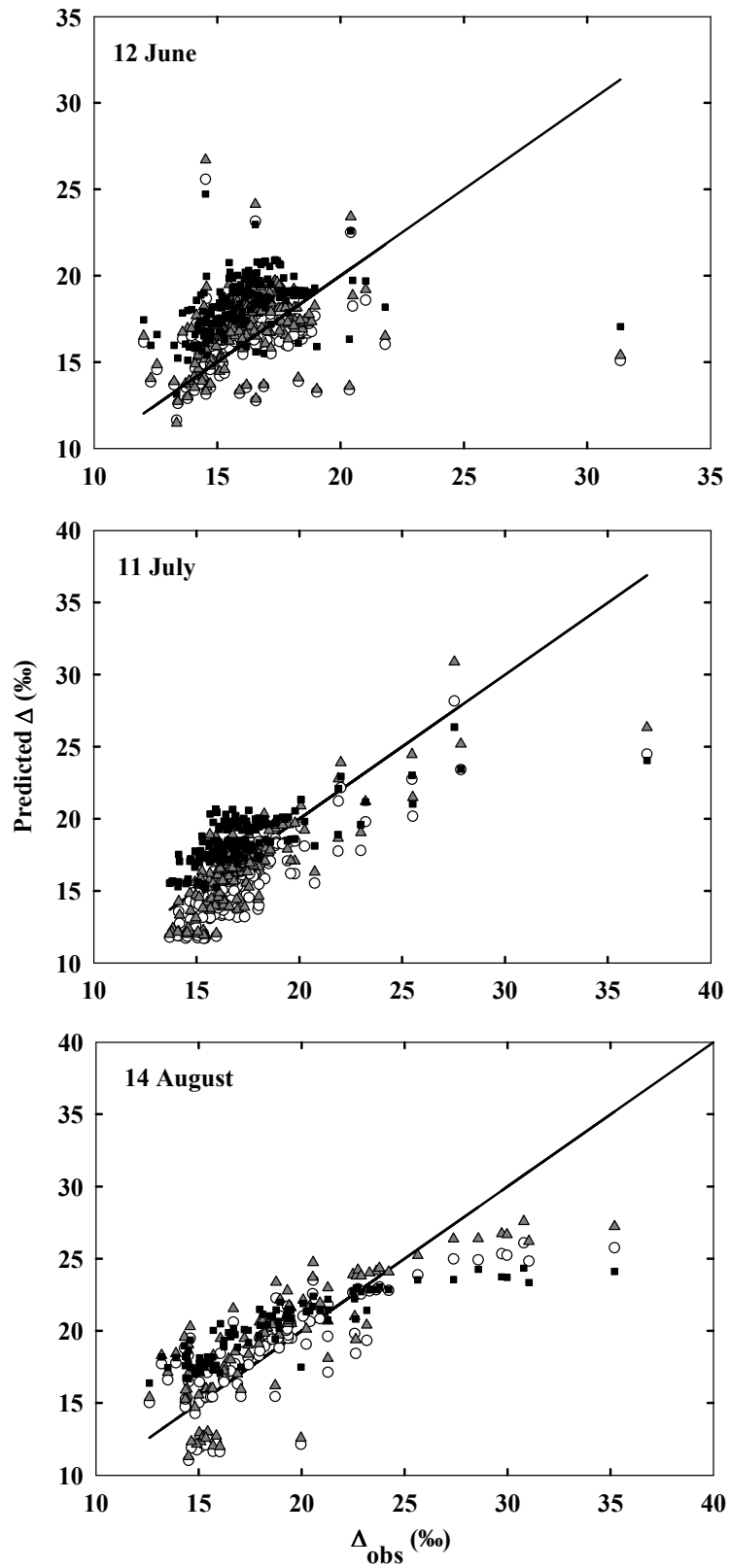
Figure 5.

Figure 6.

Figure 7.

Chapter 3

Influence of diurnal variation in internal conductance on modeled ^{13}C discrimination: results from a field study

CHRISTOPHER P. BICKFORD[1]

[1]*University of New Mexico, Department of Biology, MSC03-2020, Albuquerque, NM 87131*

Abstract

Internal CO_2 conductance (g_i) can limit carbon assimilation and influence carbon isotope discrimination (Δ) under some environmental conditions but environmental regulation of g_i is not well understood. We used high frequency field measurements to test the importance of g_i in predicting Δ using the comprehensive Farquhar, O'Leary & Berry (1982) model of Δ (Δ_{comp}) when g_i was parameterized using three different methods based on: mean g_i, the relationship between stomatal conductance (g_s) and g_i, and the relationship between time of day (*TOD*) and g_i. Incorporating mean g_i and *TOD*-based g_i improved Δ_{comp} predictions compared to the simple model of Δ (Δ_{simple}) that omits fractionation factors associated with g_i and decarboxylation, but predictions using g_s-based g_i did not outperform Δ_{simple}. Sensitivity tests suggest *b*, the fractionation due to carboxylation, was lower (24‰) than the value commonly used in Δ_{comp} (29‰). These results demonstrate the limits of Δ_{simple} while reinforcing the need for improved parameterization of Δ_{comp} by showing both g_i and *b* impact Δ and that variability in both terms should be accounted for to better predict Δ.

Introduction

Low internal CO_2 conductance from substomatal cavities to sites of carboxylation (g_i) can reduce the partial pressure of CO_2 (pCO_2) at the site of carboxylation, limit photosynthesis (*A*), and affect carbon isotope discrimination (Δ). g_i varies on numerous time-scales in response to environmental drivers, from rapid variation in response to

changes in intercellular [CO_2] (Flexas *et al.* 2007) to shifts in response to temperature (Bernacchi *et al.* 2002), water stress (Ethier & Livingston 2004), light gradients (Piel *et al.* 2002; Flexas *et al.* 2007a), and others (see Flexas *et al.* 2008 for a review). Scaling relationships between g_i and photosynthetic capacity have been shown (Evans & Caemmerer 1996; Le Roux *et al.* 2001; Ethier *et al.* 2006) and challenged (Warren & Adams 2006). Similarly, a linkage between g_i and g_s has been demonstrated (Loreto *et al.* 1992; Lauteri *et al.* 1997; Hanba *et al.* 2003; Flexas *et al.* 2002; Ethier *et al.* 2006) and is intriguing because of the potential for high frequency modeling of g_s and subsequent estimates of g_i. Internal conductance has also been recognized as an important factor influencing the $^{13}C/^{12}C$ ratio of leaf material ($\delta^{13}C_L$; Le Roux *et al.* 2001; Hanba, Kogami & Terashima 2003; Warren & Adams 2006) and ecosystem respiration ($\delta^{13}C_{resp}$; Ogée *et al.* 2003, Cai *et al.* 2008) which has implications for interpreting water use efficiency and terrestrial carbon exchange, among other applications. Δ is a strong regulator of $\delta^{13}C_L$ and $\delta^{13}C_{resp}$ (Bowling, Pataki & Randerson 2008), and therefore a better understanding of g_i in leaf-level predictions of discrimination may improve interpretation of $\delta^{13}C$ signals from multiple sources. Studies testing the role of g_i in Δ predictions are limited, but differ by showing the influence of g_i was either negligible (Wingate *et al.* 2007) or important (Le Roux *et al.* 2001; Bickford *et al.* 2009).

Δ is influenced by numerous environmental and physiological regulators and well correlated with key physiological indicators. The ratio of intercellular to ambient pCO_2 (p_i/p_a) is a physiological parameter that succinctly describes the variability in the pCO_2 gradient driven by A and stomatal conductance (g_s) and its linear relationship with Δ has been widely observed over the last three decades (Farquhar *et al.* 1982; Farquhar,

Ehleringer & Hubick 1989; Brugnoli & Farquhar 2000). p_i/p_a is integral to two models of

Δ: a comprehensive model that incorporates fractionation factors associated with

diffusion, carboxylation and decarboxylation processes (Δ_{comp}; Farquhar *et al*. 1982b) and

a simplified version of Δ_{comp} that omits fractionation factors associated with

decarboxylation activity and much of the diffusion pathway (Δ_{simple}; Farquhar *et al*.

1982b). The parsimonious Δ_{simple} evolved from the same theoretical work as Δ_{comp}

(Farquhar *et al*. 1982b) and gained wide usage primarily because of its simplicity and

power in explaining observations of Δ, but also because the effects of decarboxylation

activity and g_i were thought to be negligible in predicting Δ.

Mechanistic models are used to predict Δ across a variety of temporal and spatial

scales, where variation is driven by p_i/p_a interacting with key model parameters (Farquhar

et al. 1982b). In addition to p_i/p_a, the key drivers of Δ_{simple} include 1) the carboxylation

term, *b*, that represents net fractionation associated with phosphoenolpyruvate (PEP)

carboxylase and Ribulose-1,5-bisphosphate carboxylase/oxygenase (Rubisco), and 2) the

fractionation associated with diffusion in air and through stomata (*a*; 4.4‰) (Farquhar *et*

al. 1989). *b* is typically estimated at ~27‰ in Δ_{simple}, or ~2‰ lower than early

measurements of the full Rubisco fractionation (~29‰; Roeske & O'Leary 1984), to

account for omitted fractionation factors (Farquhar & Richards 1984). Recent work

suggests net Rubisco fractionation may be between 25-30‰ (Tcherkez & Farquhar 2005)

and gross Rubisco fractionation may be as low as 27.4‰ in tobacco (*Nicotiana tabacum*;

McNevin *et al*. 2007) while *b* is estimated to be 26‰ in *Senecio* (Lanigan *et al*. 2008).

The comprehensive mechanistic Δ model incorporates the factors discussed above

plus fractionation associated with CO_2 diffusion, including g_i, and decarboxylation

activity. As previously discussed, g_i is dynamic and may influence Δ by reducing the diffusion rate from stomatal cavities to the chloroplast. The influence of day respiration (R_d), its associated fractionation factor (e), and fractionation associated with photorespiration (f), was thought to be negligible in early studies of g_i and Δ (Evans *et al*. 1986, Caemmerer & Evans 1991) but recent evidence suggests these may be non-negligible variables (Ghashghaie *et al*. 2003), with f values ranging from ~ +7–13‰ (Tcherkez 2006, Lanigan *et al*. 2008). R_d is difficult to measure and not well understood, but existing studies demonstrate inhibition of respiration rate under illuminated conditions (Tcherkez *et al*. 2005) and biochemical differences between R_d and dark respiration (R; Tcherkez *et al*. 2008). Similarly, e is very difficult to estimate and no direct measurements currently exist in the literature. Consequently, e is frequently estimated based on the dark respiration fractionation (e_d; Ghashghaie *et al*. 2001; Tcherkez *et al*. 2003; Barbour *et al*. 2007) though the similarity, if any, of the isotope effects in R and R_d are not yet well understood (Tcherkez *et al*. 2008).

In this study we used tunable diode laser spectroscopy (*TDL*) coupled to infra-red gas analyzers (*IRGA*) to measure g_i and Δ of *Juniperus monosperma* trees at high frequency on days representative of the growing season at a high elevation semi-arid field site in 2007. The objectives of this study were to 1) measure the diurnal variation of g_i, 2) quantify the relationship between diurnal g_i and *i*) g_s and *ii*) time of day (*TOD*), 3) assess model sensitivity to variation in eR_d and b, 4) measure the diurnal variation in Δ and examine the relationship between Δ and environmental and physiological drivers and 5) assess the performance of Δ_{comp}, when fitted with diurnally variable g_i, compared to predictions from Δ_{simple}.

Methods

The study was conducted on 1 June, 20 June, 19 July, and 23 August 2007 on Mesita del Buey near Los Alamos, NM USA (elev. 2140m) at a field site described in Breshears (2008) and Bickford *et al*. (2009). Precipitation at the site was 156.2 mm between May–August 2007, but was 65.5 mm in the January–April period preceding measurements.

Leaf gas exchange measurements

We conducted two simultaneous measurements of leaf gas exchange: 1) on the crowns of three mature juniper trees ($j_{ambient}$) which we rotated through from ~0600–1800 on each day with measurements conducted maintaining the chamber environment similar to ambient conditions and, 2) on an adjacent mature juniper tree ($j_{manipulate}$) measured continuously throughout each day but subject to light manipulations. Measurements were occasionally interrupted by rainfall, and did not resume until foliage was dry. Among the three rotational trees comprising $j_{ambient}$ we measured leaf gas exchange and ^{13}C discrimination in response to ambient conditions. For both $j_{ambient}$ and $j_{manipulate}$ we engaged temperature regulation in the chamber when leaf temperature (T_L), measured by energy balance, $\geq 35°C$. We manipulated incoming irradiance in $j_{manipulate}$ by using a plastic shade to reduce incident light by ~50% one or two times per hour to regulate net photosynthetic rate (A; µmol m^{-2} s^{-1}). Shading was maintained for 15–25 minute intervals to induce sufficient variation in A within each hour across the diurnal measurement period. Natural variation in irradiance occurred during both shaded and un-shaded periods and contributed to a wide range of A. While all light manipulations were

performed on one tree ($j_{manipulate}$), we did measure different leaves over the course of each day and across the season including two on 1 June, three on 20 June, two on 19 July, and three on 23 August.

We measured leaf gas exchange by providing buffered air, via two 50L buffer volumes, to two LICOR 6400 portable photosynthesis systems (*IRGA*; LI-COR Biosciences Inc., Lincoln, NE USA); one *IRGA* was used to measure $j_{ambient}$ and the other to measure $j_{manipulate}$. Each *IRGA* was fitted with a conifer chamber (LI-COR 6400-05) and incoming and outgoing gas streams were plumbed to a *TDL* (TGA100A, Campbell Scientific Inc., Logan, UT) for measurement of the $[^{12}C^{16}O^{16}O]$ and $[^{13}CO_2]$ within each gas stream. Lines connecting each *IRGA* and the *TDL* were different lengths, resulting in different lag times, and we accounted for the 33 s and 50 s lag between the two *IRGA*'s and the *TDL* when summarizing data between the instruments. We used three minute *TDL* measurement cycles where each calibration tank (see below) was measured for 40 s, of which the last 10 s were used to calculate the means for both isotopologues, and 25 s for each of the four measurement inlets, of which the last 15 s were used for calculating concentrations. Details of the instrument coupling and measurement cycle calibration follow procedures described in Bickford *et al*. (2009).

Working standard (WS) calibration tanks spanning the range of expected $[CO_2]$ measurements used to calibrate each measurement cycle were (mean ± standard error (SE)) 548.648 ± 0.04 µmol/mol ($^{12}C^{16}O^{16}O$): 5.920 ± 0.0005 µmol/mol ($^{13}C^{16}O^{16}O$): 2.212 ± 0.0001 µmol/mol ($^{12}C^{18}O^{16}O$) for the high WS tank and 347.248 ± 0.25 µmol/mol ($^{12}C^{16}O^{16}O$): 3.747 ± 0.003 µmol/mol ($^{12}C^{16}O^{16}O$): 1.399 ± 0.001 µmol/mol ($^{12}C^{18}O^{16}O$) for the low WS tank during 1 June, 20 June, and 19 July measurements. The

[CO$_2$] of a new high WS calibration tank used in the 23 August measurements was measured as 535.972 ± 0.32 μmol/mol ($^{12}C^{16}O^{16}O$): 5.785 ± 0.003 μmol/mol ($^{13}C^{16}O^{16}O$): 2.161 ± 0.001 μmol/mol ($^{12}C^{18}O^{16}O$) while the low WS tank was the same as described above. All WS calibration tanks were calibrated for four hours monthly against WMO certified tanks that were filled and $\delta^{13}C$ calibrated at the Stable Isotope Lab of the Institute for Arctic and Alpine Research, a cooperating agency of the Climate Monitoring division of the National Oceanic and Atmospheric Administration's Earth Research Laboratory. The [CO$_2$] of the WMO traceable tanks used in this study were, for the high tank, 539.568 μmol/mol ($^{12}C^{16}O^{16}O$): 5.933 μmol/mol ($^{13}C^{16}O^{16}O$): 2.208 μmol/mol ($^{12}C^{18}O^{16}O$) and for the low tank, 339.433 μmol/mol ($^{12}C^{16}O^{16}O$): 3.764 μmol/mol ($^{13}C^{16}O^{16}O$): 1.401 μmol/mol ($^{12}C^{18}O^{16}O$). Measurements of [CO$_2$] concentration occasionally exceeded the lower span of the WS calibration tanks (maximum deviation: 42.6 μmol/mol), but post-hoc tests of the *TDL* demonstrated a linear measurement response beyond lowest the range of CO$_2$ values observed in this study (Bickford *et al.* 2009).

Predawn leaf water potential (Ψ_w) was measured using a Scholander-type pressure bomb (PMS Instruments Co., Corvallis, OR, USA) on six mature juniper trees near our study trees on 23 May, 27 June, 25 July, and 23 August 2007. Soil water content was measured at depths of 0.02–0.3m using eleven neutron probes (503DR Hydrophobe Neutron Moisture Probes, Campbell Pacific Nuclear, Inc., Pacheco, CA) at two week intervals between 23 May and 9 August 2007.

Model parameterization

We tested whether variable g_i improved model predictions of Δ_{obs} in $j_{ambient}$ using a comprehensive model of Δ (Δ_{comp}; Farquhar et al. 1982b),

$$\Delta_{comp} = a_b \frac{p_a - p_s}{p_a} + a \frac{p_s - p_i}{p_a} + (b_s + a_w) \frac{p_i - p_c}{p_a} + b \frac{p_c}{p_a} - \frac{\frac{eR_d}{k} + f\Gamma^*}{p_a} \qquad (1)$$

where a_b, a_w, and b_s represent the fractionation factors associated with CO_2 diffusion through the leaf boundary layer (2.9‰), water (0.7‰), and fractionation attributed with CO_2 entering solution (1.1‰). The variables p_a, p_s, p_i, and p_c represent pCO_2 (Pa) in the chamber surrounding the leaf, at the leaf surface, in the intercellular spaces, and at the sites of carboxylation, respectively. Γ^*, R_d, k, f, and e represent the CO_2 compensation point in the absence of day respiration (Pa), day respiration rate (μmol m^{-2} s^{-1}), carboxylation efficiency (μmol m^{-2} s^{-1} Pa^{-1}), and fractionations associated with photorespiration and day respiration (‰), respectively.

Parameters p_a, p_s, p_i, and p_c were calculated by incorporating atmospheric pressure in Los Alamos (~79 kPa) with mole fraction measurements of [CO_2]. We estimated R_d at 1.5 μmol m^{-2} s^{-1} based on reported measurements of dark respiration in juniper (Bickford et al. 2009), calculated k as A/p_c for each three minute cycle, and calculated Γ^* based on T_L (Brooks & Farquhar 1985). The photorespiratory, f, and day respiratory fractionation, e, were estimated at 11.6‰ (Lanigan et al. 2008) and $-$3‰, respectively. e has often been estimated based on the dark respiration fractionation, and previous work suggests juniper exhibits a 2-3‰ dark respiration fractionation (Bickford et al. 2009). Recent evidence demonstrates biochemical shifts between light and dark respiration that may influence the isotopic signature of respired CO_2 (Tcherkez et al. 2008), but currently there are no data in the literature providing estimates of the offset

between day and dark respiratory fractionation. Because uncertainty in e, R_d, and b could contribute to model uncertainty we tested the sensitivity of Δ_{comp} to variation in each and compared model predictions to Δ_{obs}. In these sensitivity tests Δ_{comp} was fitted with a $g_i =$ 0.71 μmol m^{-2} s^{-1} Pa^{-1} and both Δ_{comp} and Δ_{simple} were tested against all Δ_{obs} values (n = 705), where Δ_{simple} is:

$$\Delta_{simple} = a + (b - a) \cdot \frac{p_i}{p_a} \tag{2}$$

and b is equal to 27‰ to account for omitted fractionation factors (Farquhar & Richards 1984).

We parameterized g_i in Δ_{comp} in three ways for inter-model testing, calculating Δ_{comp} using g_{i1} (Δ_{comp1}), g_{i2} (Δ_{comp2}), and g_{i3} (Δ_{comp3}). All three variations of Δ_{comp} and Δ_{simple} were tested against Δ_{obs}, but Δ_{obs} values occurring outside the range of conditions of regression parameters associated with g_{i2} and g_{i3} were excluded from all inter-model comparisons (see **Results**). Model performance was evaluated using model bias and the root mean squared error (RMSE) as test statistics. Both were calculated from residuals where all models conformed to a slope of one and intercept of zero (i.e. residuals = model prediction − Δ_{obs}). The mean of these residuals represents model bias, while the standard deviation of the residuals represents the RMSE (Bickford *et al.* 2009).

Δ and Diurnal g_i

We calculated leaf carbon isotope discrimination (Δ_{obs}) from *TDL* generated data:

$$\Delta_{obs} = \frac{\xi(\delta_o - \delta_e)}{1 + \delta_o - \xi(\delta_o - \delta_e)} \tag{3}$$

where δ_e and δ_o equal the $\delta^{13}C$ of the entering and outgoing chamber gas streams,

respectively, and ξ equals $c_e/(c_e-c_o)$ and c_e and c_o are the $[CO_2]$ of the gas entering and

exiting the leaf chamber, respectively. Measurement error in Δ_{obs} was estimated

following Bickford *et al*. (2009). We estimated g_i in $j_{manipulate}$ from 40–80 minute periods

of leaf gas exchange and isotopic data using slope-based methods (Evans *et al*. 1986),

$$g_i = (b-b_s-a_w)/r_i \tag{4}$$

where r_i is the internal resistance to CO_2 diffusion and is proportional to the slope of the

linear regression between A/p_a and predicted discrimination (Δ_i) minus Δ_{obs} (Figure 1); Δ_i

is Δ_{simple} with $b = 29‰$. We determined the significance of each slope from zero (P $\leq$

0.05) using simple linear regression (SLR), and used these g_{is} estimates to quantify g_i

three ways for model testing. First we calculated a mean g_i from all g_{is} estimates (g_{i1}).

Second, we fit a SLR between time of day (*TOD*) and g_i measured within each day. On

days when a significant relationship was found between *TOD* and g_i the data were pooled

across dates, analyzed using SLR, and the resulting expression was used to estimate g_i

(g_{i2}). Thirdly, we transformed each g_i estimate expressed in partial pressure ($\mu mol\ m^{-2}\ s^{-1}$

Pa^{-1}) to a flux density (mol $CO_2\ m^{-2}\ s^{-1}$). Calculations showed incorporating partial

pressure resulted in 21.1% higher g_{is} estimates at 79 kPa so we added 21.1% to each flux

density estimate of g_i to account for underestimation due to these pressure considerations.

These transformed g_i were then compared to stomatal conductance of CO_2 (gs_{CO2}; mol

$CO_2\ m^{-2}\ s^{-1}$) data using SLR. gs_{CO2} was calculated as stomatal conductance of H_2O

(gs_{H2O}) divided by 1.6 to account for differences in diffusivity between water vapor and

CO_2 (Farquhar & Sharkey 1982). This relationship was tested to determine if slopes were

significantly different from zero (P $\leq$ 0.05; SLR) on each measurement date. The

expression resulting from all dates where there was a significant gs_{CO2}-g_i relationship was used to estimate g_i (g_{i3}). All statistical tests were performed in JMP 5.0.1 (SAS Institute Inc., Cary, NC).

Results

Diurnal g_i

g_i ranged between 0.11–1.97 µmol m^{-2} s^{-1} Pa^{-1} in $j_{manipulate}$ across the four measurement days (Figure 2). Mean g_i was different between 1 June (mean ± SE = 1.12 ± 0.65 µmol m^{-2} s^{-1} Pa^{-1}) and 20 June (0.60 ± 0.33 µmol m^{-2} s^{-1} Pa^{-1}; P = 0.04), but not between other dates (P > 0.05). There was a significant relationship between gs_{CO2} and g_i (P ≤ 0.03; Figure 3) and *TOD* and g_i (P ≤ 0.01) on 20 June and 19 July, but not on other dates. The linear expression $g_i = -0.043 + 2.455gs_{CO2}$ described the gs_{CO2}–g_i relationship (P = 0.0002, R^2 = 0.58, F = 22.22) between gs_{CO2} values of 0.02–0.06 mol CO$_2$ m^{-2} s^{-1}, thus excluding periods when gs_{CO2} fell below 0.02 mol m^{-2} s^{-1} from model testing (see *Model performance* below). The linear expression $g_i = 1.623 - 2.138TOD$ described the *TOD*–g_i relationship (P ≤ 0.0001, R^2 = 0.74, F = 45.02) across the day between 06:00–17:00, excluding time periods beyond 17:00 on 1 June from model testing (see *Model performance* below). Linear slopes used to estimate g_i showed strong relationships between $\Delta_i - \Delta_{obs}$ and A/p_a (Table 1, Figure 1).

Δ_{obs}, physiological, and environmental parameters

Mean Δ_{obs} in $j_{ambient}$ was 14.3 ± 0.2‰ on 1 June, 16.3 ± 0.2‰ on 20 June, 17.6 ± 0.4‰ on 19 July, and 15.4 ± 0.3‰ on 23 August. Δ_{obs} was similar on the 20 June and 23 August

measurement dates (Tukey's Honestly Significant Differences (HSD), P > 0.05) but was

significantly different on all other dates (P < 0.0001; Figure 4). When pooled across

months physiological parameters exhibited significant but weak linear relationships with

Δ_{obs} including A (P < 0.0001, R^2 = 0.22, F = 194.81), g_s (P < 0.0001, R^2 = 0.03, F =

20.30), and p_i/p_a (P < 0.0001, R^2 = 0.26, F = 247.46) (Figure 5). One measurement date,

19 July, showed a curvilinear trend between Δ_{obs} and p_i/p_a that was better described by a

second order polynomial (P < 0.0001, R^2 = 0.84, F = 380.18) compared to a linear

regression (P < 0.0001, R^2 = 0.71, F = 338.97) (data not shown). We attribute the diffuse

pattern seen at higher p_i/p_a (> 0.7) to variation among measured trees (data not shown). A

was not significantly different between dates (Tukey's HSD, P > 0.05; Table 2); g_s was

similar on 20 June and 19 July, but was different on all other days (P ≤ 0.05; Table 2).

There were weak but significant relationships between Δ_{obs} and T_L on 1 June (P =

0.02, R^2 = 0.04, F = 8.92) and 19 July (P = 0.01, R^2 = 0.05, F = 6.81) but not other dates

(P ≥ 0.05). Similarly, there were weak but significant relationships between Δ_{obs} and VPD

on each day (P ≤ 0.04), but not when VPD data were pooled across months (P = 0.06, R^2

= 0.005). VPD was significantly higher on 1 June and lower on 23 August compared to

other days (Tukey's HSD, P ≤ 0.05), but was similar on remaining days (P > 0.05; Table

2). Finally, there was a weak but significant linear relationship between Δ_{obs} and PPFD

across all dates (P < 0.0001, R^2 = 0.09), but a second order polynomial better described

the relationship (P < 0.0001, R^2 = 0.25). Soil water content at 200mm over the study

period ranged from a high of 19.2% on 23 May to a low of 12.0% on 25 July, before

recovering to 13.9% on 9 August. Ψ_w measured in nearby juniper trees (n = 6) ranged

between −0.62 ± 0.06 (23 May) and −3.4 ± 0.33 MPa (25 July), before increasing to

−2.75 ± 0.34 MPa (23 August). The relationship between Ψ_w and Δ_{obs} was not significant ($P = 0.15$, $R^2 = 0.75$).

Model performance

The performance of Δ_{comp} and its comparison to Δ_{simple} varied depending on how g_i was parameterized. To facilitate model comparison all periods of gs_{CO2} or *TOD* outside the range of parameterization for g_{i2} and g_{i3} were excluded from all four models during testing (n = 137 Δ_{comp} values removed, n = 568 used in each Δ_{comp} and Δ_{simple} analysis; see *Diurnal g_i* above). As determined by lowest RMSE, Δ_{comp1} and Δ_{comp2} performed better than Δ_{comp3} and Δ_{simple} throughout the study. Δ_{comp1} performed best on 20 June and 19 July and Δ_{comp2} performed best on 1 June and 23 August (Table 3). Δ_{comp3} showed lower error than Δ_{simple} on all days after 1 June (Table 3; Figure 7). Model predictions were also pooled across the whole study and compared to pooled Δ_{obs} data. Among pooled data Δ_{comp1} and Δ_{comp2} still exhibited relatively lower error than Δ_{comp3} and Δ_{simple} (Table 3), though model bias was higher in Δ_{comp1} (bias = 3.45‰ vs. 3.27‰ for Δ_{comp2}; Table 3). A primary conclusion from Table (3) is that all models consistently over-predicted Δ by at least 1‰.

Sensitivity tests showed reduced model bias and RMSE when eR_d and b were set to low values (compare Tables 3 and 4). Model bias increased 60% and error decreased 7.4% as eR_d shifted from more positive (−1‰) to more negative (−9‰) values when b was 29‰. Across tested eR_d values the use of lower b values in Δ_{comp} consistently reduced model bias and error. Δ_{simple} showed a 94% reduction in model bias and 1.6% reduction in error when fit with $b = 22$‰ instead of $b = 27$‰ (Table 4). Excluding 19

July, all variations of Δ_{comp} and Δ_{simple} overestimated Δ_{obs} by 2–6‰, as determined by model bias, though accounting for the variance, as in the RMSE term, reduced total error to between 1.0–2.4‰ on individual days. The pooled data were skewed by the high bias and error in the 23 August data but reveal better performance by Δ_{simple} than seen on individual dates, including modest improvement in model error compared to Δ_{comp3}. Using RMSE as the metric, the best fit to Δ_{obs} was found using Δ_{comp} with $eR_d = -9‰$ and $b = 24‰$.

Discussion

Diurnal g_i

Two diurnal g_i trends were evident across the study. On 1 June g_i increased through most of the morning period to relatively high values (~2 μmol m^{-2} s^{-1} Pa^{-1}) and then decreased in the afternoon period. This trend of low to high g_i over the early morning to mid-day period resembles previous observation of diurnal g_i in juniper (Bickford *et al.* 2009). Predawn Ψ_w was relatively high during both periods, and higher leaf water status may have contributed to the morning increase. In the other three days, however, a different pattern was observed: the highest g_i (~1 μmol m^{-2} s^{-1} Pa^{-1}) was observed in the early morning, with a linear decline across two of the three days (Fig. 2). On 23 August the decline occurs in the morning, with g_i stabilizing around ~0.5 μmol m^{-2} s^{-1} Pa^{-1} for the remainder of the day. The diurnal decline in g_i is consistent with previous work showing reduced g_i under water stressed conditions (Warren, Livingston & Turpin 2004; Flexas *et al.* 2004), however, the range of Ψ_w seen during this period of the study would be characterized as moderate water stress in juniper (Linton, Sperry & Williams 1998;

McDowell *et al.* 2008). g_i was significantly related to g_s and *TOD* on two of four days.

The predictive power of the g_i-*TOD* could likely be improved by accounting for variation

in the early evening time period. Below g_s of ~0.035 mol CO_2 m^{-2} s^{-1} g_i was limiting CO_2

transfer to the sites of carboxylation; most g_s measurements were above 0.035 mol CO_2

m^{-2} s^{-1} and thus stomatal limitations often provided the greatest diffusion resistance. Our

findings agree with the strong g_s-g_i relationship among 15 species shown by Loreto *et al.*

(1992), where g_i was $1.4g_s$, and in *Nicotaina* (Galmes *et al.* 2006), but differ from data in

other species showing generally lower g_i compared to g_s (Hanba *et al.* 2003). Our g_s-g_i

data deviate from the 1:1, likely due to different regulatory processes between stomatal

and internal conductance to CO_2, but others have observed nearly 1:1 g_s-g_i relationships

(Lauteri *et al.* 1997).

Δ, environmental & physiological parameters

Diurnal patterns across the study were consistent with previous studies showing

environmental regulation of Δ_{obs}. As previously observed in model and empirical studies

VPD and PPFD acted as environmental drivers of Δ (Baldocchi & Bowling 2003; Chen

& Chen 2007; McDowell *et al.* 2008b; Bickford *et al.* 2009), likely through their strong

influence on *A* and g_s. Ψ_w co-varied with Δ, decreasing when Δ was increasing from 1

June to 19 July, and Δ decreased when Ψ_w again increased in August. Δ was comparable

to previous observations in juniper during the same months in 2006, but was lower on 23

August (Bickford *et al.* 2009). Predawn Ψ_w was substantially more negative in August

2007 (−2.75 MPa) compared to August 2006 (−0.58 MPa; McDowell *et al.* 2008b) and

may have contributed to the seasonal Δ pattern. The non-significant relationship between Ψ_w and mean Δ_{obs} was likely due to low sample size (n=4).

The variation in the physiological parameters A, g_s and p_i/p_a was correlated with Δ_{obs}. Δ_{obs} was generally higher when A was low and g_s and p_i/p_a were high (Figure 5). Conversely, Δ_{obs} tended to be lower when A was high and p_i/p_a was low. A large range of Δ_{obs} was seen at low g_s, consistent with previous work showing relatively high Δ when g_s and A are low (Bickford *et al*. 2009). It is likely that isotopic measurements indicating moderate to high Δ_{obs} (~25–35‰) occurring at low g_s (< 0.05 mol m^{-2} s^{-1}) are being more strongly influenced by respiratory and/or photorespiratory activity (Bickford *et al*. 2009).

Model performance

Overall Δ_{comp} performed best in predicting Δ_{obs} when fitted with g_{i1} and g_{i2}, while Δ_{comp3} and Δ_{simple} produced poorer predictions of Δ_{obs} (Table 3), and supports recent work showing improved model fit when including g_i in model predictions versus using simpler models (Cai *et al*. 2008; Bickford *et al*. 2009). Our results demonstrate no substantial improvement when using Δ_{comp2} compared to Δ_{comp1}, indicating the validity of using a mean g_i value to predict juniper Δ over the diurnal periods and across the seasonal gradient in this study. This finding supports previous work showing improved model fit when utilizing a mean g_i in Δ_{comp} across diurnal and seasonal timescales (Bickford *et al*. 2009), but contrasts with recent evidence showing improved model predictions of respired $\delta^{13}C$ values when g_i was linked to variation in g_s compared to using a static g_i in model predictions (Cai *et al*. 2008). The discrepancy between our observation of diurnal shifts in g_i and the null effect of incorporating this variability into model predictions may

be due to the use of a mean g_i that was high enough so that resistance in the diffusion

pathway was minimized to an extent that did not substantially effect model predictions.

Alternatively, our model assessment method may have lacked sufficient sensitivity to

discern improvements brought about by using Δ_{comp2}. The predictive performance of

Δ_{simple} and Δ_{comp3} was similar enough that their performance ranking varied depending on

the temporal scale of the analysis, with Δ_{comp3} showing lower error on most days but

Δ_{simple} outperforming when data were pooled across the whole study. This shows that

improper parameterization can override the expected predictive advantage of Δ_{comp} and

produce inferior results compared to a more parsimonious model. Model bias was

relatively high on most days (Figure 6), particularly 23 August, and in the pooled data

(Table 3), showing all models consistently overestimated Δ_{obs}. The most likely reason for

this is model parameterization error (discussed below in our sensitivity analysis). Viewed

from the whole study perspective there was lower model bias and error in Δ_{comp1} and

Δ_{comp2} compared to Δ_{simple}, supporting the use of a carefully parameterized Δ_{comp} for leaf-

level predictions of Δ.

Sensitivity tests showed that, in addition to g_i, variation in eR_d and b improved

model performance. Lowering eR_d resulted in reduced error for a given b value, but

consistently increased model bias. Step-change reductions in b from the value we used

(29‰), however, resulted in consistently lower model bias and error. Two factors could

explain these findings, namely that the fractionation associated with b is lower than has

been reported until recently or that R_d was higher and e more negative than we estimated.

The simultaneous reduction in model bias and error we observed when reduced b values

were implemented suggests b is the stronger regulator of model performance, but without

assays of PEP and Rubisco activity only limited conclusions can be made. A lower b could be explained by relatively high PEP carboxylation activity proportional to Rubisco activity (Farquhar & Richards 1984; Lanigan *et al*. 2008) or a lower intrinsic isotope effect of the carboxylases comprising b (Raven & Farquhar 1990; Brugnoli & Farquhar 2000). PEP carboxylation is typically associated with C_4 photosynthesis and results in low discrimination against ^{13}C ($\sim -5.7‰$; Farquhar *et al*. 1989), but the extent of PEP carboxylase activity in C_3 photosynthesis is not well understood. Alternatively, the influence of respiratory activity may have been higher than we estimated in this study. We based our estimates on previous work showing high dark respiration rate, which we used as a surrogate estimator of R_d, and a 2–3‰ dark respiration fractionation in juniper (Bickford *et al*. 2009). Error may have been introduced if R_d was subject to diurnal variation we did not account for, or if a substantial offset exists between e and the dark respiration fractionation. Recent evidence shows the day and dark respiratory biochemical pathways are not the same, and may result in different isotopic fractionation (Tcherkez *et al*. 2008), however the magnitude of the difference is not yet understood.

Δ_{simple} was less sensitive to variation in b compared to Δ_{comp}, but sensitivity tests demonstrated variability in b may be greater than currently assumed. Previous studies using Δ_{simple} have shown b values < 27‰ resulting in the best fit of observed Δ (Brugnoli & Farquhar 2000), and this is usually attributed to the reduced b value accounting for omitted fractionation factors. We tested Δ_{comp} and Δ_{simple} with the same Δ_{obs} dataset, however, and found improvement in both models when lower b values were used, supporting the use of species specific b values in Δ_{comp} to improve model predictions. Further studies of the net carboxylation fractionation in other groups of higher plants (i.e.

conifers and deciduous woody species) are needed to better understand variation in *b*.
Overall, the results of our model tests and sensitivity analysis show non-negligible model
error in predicting leaf Δ, but suggest better understanding and incorporation of the
variability in key parameters such as g_i, *b*, *e*, and R_d may aid in more accurate and precise
model fits. In the interim, modelers interested in predicting diurnal Δ across seasonal and
annual time scales and at larger organizational scales should consider the relative
sensitivity of Δ_{comp} to proper parameterization versus results from the parsimonious
Δ_{simple}.

Acknowledgements

References

Baldocchi DD, Bowling D.R. 2003. Modelling the discrimination of $^{13}CO_2$ above and
within a temperate broad-leaved forest canopy on hourly to seasonal times scales. *Plant,
Cell and Environment* **26:** 231-244.

Barbour MM, McDowell NG, Tcherkez G, Bickford CP, Hanson DT. **2007.** A new
measurement technique reveals rapid post-illumination changes in the carbon isotope
composition of leaf-respired CO_2. *Plant, Cell and Environment* **30:** 469-482.

Bernacchi CJ, Portis AR, Nakano H, von Caemmerer S, Long SP. **2002.**
Temperature response of mesophyll conductance. Implications for the determination of
rubisco enzyme kinetics and for limitations to photosynthesis in vivo. *Plant Physiology*
130: 1992-1998.

Bickford CP, McDowell NG, Erhardt EB , Hanson DT. **2009.** High frequency field
measurements of carbon isotope discrimination and internal conductance in a semi-arid

species, *Juniperus monosperma. Plant, Cell and Environment*.

Bowling DR, Pataki DE, Randerson JT. **2008.** Carbon isotope in terrestrial ecosystem pools and CO_2 fluxes. *New Phytologist Tansley Review* **178**: 24-40.

Breshears DD. **2008.** Structure and function of woodland mosaics: consequences of patch-scale heterogeneity and connectivity along the grassland-forest continuum. In: O. W. Van Auken, ed. *Western North American Juniperus Woodlands- A Dynamic Vegetation Type*. Springer, 58-92.

Brooks A, Farquhar GD. **1985.** Effect of temperature on the CO_2/O_2 specificity of ribulose-1,5-bisphosphate carboxylase/oxygenase and the rate of respiration in the light. *Planta* **165:** 397-406.

Brugnoli E, Farquhar GD. **2000.** Photosynthetic fractionation of carbon isotopes. In: Leegood RC, Sharkey TD, von Caemmerer S, eds. *Photosynthesis: Physiology and Metabolism*. The Netherlands: Kluwer Academic, 399-434.

Cai T, Flanagan LB, Jassal RS, Black TA. **2008.** Modelling environmental controls on ecosystem photosynthesis and the carbon isotope composition of ecosystem-respired CO_2 in a coastal Douglas-fir forest. *Plant, Cell and Environment*: **31**: 435-453.

Chen B, Chen JM. **2007.** Diurnal, seasonal and interannual variability of carbon isotope discrimination at the canopy level in response to environmental factors in a boreal forest ecosystem. *Plant, Cell and Environment* **30:** 1223-1239.

Ethier G.J., Livingston N.J. 2004. On the need to incorporate sensitivity to CO_2 transfer conductance into the Farquhar-von Caemmerer-Berry leaf photosynthesis model. *Plant, Cell, and Environment* **27:** 137-153.

Ethier G.J., Livingston N.J., Harrison D.L., Black T.A., Moran J.A. 2006. Low stomatal and internal conductance to CO_2 versus Rubisco deactivation as determinants of the photosynthetic decline of ageing evergreen leaves. *Plant, Cell and Environment* **29:** 2168-2184.

Evans JR, Sharkey TD, Berry JA, Farquhar GD. **1986.** Carbon isotope discrimination measured concurrently with gas exchange to investigate CO_2 diffusion in leaves of higher plants. *Australian Journal of Plant Physiology* **13:** 281-292.

Evans JR, von Caemmerer S. **1996.** Carbon dioxide diffusion inside leaves. *Plant Physiology* **110:** 339-346.

Farquhar GD, Ball MC, Caemmerer S, Roksandic Z. **1982.** Effect of salinity and humidity on $\delta^{13}C$ value of halophytes—Evidence for diffusional isotope fractionation determined by the ratio of intercellular/atmospheric partial pressure of CO_2 under different environmental conditions. *Oecologia* **52:** 121-124.

Farquhar GD, Ehleringer JR, Hubick KT. **1989.** Carbon isotope discrimination and

photosynthesis. *Annual Review of Plant Physiology and Plant Molecular Biology* **40:** 503-537.

Farquhar GD, Richards RA. **1984.** Isotopic composition of plant carbon correlates with water-use efficiency of wheat genotypes. *Australian Journal of Plant Physiology* **11:** 539-552.

Farquhar GD, O'Leary MH, Berry JA. **1982.** On the relationship between carbon isotope discrimination and the intercellular carbon dioxide concentration in leaves. *Australian Journal of Plant Physiology* **9:** 121-137.

Farquhar GD, Sharkey TD. **1982.** Stomatal conductance and photosynthesis. *Annual Review of Plant Physiology* **33:** 317-345.

Flexas J, Bota J, Loreto F, Cornic G, Sharkey TD. **2004.** Diffusive and metabolic limitations to photosynthesis under drought and salinity in C_3 plants . *Plant Biology* **6:** 269-279.

Flexas J, Bota J, Escalona JM, Sampol B, Medrano H. **2002.** Effects of drought on photosynthesis in grapevines under field conditions: an evaluation of stomatal and mesophyll limitations. *Functional Plant Biology* **29:** 461-471.

Flexas J, Diaz-Espejo A, Galmčs J , Kaldenhoff R, Medrano H, Ribas-Carbo M. **2007.** Rapid variations of mesophyll conductance in response to changes in CO_2 concentration around leaves. *Plant, Cell and Environment* **30:** 1284-1298.

Flexas J, Ribas-Carbo M, Diaz-Espejo A, Galmes J, Medrano H. **2008.** Mesophyll conductance to CO_2: current knowledge and future prospects. *Plant, Cell and Environment* **31**: 602-621.

Galmes J, Medrano H, Flexas J. **2006.** Acclimation of Rubisco specificity factor to drought in tobacco: discrepancies between *in vitro* and *in vivo* estimations. *Journal of Experimental Botany* **57 :** 3659-3667.

Ghashghaie J, Duranceau M, Badeck F-W, Cornic G, Adeline M-T, Deleens E . **2001.** $\delta^{13}C$ of CO_2 respired in the dark in relation to $\delta^{13}C$ of leaf metabolites: comparison between *Nicotiana sylvestris* and *Helianthus annuus* under drought. *Plant, Cell and Environment* **24:** 505-515.

Ghashghaie J, Badeck FW, Lanigan G, Nogues S, Tcherkez G, Deleens E, Cornic G, Griffiths H. **2003.** Carbon isotope fractionation during dark respiration and photorespiration in C_3 plants. *Phytochemistry Reviews* **2:** 145-161.

Hanba YT, Kogami H, Terashima I. **2003.** The effect of internal CO_2 conductance on leaf carbon isotope ratio. *Isotopes in Environmental Health Studies* **39:** 5-13.

Lanigan GJ, Betson N, Griffiths H, Seibt U. **2008.** Carbon isotope fractionation during photorespiration and carboxylation in *Senecio*. *Plant Physiology* **148:** 2013-2020.

Lauteri M, Scartazza A, Guido MC, Brugnoli E. **1997.** Genetic variation in photosynthetic capacity, carbon isotope discrimination and mesophyll conductance in provenances of *Castanea sativa* adapted to different environments. *Functional Ecology* **11:** 675-683.

Le Roux X, Bariac T, Sinoquet H, Genty B, Piel C, Mariotti A, Girardin C, Richard P. **2001.** Spatial distribution of leaf water-use efficiency and carbon isotope discrimination within an isolated tree crown. *Plant, Cell and Environment* **24:** 1021-1032.

Linton MJ, Sperry JS, Williams DG. **1998.** Limits to water transport in *Juniperus osteosperma* and *Pinus edulis*: implications for drought tolerance and regulation of transpiration. *Functional Ecology* **12:** 906-911.

Loreto F, Harley PC, Di Marco G, Sharkey TD. **1992.** Estimation of mesophyll conductance to CO_2 flux by three different methods. *Plant Physiology* **98:** 1437-1443.

McDowell N, Baldocchi D., Barbour M, Bickford C., Cuntz M., Hanson D., Knohl A., Powers H., Rahn T., Randerson J., Riley W., Still C., Tu K., Walcroft A. 2008. Understanding the stable isotope composition of biosphere-atmosphere CO_2 exchange. *Eos* **89:** 94-95.

McDowell NG, Pockman WT, Allen C, Breshears DD, Cobb N, Kolb T, Plaut J, Sperry J, West A, Williams D, Yepez EA. **2008.** Mechanisms of plant survival and mortality during drought: Why do some plants survive while others succumb to drought? *New Phytologist Tansley Review* **178**: 719-739.

McNevin DB, Badger MR, Whitney SM, von Caemmerer S, Tcherkez GGB, Farquhar GD. **2007.** Differences in carbon isotope discrimination of three variants of D-Ribulose-1,5-bisphosphate carboxylase/oxygenase reflect differences in their catalytic mechanisms. *Journal of Biological Chemistry* **282:** 36068-36076.

Ogee J, Peylin P, Ciais P, Bariac T, Brunet Y, Berbigier P, Roche C, Richard P, Bardoux G, Bonnefond J-M. **2003.** Partitioning net ecosystem carbon exchange into net assimilation and respiration using $^{13}CO_2$ measurements: a cost-effective sampling strategy. *Global Biogeochemical Cycles* **17:** 1070-1070.

Piel C, Frak E, Le Roux X, Genty B. **2002.** Effect of local irradiance on CO_2 transfer conductance of mesophyll in walnut. *Journal of Experimental Botany* **53:** 2423-2430.

Raven JA, Farquhar GD. **1990.** The influence of N metabolism and organic acid synthesis on the natural abundance of isotopes of carbon in plants. *New Phytologist* **116:** 505-529.

Roeske CA, O'Leary MH. **1984.** Carbon isotope effects on the enzyme-catalyzed carboxylation of ribulose bisphosphate . *Biochemistry* **23:** 6275-6284.

Tcherkez Guillaume. **2006.** How large is the carbon isotope fractionation of the

photorespiratory enzyme glycine decarboxylase? *Functional Plant Biology* **33:** 911-920.

Tcherkez G, Bligny R, Gout E, Mahe A, Hodges M, Cornic G. **2008.** Respiratory metabolism of illuminated leaves depends on CO_2 and O_2 conditions. *Proceedings of the National Academy of Science* **105:** 797-802.

Tcherkez G, Cornic G, Bligny R, Gout E, Ghashghaie J. **2005.** In vivo respiratory metabolism of illuminated leaves. *Plant Physiology* **138:** 1596-1606.

Tcherkez G, Farquhar GD. **2005.** Carbon isotope effect predictions for enzymes involved in the primary carbon metabolism of plant leaves. *Functional Plant Biology* **32:** 277-291.

Tcherkez G, Nogues S, Bleton J, Cornic G, Badeck F, Ghashghaie J. **2003.** Metabolic origin of carbon isotope composition of leaf dark-respired CO_2 in French bean. *Plant Physiology* **131:** 237-244.

von Caemmerer S, Evans JR. **1991.** Determination of the average partial pressure of CO_2 in the chloroplasts from leaves of several C_3 plants. *Australian Journal of Plant Physiology* **18:** 287-305.

Warren CR, Livingston NJ, Turpin DH. **2004.** Water stress decreases the transfer conductance of Douglas-fir (*Pseudotsuga menziesii*) seedlings. *Tree Physiology* **24:** 971-979.

Warren CR, Adams MA. **2006.** Internal conductance does not scale with photosynthetic capacity: implications for carbon isotope discrimination and the economics of water and nitrogen use in photosynthesis. *Plant, Cell and Environment* **29**: 192-201.

Wingate L, Seibt U, Moncrieff JB, Jarvis PG, Lloyd J. **2007.** Variations in ^{13}C discrimination during CO_2 exchange by *Picea sitchensis* branches in the field. *Plant, Cell and Environment* **30**: 600-616.

Tables

Table 1. Correlation coefficients and *P* values from the linear regressions used to calculate all slopes for estimation of internal CO_2 conductance across each measurement day.

01 June			20 June			19 July			23 August		
time	R^2	*P*	time	R^2	*P*	time	R^2	*P*	time	R^2	*P*
7:00	0.68	< 0.0001	7:00	0.32	0.005	6:30	0.68	< 0.0001	6:30	0.63	< 0.0001
9:00	0.54	0.0001	8:00	0.36	0.006	8:00	0.60	< 0.0001	7:30	0.80	< 0.0001
10:00	0.32	0.0091	9:00	0.71	< 0.0001	9:00	0.52	0.0005	8:30	0.76	< 0.0001
11:00	0.66	< 0.0001	10:00	0.76	< 0.0001	10:00	0.75	< 0.0001	9:30	0.72	< 0.0001
15:30	0.32	0.0234	11:00	0.76	< 0.0001	11:00	0.75	< 0.0001	10:30	0.64	< 0.0001
16:30	0.36	0.0047	12:00	0.59	< 0.0001	12:00	0.67	0.001	11:30	0.84	0.0006
18:00	0.55	0.0015	13:00	0.47	0.001	15:30	0.78	< 0.0001	13:30	0.60	< 0.0001
			14:30	0.56	0.0001	16:00	0.68	0.002	14:30	0.91	< 0.0001
			15:30	0.63	0.001						
			16:30	0.55	0.0003						

Table 2. Mean diurnal net photosynthetic rate (A; μmol m^{-2} s^{-1}), stomatal conductance to

H$_2$O (g_s; mol m^{-2} s^{-1}), and vapor pressure deficit (VPD; kPa), each reported with one

standard error (SE) and sample size (n). A was not different across dates (P > 0.05); g_s

and VPD were both different on 1 June and 23 August (P < 0.05) from all other days, but

20 June and 19 July were not different from one another (P > 0.05).

	A	**SE**	*g*$_s$	**SE**	*VPD*	**SE**	*n*
01-June	3.87	0.11	0.05	0.002	3.04	0.04	230
20-June	3.73	0.12	0.06	0.002	2.26	0.04	180
19-July	3.92	0.13	0.06	0.002	2.30	0.05	159
23-August	4.15	0.13	0.11	0.002	1.34	0.05	158

Table 3. Results from model prediction tests of observed discrimination (Δ_{obs}). Δ_{simple} represents the simplified model of discrimination and Δ_{comp} represents the comprehensive model of discrimination, with different forms of Δ_{comp} indicating parameterization with different internal conductance (g_i) values. Here Δ_{comp1} uses a seasonal mean g_i value of 0.71 μmol m^{-2} s^{-1} Pa^{-1}, Δ_{comp2} uses g_i derived from a regression describing the relationship between g_i and time of day, and Δ_{comp3} uses g_i calculated based on the regression between g_i and stomatal conductance of CO_2. Model bias (‰) ranged between 1.0–6.75‰ and error (RMSE; ‰) ranged from 1.0–2.4‰ across individual measurement dates, but showed reduced variation in the whole study assessment. Assessed monthly and across the whole study Δ_{comp1} and Δ_{comp2} best predicted Δ_{obs}. Δ_{comp3} outperformed Δ_{simple} on individual days, but Δ_{simple} outperformed Δ_{comp3} across the whole study. Bolded values highlight the best performing model in each month and across the study.

Model	1 June		20 June		19 July		23 August		Whole study	
	bias	RMSE	bias	RMSE	bias	RMSE	bias	RMSE	bias	RMSE
Δ_{comp1}	2.54	1.32	2.94	**1.68**	1.09	**1.87**	6.75	2.01	3.45	**2.70**
Δ_{comp2}	2.32	**1.03**	2.67	1.72	0.91	1.91	6.70	**1.90**	3.27	2.72
Δ_{comp3}	2.56	1.26	2.84	1.79	1.01	2.04	6.67	2.30	3.39	2.80
Δ_{simple}	3.65	1.09	3.25	1.96	1.56	2.48	6.72	2.35	3.88	2.75

Table 4. Results from sensitivity tests where the parameters representing the day respiration fractionation (e; ‰), day respiration rate (R_d; µmol m^{-2} s^{-1}), and fractionation during carboxylation (b) were adjusted in the comprehensive model of carbon discrimination (Δ_{comp}; eq. 1), and b was adjusted in the simplified version of carbon discrimination (Δ_{simple}; eq. 2). g_i was held constant at 0.71 µmol m^{-2} s^{-1} Pa^{-1}; all other variables are as described in *Model parameterization*. More negative eR_d and/or lower b values reduced Δ_{comp} model bias (‰) and root mean squared error (RMSE; ‰) when compared to observed discrimination (Δ_{obs}). Similarly, lower b values reduced Δ_{simple} model bias and RMSE when compared to Δ_{obs}.

eR_d	Δ_{comp} b (‰)	bias	RMSE	Δ_{simple} b (‰)	bias	RMSE
	29	2.43	2.99			
-1	27	1.15	2.93	27	3.47	3.01
	24	-0.76	2.87			
	29	3.16	2.82			
-4.5	27	1.88	2.74	24	1.5	2.97
	24	-0.03	2.65			
	29	4.09	2.77			
-9	27	2.82	2.66	22	0.19	2.96
	24	0.9	2.52			

Figures captions

Figure 1. Regression slopes of the relationship of predicted discrimination (Δ_i) minus observed discrimination (Δ_{obs}) in relationship to the ratio of net photosynthetic rate (A) to the partial pressure of CO_2 in the atmosphere surrounding the leaf (p_a) used to estimate the internal CO_2 conductance. See Table 1 for P values and correlation coefficients associated with each slope.

Figure 2. Diurnal variation in internal CO_2 conductance (g_i) across the four measurement dates. g_i was significantly different between 1 June and 20 June ($P < 0.05$), but not between other dates.

Figure 3. The relationship between stomatal conductance to CO_2 (g_{sCO2}) and internal CO_2 conductance (g_i) on 20 June and 19 July. g_{sCO2} and g_i data on each date were tested for significance ($P \leq 0.05$, simple linear regression); significant relationships were pooled and the regression used to estimate g_i based on g_{sCO2} when g_{sCO2} was > 0.02 mol m^{-2} s^{-1}.

Figure 4. Diurnal variation in carbon isotope discrimination (Δ;●) and photosynthetic photon flux density (PPFD;○) on the four measurement dates. Error bars represent one SE. The abrupt shifts in Δ mid-day on 1 June can be attributed to variation among trees, but variation seen on other dates results from plant environmental response. There was a significant relationship between PPFD and Δ best described by a second order polynomial ($P < 0.0001$, $R^2 = 0.25$)

Figure 5. The relationship between observed discrimination (Δ_{obs}) and net photosynthetic rate (A), stomatal conductance to H_2O (g_s), and the ratio of partial pressure of CO_2 in intercellular spaces and the environment around the leaf (p_i/p_a). When pooled across months these parameters exhibited significant linear relationships with Δ_{obs} including A ($P < 0.0001$, $R^2 = 0.22$), g_s ($P < 0.0001$, $R^2 = 0.03$), and p_i/p_a ($P < 0.0001$, $R^2 = 0.26$).

Figure 6. Model tests of observed discrimination (Δ_{obs}). Four models were tested against Δ_{obs} including the simple model of discrimination (Δ_{simple}; ●), the comprehensive model of discrimination using a mean internal CO_2 conductance (g_i) of 0.71 μmol m^{-2} s^{-1} Pa^{-1} (Δ_{comp1}; ●), the comprehensive model of discrimination using a g_i estimated from the regression between diurnal g_i and time of day (TOD) (Δ_{comp2}; □), and the comprehensive model of discrimination using a g_i estimated from the regression describing the relationship between stomatal conductance of CO_2 and g_i (Δ_{comp3}; ▲). $\Delta_{predicted}$ represents discrimination predictions of any of the four models. In individual months and across the whole study Δ_{comp1} and Δ_{comp2} performed best, exhibiting lower model bias and error than either Δ_{comp3} or Δ_{simple}. These results support the use of a mean g_i value or g_i based on TOD in Δ_{comp} to predict diurnal carbon discrimination.
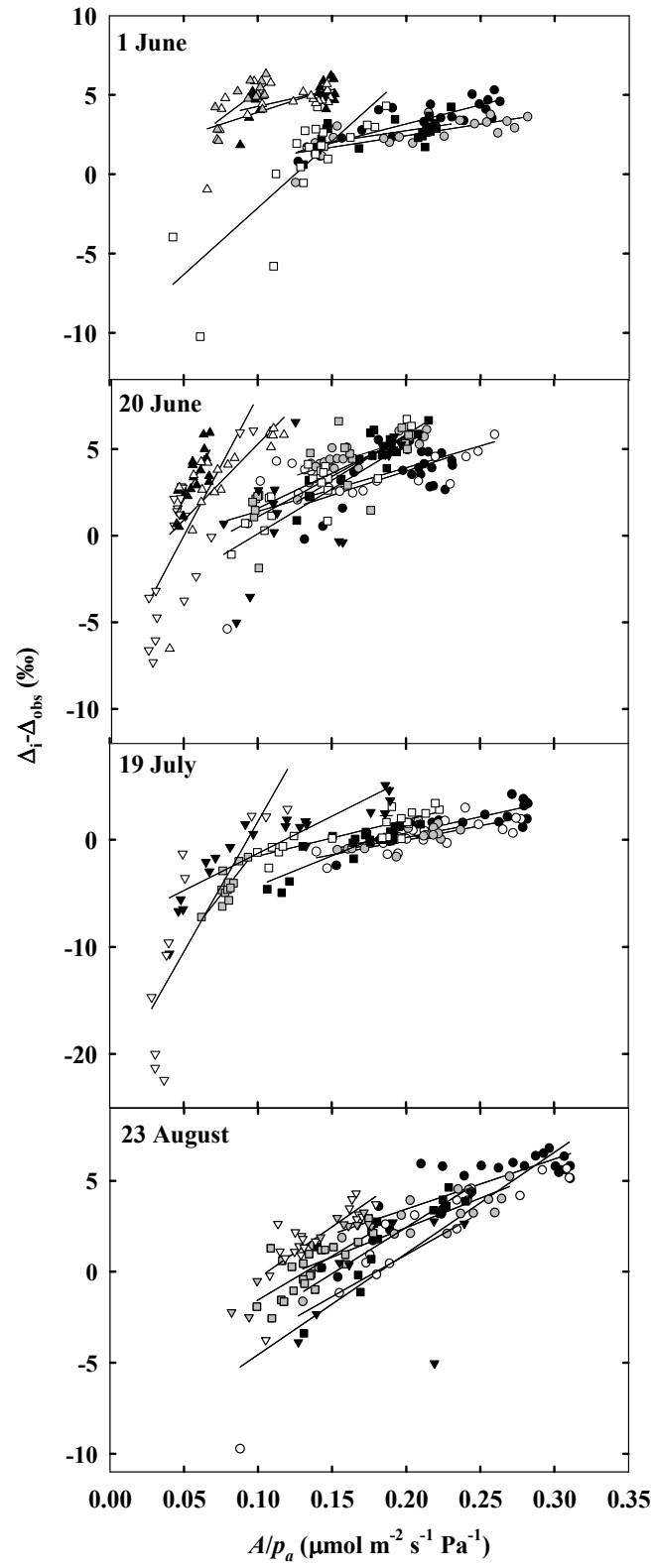
Figure 1.
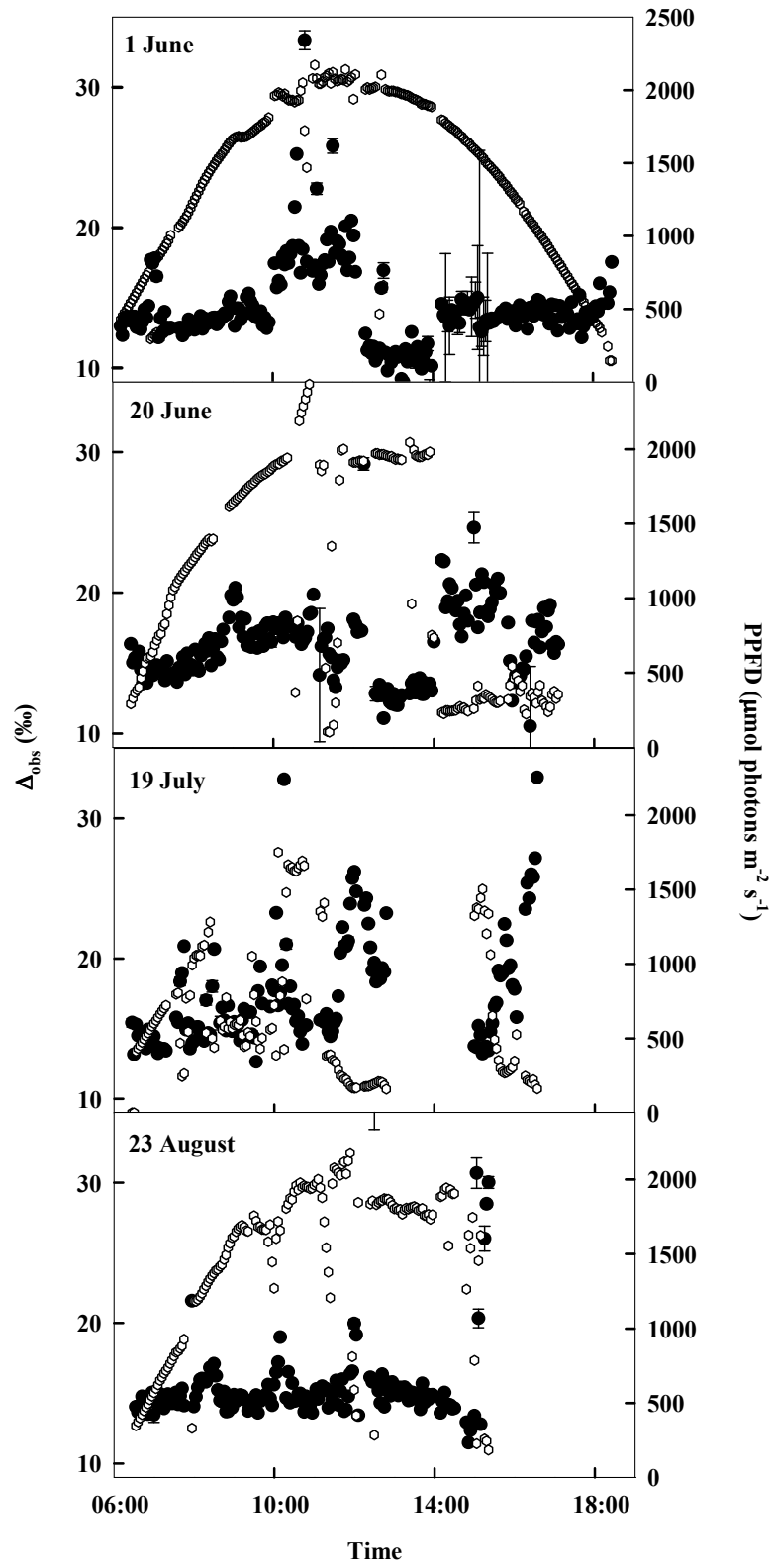
91
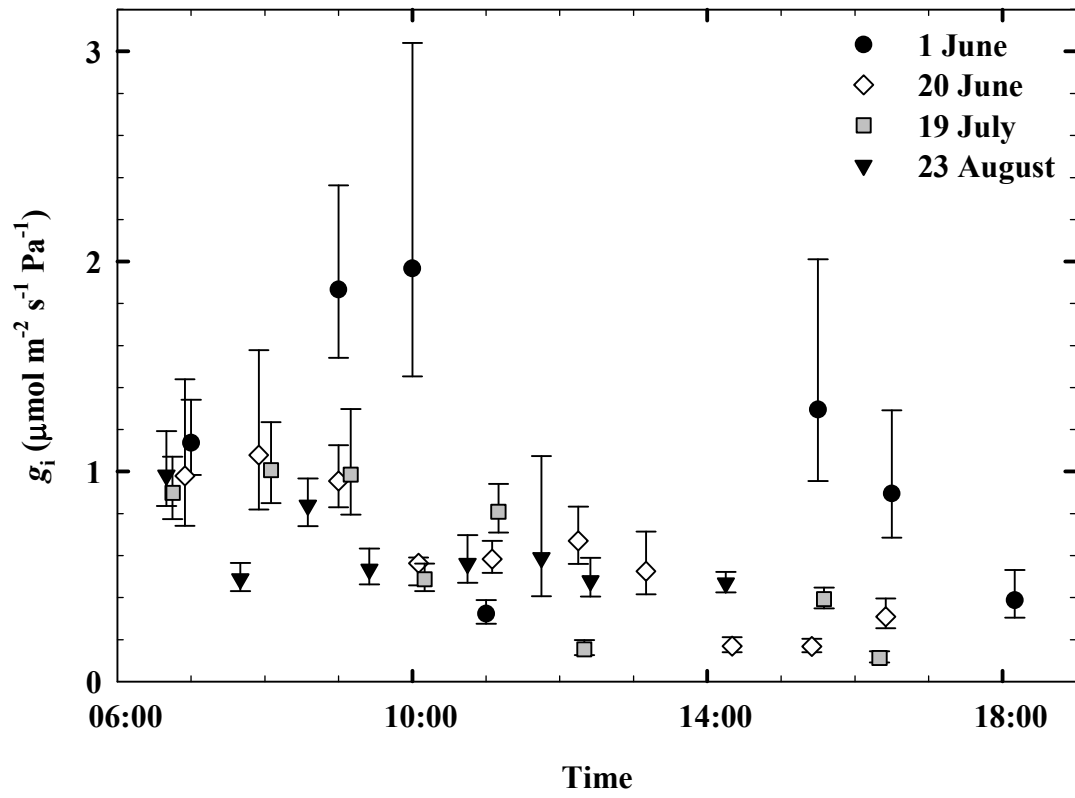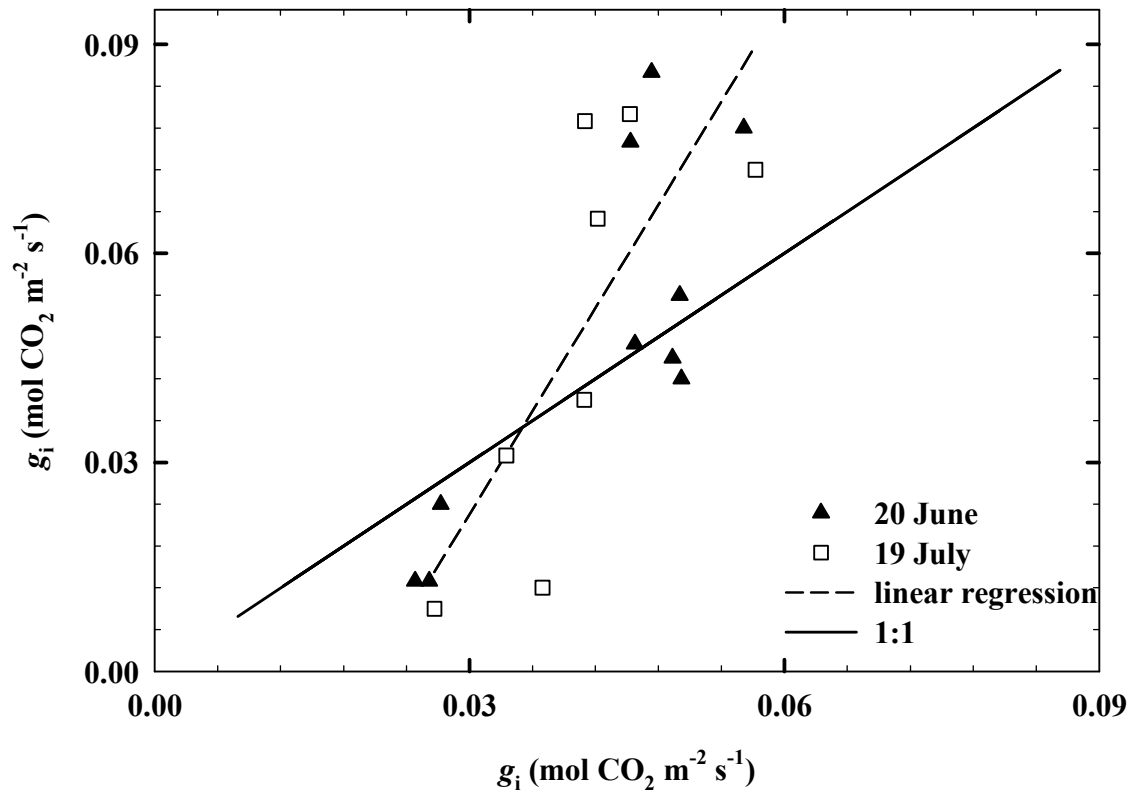
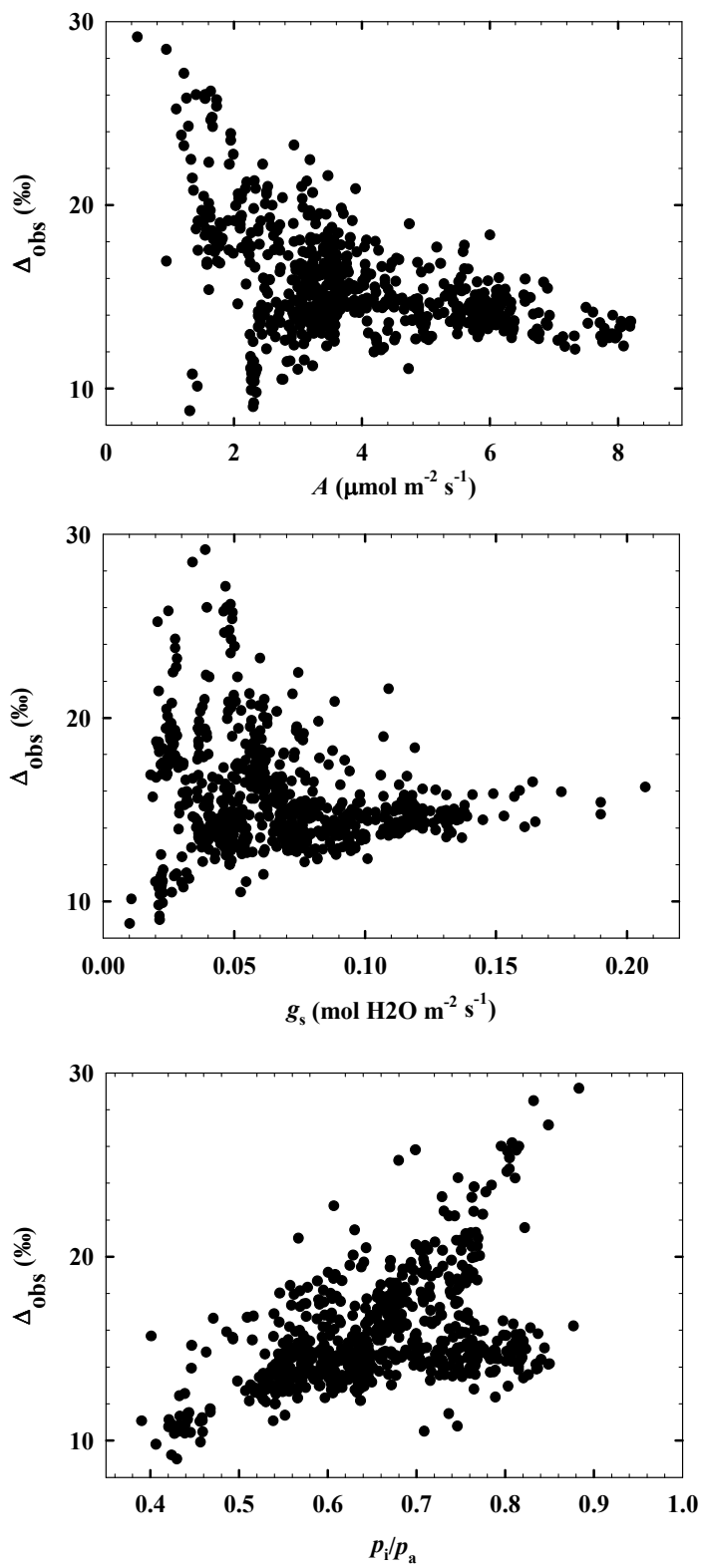**Figure 2.**
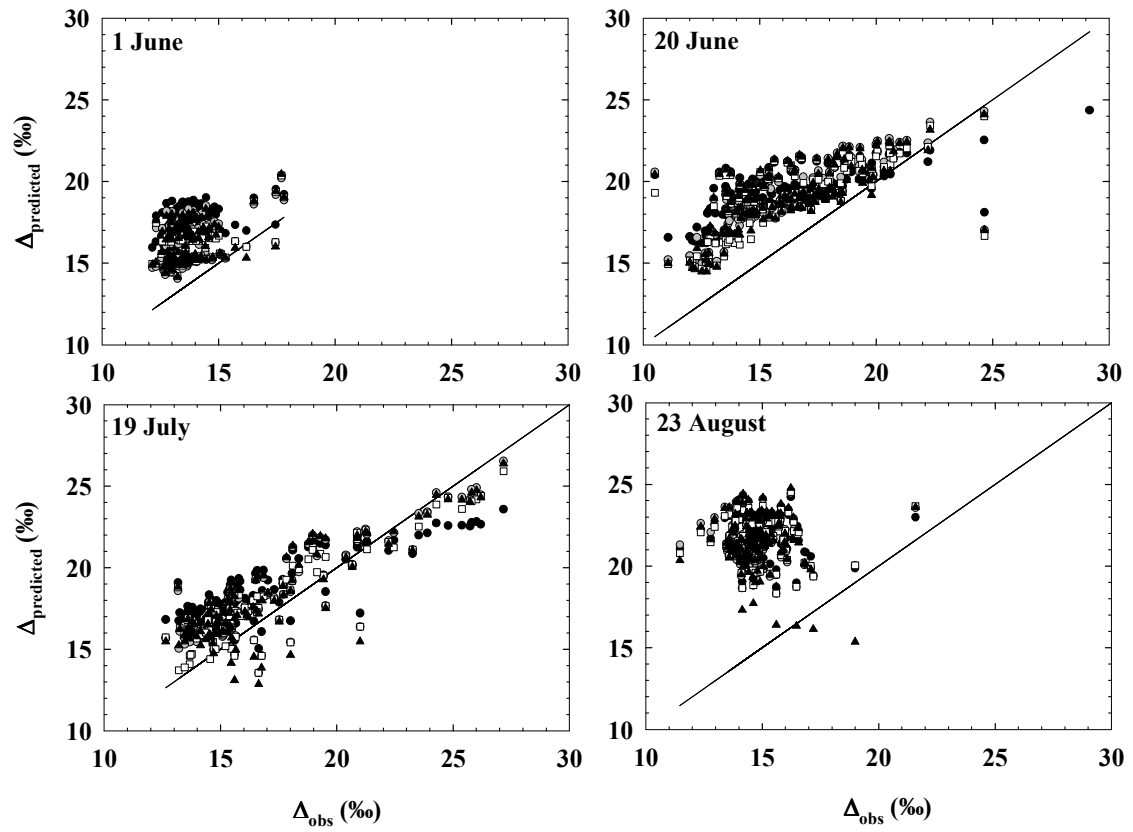
Figure 3.

Figure 4.

Figure 5.

Figure 6.

Chapter 4

Linkages between leaf water potential and internal conductance during drought in

two isohydric species

CHRISTOPHER P. BICKFORD[1]

[1]*University of New Mexico, Department of Biology, MSC03-2020, Albuquerque, NM*

87131

Running title: g_i in isohydric species

Abstract

Water deficit is known to reduce many leaf gas exchange characteristics, including the internal conductance of CO_2 from substomatal cavities to sites of carboxylation (g_i). In this study we imposed soil water deficit (*SWD*) in two isohydric species, *Populus fremontii* (poplar) and *Quercus gambelii* (oak), to investigate whether static leaf water potential during *SWD* would influence g_i activity. Using tunable diode laser spectroscopy we measured instantaneous carbon isotope discrimination (Δ) and estimated g_i from gas exchange data. Results show no statistically significant reduction in leaf water potential (Ψ_w) or g_i among droughted poplar and oak individuals in response to *SWD*. These non-significant differences in poplar g_i, however, may have generated significant changes in the relationship between Δ and the CO_2 partial pressure in intercellular airspaces and at the site of carboxylation relative to CO_2 in the ambient atmosphere, providing some evidence for an effect of *SWD* on CO_2 diffusion in leaves. Based on these data, it appears that maintenance of a constant Ψ_w diminishes the response of g_i to *SWD* and thus Ψ_w may have a regulatory role in g_i.

Keywords: mesophyll conductance, p_c/p_a, water stress, carbon isotope discrimination, decarboxylation, isohydry

Introduction

Drought has a detrimental effect on plant productivity globally. Many plant responses to soil water deficit (*SWD*) are well understood, including reduced stomatal conductance (g_s) that limits H_2O loss and carbon uptake (Lawlor & Cornic 2002, Flexas *et al*., 2004)

and biochemical impairment under severe water stress that reduces photosynthetic rate (Tezara *et al*., 1999, Flexas *et al*., 2006). Leaf water potential (Ψ_w) is a widely used indicator of plant water stress (Jones 2007), but plants exhibit different strategies for regulating Ψ_w in response to soil drought. Isohydric plants tightly regulate g_s to maintain a mid-day Ψ_w 'set point' that is largely invariant in response to moderate to severe *SWD*, whereas anisohydric plants exhibit less stringent regulation of g_s and vary Ψ_w as water availability and/or vapor pressure deficit (*VPD*) changes (Tardieu and Simmoneau 1998). Mechanisms underlying this regulatory framework are still poorly understood, though membrane aquaporin regulation may be important (Sade *et al*., 2009). Functionally, isohydric and anisohydric behavior may play a substantial role in drought survival by driving different gas exchange patterns during drought and drought recovery (McDowell *et al*., 2008; West *et al*., 2008).

In addition to stomatal control of carbon assimilation, several studies have shown that water deficit reduces the internal conductance of CO_2 from substomatal cavities to sites of carboxylation (g_i; Ridolfi and Dreyer 1997, Scartazza *et al*., 1998; Flexas *et al*., 2002; Warren, Livingston & Turpin 2004, Grassi and Magnani 2005; Galmes *et al*., 2007). Most found that g_i was reduced when water stress occurred over time periods ranging from minutes to days or weeks (Warren *et al*., 2004, Grassi and Magnani 2005) though reports exist showing no significant reductions in g_i under transient water stress (Monti *et al*., 2006) or even longer term *SWD* (Delfine *et al*., 2001). The proportion of reported species exhibiting decreased g_i during drought that are isohydric is unclear, though some reports suggest a correlation between variable g_i and anisohydric behavior (Warren *et al*., 2004) and others suggest little change in g_i in some isohydric plants

during *SWD* (Galmes *et al*., 2007). These reductions in g_i impact photosynthetic rate (A; Flexas *et al*., 2002, 2006) and measurement (Scartazza *et al*., 1998) and modeling of carbon isotope discrimination (Δ) by regulating the CO_2 diffusion pathway (Le Roux *et al*., 2001; Bickford *et al*., 2009). Recently, evidence has been put forward demonstrating that aquaporin proteins are facilitating the movement of CO_2 across cell membranes (Flexas *et al*., 2006b, Uehlein *et al*., 2008) and play a regulatory role under drought conditions (Miyazawa *et al*., 2008), however, environmental regulation of aquaporin activity is not well understood (Kaldenhoff *et al*., 2008).

Carbon isotope discrimination is the primary regulator of the $^{13}CO_2/^{12}CO_2$ ($\delta^{13}C$) signature fixed into sugars and other plant C products (Farquhar, Ehleringer & Hubick 1989), though post-photosynthetic fractionations can induce variation among different organs and substrate pools (Bowling *et al*., 2008; Gessler *et al*., 2008). Δ is known to respond to environmental change as it is linearly related to the ratio of CO_2 partial pressure (pCO_2) in intercellular air spaces and the atmosphere (p_i/p_a) (Farquhar *et al*., 1989, Brugnoli and Farquhar 2000). The strong influence of drought and/or high *VPD* conditions on g_s rapidly affects Δ by restricting CO_2 diffusion from the atmosphere to intercellular air spaces (Farquhar *et al*., 1989). Many studies have used the linear relationship between Δ and p_i/p_a to make inferences about stomatal conductance or photosynthetic rate (A), nevertheless, Δ occurs at the carboxylase and thus the ratio of pCO_2 at the site of carboxylation and in the atmosphere (p_c/p_a) is the more accurate parameter for correlation (Seibt *et al*., 2008).

The net flux and apparent isotopic fractionation associated with respiratory and photorespiratory activity (Δ_{ef}) during light reactions may also be important for

interpreting Δ. Recent work suggests the isotopic fractionation associated with photorespiration (f) is between 10–12‰ (Tcherkez 2006, Lanigan *et al*., 2008). Dark respiration (R) is inhibited in the light (Atkin *et al*., 2000, Tcherkez *et al*., 2005), and biochemically distinct from day respiration (R_d) processes as only portions of the dark respiration pathway are fully active in the light (Tcherkez *et al*., 2008). Currently, the isotopic fractionation associated with R_d (e) is not well understood and, consequently, measurements of the fractionation occurring during R are often used as a surrogate estimator. Studies have demonstrated isotopic enrichment occurring during R in response to drought (Duranceau *et al*., 1999), temperature (Tcherkez *et al*., 2003), and light exposure (Barbour *et al*., 2007). The cumulative effect of Δ_{ef} can be estimated from isotopic gas exchange data (Evans *et al*., 1986) and recent evidence suggests it may be important for predicting leaf Δ in some species (Wingate *et al*., 2007; Bickford *et al*., 2009), though the effects of drought on the interaction of R_d and photorespiratory processes are not well understood.

In this study we coupled a portable photosynthesis system to a tunable diode laser to obtain high frequency measurements of the concentration and composition of leaf gas exchange occurring in two isohydric species: *Populus fremontii* S. Watson (poplar) and *Quercus gambelii* Nuttall (oak). The aims of this study were to 1) test the hypothesis that that Ψ_w has a regulatory role in g_i among isohydric plants during *SWD*, 2) test whether drought had a significant effect on Δ_{ef}, and 3) examine the relationship between observed carbon isotope discrimination (Δ_{obs}) and *VPD*, p_i/p_a and p_c/p_a.

Methods

The study was conducted in two experiments, hereafter referred to as the poplar and oak experiments. In both experiments we measured the concentration and isotopic composition of leaf gas exchange to assess variation in g_i in response to *SWD* and Ψ_w. We coupled a portable photosynthesis system (*IRGA*; LICOR 6400, LICOR Biosciences Inc., Lincoln, NE, USA) fitted with a custom leaf chamber to a tunable diode laser (*TDL*; TGA100A, Campbell Scientific Inc., Logan, UT, USA) as described in Bickford *et al.*, (2009). The custom leaf chamber has a glass top and is capable of illuminating up to 75 cm^2 of leaf area when used with the external white LED light source (Photon Systems Instruments SL3500-W-D, Brno, Czech Republic). Boundary layer conductance in the chamber is ≥ 1.8 mol m^{-2} s^{-1}. For the poplar experiment, the working standard (WS) calibration tanks spanning the range of expected sample $[CO_2]$ used to calibrate each 3 minute measurement cycle were (mean ± standard error (SE)) 535.972 ± 0.32 μmol/mol ($^{12}C^{16}O^{16}O$): 5.785 ± 0.003 μmol/mol ($^{13}C^{16}O^{16}O$): 2.161 ± 0.001 μmol/mol ($^{12}C^{18}O^{16}O$) for the high WS tank and 347.248 ± 0.25 μmol/mol ($^{12}C^{16}O^{16}O$): 3.747 ± 0.003 μmol/mol ($^{12}C^{16}O^{16}O$): 1.399 ± 0.001 μmol/mol ($^{12}C^{18}O^{16}O$) for the low WS tank. The WS calibration tanks were calibrated for four hours monthly against WMO-certified tanks that were filled and $\delta^{13}C$ calibrated at the Stable Isotope Lab of the Institute for Arctic and Alpine Research, a cooperating agency of the Climate Monitoring division of the National Oceanic and Atmospheric Administration's Earth Research Laboratory. The $[CO_2]$ of the WMO traceable tanks used in this study were, for the high tank, 539.568 μmol/mol ($^{12}C^{16}O^{16}O$): 5.933 μmol/mol ($^{13}C^{16}O^{16}O$): 2.208 μmol/mol ($^{12}C^{18}O^{16}O$) and for the low tank, 339.433 μmol/mol ($^{12}C^{16}O^{16}O$): 3.764 μmol/mol ($^{13}C^{16}O^{16}O$): 1.401

μmol/mol ($^{12}C^{18}O^{16}O$). Measurements of [CO_2] concentration occasionally exceeded the lower span of the WS calibration tanks in the poplar experiment (maximum deviation: 78.0 μmol/mol), but post-hoc tests of the *TDL* (Bickford *et al.* 2009) demonstrated a linear measurement response to 247.43 μmol/mol, a [CO_2] lower than observed in this study. Ambient air was provided to the *IRGA* via a 50L buffer volume. For the oak experiment working standard (WS) calibration tanks spanning the range of expected [CO_2] measurements used to calibrate each 2 minute measurement cycle were (mean ± standard error (SE)) 473.336 ± 0.25 μmol/mol ($^{12}C^{16}O^{16}O$): 5.18321 ± 0.003 μmol/mol ($^{13}C^{16}O^{16}O$): 1.938 ± 0.001 μmol/mol ($^{12}C^{18}O^{16}O$) for the high WS tank and 243.47378 ± 0.10 μmol/mol ($^{12}C^{16}O^{16}O$): 2.66630 ± 0.001 μmol/mol ($^{13}C^{16}O^{16}O$): 0.996 ± 0.001 μmol/mol ($^{12}C^{18}O^{16}O$) for the low WS tank. These WS tanks were calibrated for three hours with the previously described WMO-traceable standard tanks. During the oak experiment air provided to the *IRGA* came from disposable CO_2 gas cylinders filled from a natural well ($\delta^{13}C = -4$‰; Liss America, Macedon, New York, USA).

We performed the poplar experiment in a greenhouse located at Los Alamos National Laboratory in Los Alamos, NM, USA (elev. 2140m; atmospheric pressure = ~79 kPa). Daytime temperature across the growth period ranged between 21.5 and 33.4° C, and a shade cloth covering the greenhouse reduced the maximum photosynthetic photon flux (PPF) to ~1050 μmol photons m^{-2} s^{-1}. Plants were started from cuttings and transferred to 7L pots, where they grew between May and August 2007, when measurements commenced. Pots were filled with Metro-Mix 300 growing medium (Sun-Gro Horticulture Distribution Inc., Bellevue, WA, USA) and fertilized 3 times weekly with 20-20-20 solution (Fertilome, Voluntary Purchasing Group). We withheld water

from seven trees for 2 d prior to gas exchange measurements to induce soil water deficit. 500mL H_2O was added to all droughted plant pots whose soil water content (SWC) fell below 15% at the end of day 1 measurements to bring SWC up to ~25%. During the two measurement days we measured volumetric SWC hourly on all plants using a soil water content measurement system (Hydrosense, Campbell Scientific Inc., Logan, UT, USA). During gas exchange measurements leaf temperature (T_L) was regulated between 26-31° C. T_L was measured using a thermocouple temperature sensor (Type E, Omega Engineering Inc., Stamford, CT, USA) in contact with lower side of the leaf. PPF was varied in step-change reductions from ~1550 to 200 μmol m^{-2} s^{-1}. Immediately following gas exchange measurements we collected a leaf punch from the portion of the lamina measured and placed the punch in a calibrated leaf psychrometer (C-52 sample chamber, Wescor Environmental Products Division, Logan, UT, USA) coupled to a CR-7 datalogger (Campbell Scientific Inc., Logan, UT, USA) for measurement of Ψ_w. We determined leaf area using a leaf area meter (LI-3100; LICOR Biosciences Inc., Lincoln, NE, USA), and present leaf area corrected gas exchange data.

The oak study was conducted at the University of New Mexico in Albuquerque, NM, USA (elev. 1524m; ~ atmospheric pressure = 84.8 kPa) on September 17 and 19, 2008. We grew oak plants from seed in 2.5L pots in a greenhouse between October 2007 and September 2008, when we conducted the study. Pots were filled with Metro-Mix 360 growing medium (Sun-Gro Horticulture Distribution Inc., Bellevue, WA, USA) and fertilized weekly with 20-20-20 N-P-K solution (Jack's 20-20-20; J.R. Peters, Inc., Allentown, PA, USA). Greenhouse temperature ranged between 18 and 27° C and maximum daytime irradiance was ~1100 μmol photons m^{-2} s^{-1}. We withheld water from

eight plants for 10 d prior to measurements on 17 September, except for providing ~

100mL to droughted plants three days prior to 17 September measurements. Similarly,

we administered ~200mL to remaining droughted plant pots at the end of 17 September

measurements to maintain SWC at ~25% for the 19 September measurements. We

determined SWC gravimetrically by measuring pot, soil, and plant mass at the time of gas

exchange measurements (W_m), then bringing them to field capacity and measuring mass

again (W_{fc}), and finally measuring the dry mass (W_d). To quantify SWC we used the

equation $SWC = W_m - W_d / W_{fc} - W_d$. T_L was measured and maintained as in the poplar

experiment. PPF was varied in step-change reductions from ~1300 to 200 μmol m^{-2} s^{-1},

and following light measurements a dark cloth was placed over the chamber to facilitate

measurement of the dark respiration rate and $\delta^{13}C$ of dark respired CO_2 ($\delta^{13}C_{resp}$).

Immediately following gas exchange measurements the measured leaf and petiole were

excised from the stem for measurement of xylem Ψ_w using a Scholander-type pressure

bomb (PMS Instruments Inc., Corvallis, OR, USA). We determined leaf area using by

scanning measured leaves and calculating leaf using Scion Image for Windows (Scion

Corporation, Frederick, MD, USA).

We calculated five parameters from our leaf isotopic gas exchange data: Δ_{obs},

$\delta^{13}C$, g_{is}, g_{ip} and Δ_{ef}. We determined Δ_{obs} following Evans *et al.* (1986),

$$\Delta_{obs} = \frac{\xi(\delta_o - \delta_e)}{1 + \delta_o - \xi(\delta_o - \delta_e)}$$

(1)

where $\xi = c_e/(c_e - c_o)$ is the ratio of the reference CO_2 concentration entering the chamber

(c_e) relative to the sample CO_2 concentration exiting the chamber (c_o), and δ_e and δ_o are

the $\delta^{13}C$ of the reference and sample gas, respectively. All variables incorporated in Δ_{obs}

and $\delta^{13}C_{resp}$ (below) are derived from *TDL* measurements of [$^{12}CO_2$] and [$^{13}CO_2$]. We

calculated δ_o and δ_e from the molar abundance of each isotopologue and present them in ratio to the Vienna Pee Dee belemnite (VPDB) standard, that is $\delta = R_s/R_{VPDB}-1$, where δ represents either δ_o or δ_e, and R_s and R_{VPDB} represent the carbon isotope ratio of the sample and VPDB standard, respectively. We calculated mixing ratios of total $[CO_2]$ and $\delta^{13}C_{resp}$ following Barbour *et al.* (2007),

$$\delta^{13}C_{resp} = \frac{\delta_o - \delta_e(1-p)}{p} \tag{2}$$

where p equals $(c_o-c_e)/c_o$. We calculated g_i using slope-based methods in Evans *et al.* (1986),

$$g_{is} = (b-b_s-a_w)/r_i \tag{3}$$

where b, b_s, and a_w are the isotopic fractionation factors associated with carboxylation (29‰), CO_2 entering solution (1.1‰), and diffusion in the aqueous phase (0.7‰), respectively, and r_i is the internal resistance to CO_2 diffusion from substomatal cavities to sites of carboxylation. r_i is proportional to the slope of the relationship between A/p_a and $\Delta_i-\Delta_{obs}$ (Evans *et al.*, 1986), where A is photosynthetic rate, p_a is the pCO_2 in the leaf chamber, and Δ_i is the predicted discrimination,

$$\Delta_i = a_b \frac{p_a - p_s}{p_a} + a \frac{p_s - p_i}{p_a} + b \frac{p_i}{p_a} \tag{4}.$$

Variables a_b, p_s and p_i represent fractionation associated with diffusion through air (2.9‰), pCO_2 at the leaf surface, and pCO_2 in intercellular spaces, respectively. We used positive r_i slopes that were significantly different from zero ($P \leq 0.05$) to calculate g_i, excluding any slope that displayed a negative relationship between A/p_a and $\Delta_i-\Delta_{obs}$ because negative slopes produce negative g_i estimates. We estimated Δ_{ef} from significant ($P \leq 0.05$) y-intercepts of the regressions used to calculate r_i, following theory developed

106

in Evans *et al*. (1986). We used point-based methods of calculating g_i (g_{ip}) to determine if g_i varied with A/p_a across range of values we used in g_{is} where g_{ip} is estimated following Evans *et al*. (1986),

$$g_{ip} = \frac{(b - b_s - a_w)A/p_a}{\Delta_i - \Delta_{obs} - \Delta_{ef}}$$ (5)

and Δ_{ef} is calculated as:

$$\Delta_{ef} = \frac{\dfrac{eR_d}{k} + f\Gamma^*}{p_a}$$ (6)

Variables e and f represent fractionation associated with day respiration (estimated at $-3‰$) and photorespiration ($11.6‰$; Lanigan *et al*., 2008), respectively, and R_d, k, and Γ^* represent day respiration ($\mu mol\ m^{-2}\ s^{-1}$), carboxylation efficiency ($\mu mol\ m^{-2}\ s^{-1}\ Pa^{-1}$), and the photo-compensation point in the absence of day respiration (Pa), respectively. Variability in R_d is not well understood among species or in response to stressors but has previously been shown to be approximately $0.5R$ (Tcherkez *et al*., 2005) where R is dark respiration rate; here we estimate $R_d = 0.5\ \mu mol\ m^{-2}\ s^{-1}$ based on oak R. We estimated k by calculating a mean A/p_c value from oak ($0.71\ \mu mol\ m^{-2}\ s^{-1}\ Pa^{-1}$) and poplar ($2.3\ \mu mol\ m^{-2}\ s^{-1}\ Pa^{-1}$) gas exchange measurements. We calculated Γ^* based on T_L (Brooks and Farquhar 1985); Γ^* ranged between 3.57 and 4.80 Pa in poplar and between 4.01 and 4.99 Pa in oak leaves.

Statistical analysis

We assessed potential error in our calculations of Δ_{obs} and $\delta^{13}C_{resp}$ using bootstrap methods and in g_i and Δ_{ef} using regression statistics. We used the standard deviation (SD) of the $[^{12}CO_2]$ and $[^{13}CO_2]$ measurements to generate 10000 bootstrap resamples of each

Δ_{obs} and $\delta^{13}C_{resp}$ value following methods in Bickford *et al.* (2009) and used the standard error (SE) of the variation in bootstrap resamples as an estimate of the SE in Δ_{obs} or $\delta^{13}C$. We estimated the uncertainty in g_{is} by transforming the SE associated with r_i to the g_{is} scale (Eqn. 3; Bickford *et al.*, 2009) and the uncertainty in Δ_{ef} using the SE associated with the y-intercept of the regression. Uncertainty in g_{ip} was determined by incorporating $\Delta_{obs} \pm$ SE for each point and transforming these to the g_{ip} scale (eq. 5). All error propagation was performed in R (R Core Development Team 2008); all other statistical tests were performed in JMP 5.0.1 (SAS Institute Inc., Cary, NC, USA).

Results

Soil water deficit did not significantly reduce g_{is} in droughted poplar (drought g_{is} mean $\pm$ SE = 6.62 $\pm$ 1.03 μmol m^{-2} s^{-1} Pa^{-1} versus control g_{is} = 7.55 $\pm$ 0.84 μmol m^{-2} s^{-1} Pa^{-1}; P = 0.5, t = 0.702) or droughted oak (1.56 $\pm$ 0.35 μmol m^{-2} s^{-1} Pa^{-1} versus control = 1.96 $\pm$ 0.20 μmol m^{-2} s^{-1} Pa^{-1}; P = 0.35, t = 1.07), nor did it significantly reduce Ψ_w in droughted poplar (drought mean $\pm$ SE = -1.35 ± 0.06 MPa versus control = -1.24 ± 0.05 MPa; P = 0.2, t = 1.308) or droughted oak (mean drought Ψ_w = -1.85 ± 0.18 MPa versus control Ψ_w = -1.96 ± 0.16 MPa; P = 0.65, t = -0.47) (Figure 1, Table 1). Slopes used to calculate poplar and oak g_{is} were generally strong (mean R^2 = 0.74; Table 2). SWC was significantly higher in control poplar (48.8 $\pm$ 3.0%) compared with droughted poplar (23.7 $\pm$ 1.6%; P = 0.0002, t = 6.29, n = 10) and in control oak (75.7 $\pm$ 0.86%) compared with droughted oak (22.9 $\pm$ 2.32%; P < 0.0001, t = 24.12, n = 12). 33% of droughted poplars experienced shoot dieback as a result of the drought treatment. Leaf temperature was significantly higher in droughted poplar plants compared to control poplar plants

(drought $T_L = 29.01 \pm 0.19°C$ vs. control $T_L = 27.62 \pm 0.13°C$; $P < 0.0001$, $t = -6.11$) but

not in droughted oak ($T_L = 29.19 \pm 0.16°C$) compared to control oak plants ($29.18 \pm$

$0.10°C$; $P = 0.97$).

There were significant negative relationships between g_{ip} and A/p_a in control ($P <$

0.0001, $F = 68.59$, $n = 99$, slope $= -4.23$) and droughted poplar ($P = 0.04$, $F = 4.28$, $n =$

77, slope $= -1.74$) but no significant relationship between g_{ip} and A/p_a in control ($P =$

0.11, $F = 2.63$, $n = 99$) or droughted oak plants ($P = 0.46$, $F = 0.56$, $n = 86$). Consequently,

we also present estimates of poplar g_{ip} calculated under saturating PPF conditions ($>$

1000 μmol m^{-2} s^{-1}). g_{ip} estimates were higher than g_{is} estimates ($P = 0.001$, paired t-test, n

$= 10$) with mean g_{ip} equal to 11.33 ± 1.2 μmol m^{-2} s^{-1} Pa^{-1} compared with a mean g_{is} of

7.17 ± 0.63 μmol m^{-2} s^{-1} Pa^{-1} (Table 3). In contrast to tests between g_{is} and SWC, there

was a significant decrease in g_{ip} among droughted poplar plants (mean $\pm$ SE $= 7.87 \pm$

0.97 μmol m^{-2} s^{-1} Pa^{-1}) compared to controls (13.44 ± 1.1 μmol m^{-2} s^{-1} Pa^{-1}; $P = 0.004$, $t =$

3.79, $n = 12$).

Water deficit reduced Δ_{obs}, A and g_s in droughted poplar ($P < 0.0001$ for all) and

droughted oak ($P < 0.05$ for all; Table 1) compared to controls. The relationship between

Δ_{obs} and VPD was negative and linear in control ($P < 0.0001$, $F = 110.37$, $R^2 = 0.50$) and

droughted poplar plants ($P < 0.0001$, $F = 92.21$, $R^2 = 0.50$) but was better described by a

log transformed second order polynomial when control and drought data were pooled (P

< 0.0001, $F = 257.97$, $R^2 = 0.74$; Figure 2a). The relationship between g_s and VPD was

also negative and linear in control ($P < 0.0001$, $F = 41.77$, $R^2 = 0.28$) and droughted

poplar plants ($P < 0.0001$, $F = 66.14$, $R^2 = 0.41$) but when control and drought data were

pooled the relationship was better described by a log transformed second order

polynomial (P < 0.0001, F = 292.88, R^2 = 0.76; Figure 2b). A negative linear relationship existed between Δ_{obs} and VPD in droughted oak plants (P = 0.002, F = 10.97, R^2 = 0.17), but control oaks exhibited a positive linear relationship between Δ_{obs} and VPD (P < 0.0001, F = 19.05, R^2 = 0.19; Figure 2c). Significant negative relationships existed between g_s and VPD in both control (P = 0.0007, F = 12.54, R^2 = 0.14) and droughted oak (P < 0.0001, F = 246.76, R^2 = 0.82; Figure 2d). Mean p_i/p_a was higher in control poplar plants (0.81 ± 0.01) compared with droughted poplar plants (0.61 ± 0.01; P < 0.0001, t = 11.69; Figure 3a); mean p_c/p_a was also higher in control poplar plants (0.61 ± 0.01) compared with drought plants (0.53 ± 0.02; P < 0.0001, t = 3.98; Figure 3b). Similarly, mean p_i/p_a was higher in control oak (0.70 ± 0.01) versus droughted oak plants (0.64 ± 0.02; P = 0.002, t = 3.17; Figure 3c) and p_c/p_a was higher in control (0.52 ± 0.02) versus droughted plants (0.46 ± 0.02; P = 0.03, t = 2.14; Figure 3d). There were significant linear relationships between Δ_{obs} and p_i/p_a in both control and droughted poplar (P < 0.0001) and oak (P < 0.0001) as well as significant relationships between Δ_{obs} and p_c/p_a among all poplar (P < 0.0001) and oak plants (P < 0.0001; Figure 3). As determined by overlapping 95% confidence intervals, the slopes representing the relationship between Δ_{obs} and p_i/p_a and Δ_{obs} and p_c/p_a did not differ between control and droughted poplar plants or control and treatment oak plants.

Patterns in Δ_{ef} differed between poplar and oak. Half of the poplar Δ_{ef} values were not significantly different from zero (P > 0.05, Table 1), but droughted poplar exhibited significantly higher Δ_{ef} (mean ± SE = 2.85 ± 0.84‰) compared to control poplar plants (−0.34 ± 0.84‰; P = 0.04, t = −2.69, n = 12; Table 4). All oak Δ_{ef} values were significantly less than zero (P ≤ 0.03; Table 2), but were not significantly different

between control (-4.88 ± 0.75‰) and droughted oak plants (-5.07 ± 1.12‰, $P = 0.88$, $t = 0.167$, Table 4). Pooled by species, poplar showed more positive Δ_{ef} (1.26 ± 0.74‰) than oak (-4.96 ± 0.55‰; $P < 0.0001$, $t = -6.72$, $n = 24$).

R in oak two minutes post-illumination (R_{2min}) was not different between control (mean $\pm$ SE $= 0.43 \pm 0.08$ µmol m^{-2} s^{-1}) and droughted oak (0.37 ± 0.08 µmol m^{-2} s^{-1}; $P = 0.62$, $t = 0.51$, $n = 14$), but was higher four minutes post-illumination (R_{4min}) in control (1.26 ± 0.07 µmol m^{-2} s^{-1}) versus droughted oak (0.97 ± 0.11 µmol m^{-2} s^{-1}; $P = 0.05$, $t = 2.21$, $n = 14$; Table 4). This near 3-fold increase in R between R_{2min} and R_{4min} was significant ($P = 0.006$, $t = -3.21$, $n = 9$). Due to low CO_2 flux during the transition from net A to stable R most $\delta^{13}C_{resp}$ measurements collected two minutes post-illumination were associated with high uncertainty (mean $= 13.3$‰) and are not shown. $\delta^{13}C_{resp}$ measurements collected 4–6 minutes post-illumination showed no significant difference between control (-27.92 ± 2.26‰) and droughted oak plants (-31.61 ± 1.03‰; $P = 0.25$, $t = 1.26$, $n = 10$; Table 4).

Discussion

These findings show that soil water deficit does not necessarily reduce g_i if leaves exhibit isohydric leaf behavior. Both poplar and oak exhibited isohydric regulation and did not show significant differences in Ψ_w or g_i, based on g_{is} estimates, between droughted and control plants even though the drought was severe enough to cause large declines in A. This provides initial support for the hypothesis that Ψ_w has a regulatory role in g_i that contrasts with most reports showing no linkage between Ψ_w and g_i. Previous studies providing data on both Ψ_w and g_i show reduced g_i corresponding with reductions in Ψ_w in

Pseudotsuga (Warren *et al*., 2004), *Beta vulgaris* during persistent drought (Monti *et al*., 2006) and a variety of Mediterranean plants (Galmes, Medrano & Flexas 2007). Among three isohydric species examined in Galmes *et al*. (2007) one (*Diplotaxis ibicensis*) showed substantial declines in g_i while two *Limonium* species exhibited modest decreases in g_i in response to moderate-to-severe water stress. In *Beta vulgaris*, however, transient drought did not reduce Ψ_w, suggesting isohydric tendencies, and no significant reductions in g_i were observed compared to controls (Monti *et al*., 2006). The variation in *B. vulgaris* responses to drought duration and the discrepancies between our results and those observed in *D. ibicensis* demonstrate a need for further investigation of the g_i response to drought among other isohydric species.

The current consensus posits aquaporin activity as the primary regulator of g_i by facilitating CO_2 transport across cell membranes, as shown in *Nicotiana tabacum* (Flexas *et al*., 2006b, Uehlein *et al*., 2008), but the relationship between aquaporin activity and Ψ_w remains poorly understood. One recent study found linkages between PIP2 plasma membrane (PM) aquaporin gating patterns and leaf water status that directly affected g_i in *Nicotiana* by reducing CO_2 diffusion during drought (Miyazawa *et al*., 2008). Existing studies suggesting some linkage between Ψ_w and g_i include a report of PIP2 PM protein phosphorylation being partially dependent on apoplastic water potential (Johannson *et al*., 1996) and recent work proposing a role for the tonoplast aquaporin SITIP2;2 in regulating isohydric and anisohydric behavior (Sade *et al*., 2009). Further study of the interaction between aquaporin activity and Ψ_w, specifically for those proteins shown to facilitate CO_2 transfer, are needed.

Drought did significantly reduce other leaf gas exchange characteristics, confirming previous studies. As expected, *SWD* reduced Δ_{obs}, g_s and *A* in both poplar and oak (Lawlor and Cornic 2002, Flexas *et al.*, 2006, Monti *et al.*, 2006). We also examined the relationship between Δ_{obs} and atmospheric water deficits, or *VPD*, and found that both drought and control poplar, as well as droughted oak, exhibited the expected negative relationship between these two parameters but that control oak plants showed a weakly positive relationship between Δ_{obs} and *VPD* (Figure 2c). *VPD* during oak control measurements was generally < 2 kPa, low enough to facilitate moderate g_s in this semi-arid adapted species, and thus not a large constraint on *A* and Δ_{obs} across the *VPD* range we observed. The curvilinear relationships between *VPD* and both Δ_{obs} and g_s in drought and control plants demonstrates the strong regulatory importance of g_s on poplar Δ_{obs} at higher *VPD* (> 1.0 kPa; Figure 2). In contrast, oak plants exhibited relatively weak relationships between *VPD* and Δ_{obs} and g_s, possibly due to the small range of g_s we observed in both control and droughted plants. Both p_i/p_a and p_c/p_a were higher among control poplar and oak compared to drought plants, but the slopes describing their relationships with Δ_{obs} were similar across species. Our p_i/p_a and p_c/p_a estimates were mostly higher, but still comparable, to those observed in other *Quercus* and *Populus* species (Roupsard *et al.*, 1996). Among droughted plants most lower p_i/p_a and p_c/p_a values could be attributed to lower g_s, and not necessarily lower g_i. The relationship between Δ_{obs} and p_c/p_a among control and droughted poplar plants, however, extends across a similar p_c/p_a range and show lower Δ_{obs} in droughted plants when $p_c/p_a < 0.65$. This could be due to positive Δ_{ef} influencing discrimination or it could be a biologically

significant reduction in g_i among droughted poplar plants that was not captured in our statistical tests, a finding which agrees with our poplar g_{ip} estimates.

It is possible that our g_i estimates do not accurately reflect the internal conductance of CO_2 in poplar leaves. Our g_{is} estimates depended on variation in A, which we manipulated using variable PPF. Recent evidence suggests g_i can vary rapidly in response to changes in PPF and other environmental variables (Flexas *et al.*, 2007) and this may have confounded our g_{is} results. The significant variation in poplar g_{ip} that occurred over the range of A/p_a we used in this study lends support to this conclusion. The estimates we calculated using g_{ip}, however, were much higher than g_i values reported in the literature for other woody deciduous angiosperms (Flexas *et al.*, 2008) and should be interpreted conservatively. Alternatively, the g_{ip} estimates may have accurately reflected differences in poplar g_i between droughted and control plants but overestimated the actual internal conductance of CO_2.

Decarboxylation activity differed between poplar and oak, and among oak treatments. Overall Δ_{ef} was lower in oak compared with poplar, for reasons that were not made clear by our data. Δ_{ef} was similar among oak plants, being $\sim -5\permil$ in both droughted and control plants, but was different between droughted and control poplar. Among droughted poplar most Δ_{ef} values were positive, and may have had a negative forcing effect that resulted in a lower net Δ_{obs} compared with control plants. Using mechanistic models as a framework for conceptualizing the interactions occurring during diffusion, carboxylation, and decarboxylation that influence fractionation, Δ_{ef} (eq. 6) is subtracted from the sum of fractionations due to diffusion and carboxylation processes (Farquhar *et al.*, 1989), and thus positive Δ_{ef} could result in more negative Δ_{obs}. Two high

Δ_{ef} values stood out (Table 2), and made differences between poplar treatments significant. These high measurements were collected from severely drought stressed plants, and this stress level may have resulted in stomatal patchiness that could have adversely affected our p_i estimates (Farquhar 1989), and thus impacted Δ_i calculations used to estimate Δ_{ef}. The low Δ_{ef} among the oak plants highlights two points. Quantitatively, these low values show that Δ_i, the simplified predictive model of discrimination, largely under-predicted Δ_{obs}. Functionally, this suggests accounting for R_d and photorespiration, as well as their associated fractionation factors, may be important in oak to fully describe leaf isotopic exchange, as observed in juniper (Bickford *et al.*, 2009). In oak, R showed evidence of up-regulation of dark respiration activity by exhibiting a 3-fold increase in R in the minutes following illumination. There was lower R and, unexpectedly, lower $\delta^{13}C_{resp}$ among droughted oak. Lower R during short-term water deficit has been observed previously (Atkin *et al.*, 2005), but lower $\delta^{13}C_{resp}$ is typically associated with well-watered conditions (McDowell *et al.*, 2004). It is possible that supplemental watering prior to day 2 oak measurements briefly increased gas exchange activity, resulting in assimilate being formed that was isotopically similar to control plants and that was subsequently decarboxylated during measurements.

Conclusions

This study provides a new view on the correlation between leaf water relations and g_i, and supports the existence of a linkage between Ψ_w and CO_2 conductance to sites of carboxylation. Because they display static Ψ_w in response to soil water deficit, isohydric plants provide a unique platform to separate the effects of *SWD* and leaf water potential.

In contrast to numerous studies showing reduced g_i in response to drought, our study found, based on slope-based estimates, no significant reduction in g_i during *SWD* in these isohydric species. Functionally, however, either the g_i we observed in droughted poplar did affect p_c/p_a differently than control plants, or Δ_{ef} exerted stronger influence on Δ_{obs} at lower p_c/p_a. Given the minor discrepancies between our data and the few existing data sets exploring g_i in other isohydric species it is important to document g_i in other plants with similar leaf hydraulic behavior to see whether this is a widespread phenomenon. The recent work linking g_i and aquaporin activity seems a promising avenue to further investigate linkages with leaf water potential, and such study should aid our understanding of g_i in both isohydric and anisohydric plants.

Acknowledgements

References

Atkin OK, Evans JR, Ball MC, Lambers H, Pons TL. **2000.** Leaf respiration of snow gum in the light and dark. Interactions between temperature and irradiance. *Plant Physiology* **122:** 915-923.

Atkin OK, Bruhn D, Hurry VM, Tjoelker MG. **2005.** The hot and the cold: unravelling the variable response of plant respiration to temperature. *Functional Plant Biology* **32:** 87-105.

Barbour MM, McDowell NG, Tcherkez G, Bickford CP, Hanson DT. **2007.** A new

measurement technique reveals rapid post-illumination changes in the carbon isotope composition of leaf-respired CO_2. *Plant, Cell and Environment* **30:** 469-482.

Bickford CP, McDowell NG, Erhardt EB, Hanson DT. **2009.** High frequency field measurements of carbon isotope discrimination and internal conductance in a semi-arid species, *Juniperus monosperma*. *Plant, Cell and Environment*.

Bowling DR, Pataki DE, Randerson JT. **2008.** Carbon isotope in terrestrial ecosystem pools and CO_2 fluxes. *New Phytologist Tansley Review* **178**: 24-40.

Brooks A, Farquhar GD. **1985.** Effect of temperature on the CO_2/O_2 specificity of ribulose-1,5-bisphosphate carboxylase/oxygenase and the rate of respiration in the light. *Planta* **165:** 397-406.

Brugnoli E, Farquhar GD. **2000.** Photosynthetic fractionation of carbon isotopes. In: Leegood RC, Sharkey TD, von Caemmerer S, eds. *Photosynthesis: Physiology and Metabolism*. The Netherlands: Kluwer Academic, 399-434.

Delfine S, Loreto F, Alvino A. **2001.** Drought-stress effects on physiology, growth and biomass production of rainfed and irrigated bell pepper plants in the Mediterranean region. *Journal of the American Society of Horticultural Science* **126:** 297-304.

Duranceau M, Ghashghaie J, Badeck F, Deleens E, Cornic G. **1999.** δ^{13}C of CO_2 respired in the dark in relation to δ^{13}C of leaf carbohydrates in *Phaseolus vulgaris* L. under progressive drought. *Plant, Cell and Environment* **22:** 515-523.

Evans JR, von Caemmerer S. **1996.** Carbon dioxide diffusion inside leaves. *Plant Physiology* **110:** 339-346.

Farquhar GD, Ehleringer JR, Hubick KT. **1989.** Carbon isotope discrimination and photosynthesis. *Annual Review of Plant Physiology and Plant Molecular Biology* **40:** 503-537.

Farquhar GD. **1989.** Models of integrated photosynthesis of cells and leaves. *Philosophical Transactions of the Royal Society of London. Series B, Biological Sciences* **323:** 357-367.

Flexas J, Bota J, Loreto F, Cornic G, Sharkey TD. **2004.** Diffusive and metabolic limitations to photosynthesis under drought and salinity in C_3 plants. *Plant Biology* **6:** 269-279.

Flexas J, Ribas-Carbo M, Bota J., Galmes J, Henkle M, Martinez-Canellas S, Medrano H. **2006.** Decreased Rubisco activity during water stress is not induced by decreased relative water content but related to conditions of low stomatal conductance and chloroplast CO_2 concentration. *New Phytologist* **172:** 73-82.

Flexas J, Ribas-Carbo M, Hanson DT, Bota J, Otto B, Cifre J, McDowell N, Medrano H, Kaldenhoff R. **2006.** Tobacco aquaporin NtAQP1 is involved in mesophyll

conductance to CO_2 in vivo. *Plant Journal* **48:** 427-439.

Flexas J, Bota J, Escalona JM, Sampol B, Medrano H. **2002.** Effects of drought on photosynthesis in grapevines under field conditions: an evaluation of stomatal and mesophyll limitations. *Functional Plant Biology* **29:** 461-471.

Flexas J, Diaz-Espejo A, Galmčs J , Kaldenhoff R, Medrano H, Ribas-Carbo M. **2007.** Rapid variations of mesophyll conductance in response to changes in CO_2 concentration around leaves. *Plant, Cell and Environment* **30:** 1284-1298.

Flexas J, Ribas-Carbo M, Diaz-Espejo A, Galmes J, Medrano H. **2008.** Mesophyll conductance to CO_2: current knowledge and future prospects. *Plant, Cell and Environment* **31**: 602-621.

Galmes J, Medrano H, Flexas J. **2007.** Photosynthetic limitations in response to water stress and recovery in Mediterranean plants with different growth forms. *New Phytologist* **175:** 81-93.

Gessler A, Tcherkez G, Peuke AD, Ghashghaie J, Farquhar G 2008. Experimental evidence of diel variations of the carbon isotope composition in leaf, stem and phloem sap organic matter in *Ricinus communis*. *Plant, Cell and Environment* **31**: 941-953.

Grassi G, Magnani F. **2005.** Stomatal, mesophyll conductance and biochemical limitations to photosynthesis as affected by drought and leaf ontogeny in ash and oak trees. *Plant, Cell and Environment* **28:** 834-849.

Johannson I, Larsson C, Ek B, Kjellbom P. **1996.** The major integral proteins spinach leaf plasma membranes are putative aquaporins and are phosphorylated in response to Ca^{2+} and apoplastic water potential. *The Plant Cell* **8:** 1181-1191.

Jones HG. **2007.** Monitoring plant and soil water status: established and novel methods revisited and their relevance to studies of drought tolerance. *Journal of Experimental Botany* **58:** 119-130.

Kaldenhoff R, Ribas-Carbo M, Flexas San J, Lovisolo C, Heckwolf M, Uehlein N. **2008.** Aquaporins and plant water balance. *Plant, Cell and Environment* **31**: 658-666.

Lanigan GJ, Betson N, Griffiths H, Seibt U. **2008.** Carbon isotope fractionation during photorespiration and carboxylation in *Senecio*. *Plant Physiology* **148:** 2013-2020.

Lawlor DW, Cornic G. **2002.** Photosynthetic carbon assimilation and associated metabolism in relation to water deficits in higher plants. *Plant, Cell and Environment* **25:** 275-294.

Le Roux X, Bariac T, Sinoquet H, Genty B, Piel C, Mariotti A, Girardin C, Richard P. **2001.** Spatial distribution of leaf water-use efficiency and carbon isotope discrimination within an isolated tree crown. *Plant, Cell and Environment* **24:** 1021-1032.

McDowell NG, Bowling DR, Schauer A, Irvine J, Bond BJ, Law BE, Ehleringer JR. **2004.** Associations between carbon isotope ratios of ecosystem respiration, water availability, and canopy conductance. *Global Change Biology* **10:** 1767-1784.

McDowell NG, Pockman WT, Allen C, Breshears DD, Cobb N, Kolb T, Plaut J, Sperry J, West A, Williams D, Yepez EA. **2008.** Mechanisms of plant survival and mortality during drought: Why do some plants survive while others succumb to drought? *New Phytologist Tansley Review* **178**: 719-739.

Miyazawa S-I, Yoshimura S, Shinzaki Y, Maeshima M, Miyake C. **2008.** Deactivation of aquaporins decreases internal conductance to CO_2 diffusion in tobacco leaves grown under long-term drought. *Functional Plant Biology* **35:** 553-564.

Monti A, Brugnoli E, Scartazza A, Amaducci MT. **2006.** The effect of transient and continuous drought on yield, photosynthesis, and carbon isotope discrimination in sugar beet (*Beta vulgaris* L.). *Journal of Experimental Botany* **57:** 1253-1262.

Ridolfi M, Dreyer E. **1997.** Responses to water stress in an ABA-unresponsive hybrid poplar (*Populus koreana* x *trichocarpa* cv. Peace) III. Consequences for photosynthetic carbon assimilation. *New Phytologist* **135:** 31-40.

Roupsard O, Gross P, Dreyer E. **1996**. Limitation of photosynthetic activity by CO_2 availability in the chloroplasts of oak leaves from different species and during drought. *Annales Des Sciences Forestieres* **53**: 243-254.

Sade N, Vinocur BJ, Diber A, Shatil A, Ronen G, Nissan H, Wallach R, Karchi H, Moshelion M. **2009.** Improving plant stress tolerance and yield production: is the tonoplast aquaporin SITIP2;2 a key to isohydric to anisohydric conversion? *New Phytologist* **181:** 651-661.

Scartazza A, Lauteri M, Guido MC, Brugnoli E. **1998.** Carbon isotope discrimination in leaf and stem sugars, water-use efficiency and mesophyll conductance during different developmental stages in rice subjected to drought. *Australian Journal of Plant Physiology* **25:** 489-498.

Seibt U, Rajabi A, Griffiths H, Berry JA. **2008.** Carbon isotopes and water use efficiency: sense and sensitivity. *Oecologia* **155:** 441-454.

Tardieu F, Simonneau T. **1998.** Variability among species of stomatal control under fluctuating soil water status and evaporative demand: modelling isohydric and anisohydric behaviours. *Journal of Experimental Botany* **49:** 419-432.

Tcherkez Guillaume. **2006.** How large is the carbon isotope fractionation of the photorespiratory enzyme glycine decarboxylase? *Functional Plant Biology* **33:** 911-920.

Tcherkez G, Bligny R, Gout E, Mahe A, Hodges M, Cornic G. **2008.** Respiratory metabolism of illuminated leaves depends on CO_2 and O_2 conditions. *Proceedings of the National Academy of Science* **105:** 797-802.

Tcherkez G, Cornic G, Bligny R, Gout E, Ghashghaie J. **2005.** In vivo respiratory metabolism of illuminated leaves. *Plant Physiology* **138:** 1596-1606.

Tcherkez G, Nogues S, Bleton J, Cornic G, Badeck F, Ghashghaie J. **2003.** Metabolic origin of carbon isotope composition of leaf dark-respired CO_2 in French bean. *Plant Physiology* **131:** 237-244.

Tezara W, Mitchell VJ, Driscoll SD, Lawlor DW. **1999.** Water stress inhibits plant photosynthesis by decreasing coupling factor and ATP. *Nature* **401:** 914-917.

Uehlein N, Otto B, Hanson DT, Fischer M, McDowell N, Kaldenhoff R. **2008.** Function of *Nicotiana tabacum* aquaporins as chloroplast gas pores challenges the concept of membrane CO_2 permeability. *The Plant Cell* **20:** 648-657.

Warren CR, Livingston NJ, Turpin DH. **2004.** Water stress decreases the transfer conductance of Douglas-fir (*Pseudotsuga menziesii*) seedlings. *Tree Physiology* **24:** 971-979.

West AG, Hultine KR, Sperry JS, Bush SE, Ehleringer JR. **2008.** Transpiration and hydraulic strategies in a pinon-juniper woodland. *Ecological Applications* **18:** 911-927.

Wingate L, Seibt U, Moncrieff JB, Jarvis PG, Lloyd J. **2007.** Variations in ^{13}C discrimination during CO_2 exchange by *Picea sitchensis* branches in the field. *Plant, Cell and Environment* **30**: 600-616.

Tables

Table 1. Summary of results for internal conductance of CO_2 (g_i), leaf water potential (Ψ_w), soil water content (SWC), observed carbon discrimination (Δ_{obs}), net assimilation rate (A) and stomatal conductance to H_2O (g_s) in poplar and oak plants. Values are represented as means ± one SE.

Poplar	g_i (μmol m^{-2} s^{-1} Pa^{-1})	*P*	Ψ_w (MPa)	*P*	SWC (%)	*P*
control	7.55 ± 0.84	0.5	-1.24 ± 0.05	0.2	48.8 ± 3.0	0.0002
drought	6.62 ± 1.03		-1.35 ± 0.06		23.7 ± 1.6	
Oak						
control	1.96 ± 0.20	0.35	-1.96 ± 0.16	0.65	75.7 ± 0.86	< 0.0001
drought	1.56 ± 0.35		-1.85 ± 0.18		22.9 ± 2.32	
Poplar	Δ_{obs} (‰)	*P*	A (μmol m^{-2} s^{-1})	*P*	g_s (mol m^{-2} s^{-1})	*P*
control	19.53 ± 0.32	< 0.0001	32.34 ± 0.90	< 0.0001	1.46 ± 0.06	< 0.0001
drought	15.17 ± 0.44		19.35 ± 0.96		0.40 ± 0.03	
Oak						
control	21.54 ± 0.47	0.02	10.26 ± 0.44	< 0.0001	0.18 ± 0.004	< 0.0001
drought	19.82 ± 0.54		7.10 ± 0.38		0.11 ± 0.007	

Table 2. Summary of slope and intercept statistics from slope-based estimates (g_{is}) of internal conductance to CO_2 where T and C represent droughted and control poplar plants, respectively, and D and W represent droughted and control oak plants, respectively. Δ_{ef} represents the estimate of the total fractionation attributed to both respiratory and photorespiratory activity (‰). SE represents one standard error.

Poplar	Slope	SE	P	Δ_{ef}	SE	P	R^2
T1	2.82	0.39	< 0.0001	1.44	0.54	0.02	0.79
T2	5.07	1.45	0.004	-0.99	1.33	0.46	0.47
T3	5.24	1.21	0.001	1.81	0.99	0.08	0.54
T4	4.34	1.07	0.002	2.92	0.59	0.001	0.60
T5	-7.09	2.94	0.04	7.24	1.27	0.0002	0.37
T6	-1.72	2.14	0.43	4.69	1.40	0.004	0.04
C1	3.81	0.44	< 0.0001	-0.55	0.66	0.42	0.71
C2	3.79	0.20	< 0.0001	-0.99	0.33	0.01	0.95
C3	4.40	0.27	< 0.0001	-0.90	0.36	0.02	0.94
C4	4.32	0.37	< 0.0001	0.15	0.41	0.71	0.90
C5	2.34	0.29	< 0.0001	0.59	0.51	0.26	0.80
C6	3.98	0.47	< 0.0001	-0.35	0.62	0.57	0.80
Oak							
D1	10.32	1.09	< 0.0001	-1.81	0.42	0.002	0.91
D2	24.25	3.39	< 0.0001	-5.37	0.68	< 0.0001	0.77
D3	31.46	4.63	0.001	-8.33	0.95	0.0001	0.88
D4	26.47	4.14	0.0004	-6.29	0.83	0.0001	0.85
D5	12.69	3.12	0.01	-3.58	0.99	0.01	0.73
W1	13.54	1.20	< 0.0001	-4.55	0.43	< 0.0001	0.92
W2	11.05	0.02	< 0.0001	-4.07	0.29	< 0.0001	0.96
W3	19.38	2.85	0.0005	-7.75	0.88	0.0001	0.86
W4	23.10	7.42	0.04	-6.05	1.25	0.01	0.71
W5	11.38	2.75	0.001	-3.88	1.25	0.01	0.59
W6	15.05	2.00	< 0.0001	-4.31	0.68	< 0.0001	0.85
W7	10.97	2.52	0.003	-3.32	1.24	0.03	0.70

Table 3. Estimates of internal conductance of CO_2 in poplar calculated using a slope-based method (g_{is}) and a point-based method (g_{ip}) where C and T represent control and droughted poplar plants, respectively. g_{ip} estimates were significantly higher than g_{is} estimates (P = 0.001). There was a significant difference between droughted and control poplar plants using g_{ip} (P = 0.004, n = 12) but not when using g_{is} (P = 0.50).

	C1	C2	C3	C4	C5	C6
g_{is} (μmol m^{-2} s^{-1} Pa^{-1})	7.13 ± 0.85	7.19 ± 0.38	6.19 ± 0.39	6.30 ± 0.55	11.63 ± 1.49	6.84 ± 0.81
g_{ip} (μmol m^{-2} s^{-1} Pa^{-1})	16.25 ± 1.72	12.67 ± 0.38	11.53 ± 0.39	10.72 ± 2.03	17.34 ± 0.40	12.15 ± 0.71
	T1	**T2**	**T3**	**T4**		
g_{is} (μmol m^{-2} s^{-1} Pa^{-1})	9.64 ± 1.37	5.37 ± 1.67	5.19 ± 1.27	6.27 ± 1.64		
g_{ip} (μmol m^{-2} s^{-1} Pa^{-1})	12.11 ± 0.79	8.85 ± 1.54	6.36 ± 0.57	5.34 ± 0.23		

Table 4. Summary of the mean fractionation attributed to all decarboxylation activity (Δ_{ef}), dark respiration rate two minutes (R_{2min}) and four minutes post-illumination (R_{4min}), and the $^{13}C/^{12}C$ ratio of dark-respired CO_2 ($\delta^{13}C_{resp}$) four minutes post-illumination. Values are represented as means ± one SE.

Oak	Δ_{ef} (‰)	*P*	R_{2min}	*P*	R_{4min}	*P*	$\delta^{13}C_{resp}$	*P*
control	-4.88 ± 0.75	0.88	0.43 ± 0.08	0.62	1.26 ± 0.07	0.05	-27.92 ± 2.26	0.25
drought	-5.08 ± 0.89		0.37 ± 0.08		0.97 ± 0.11		-31.61 ± 1.03	

Figure captions

Figure 1. The relationship between internal conductance of CO_2 (g_i) and leaf water potential (Ψ_w; Panel a) and soil water content (SWC; Panel b) in poplar and oak plants. g_i was not different between droughted and control poplar (P = 0.5) or oak plants (P = 0.35), nor was Ψ_w different between droughted and control poplar (P = 0.2) or oak plants (P = 0.65). This demonstrates that soil water deficit does not necessarily reduce g_i in isohydric plants like poplar and oak.

Figure 2. The relationship between vapor pressure deficit (*VPD*) and observed carbon discrimination (Δ_{obs}) and stomatal conductance to H_2O (g_s). Panels a and b represent droughted (□) and control (■) poplar plants; panels c and d represent droughted (▲) and control (▲) oak plants. Error bars in all panels represent one SE. Linear and negative relationships between *VPD* and both Δ_{obs} and g_s were significant among both droughted and control poplar plants (P < 0.0001). In oak, however, linear negative relationships existed between *VPD* and g_s among treatments (P ≤ 0.0007) and between *VPD* and Δ_{obs} and droughted oak (P = 0.002), but a positive linear was found among control oak plants (P < 0.0001).

Figure 3. The relationship between observed carbon discrimination (Δ_{obs}) and the ratio of intercellular to atmospheric CO_2 partial pressure (p_i/p_a), and the relationship between Δ_{obs} and the ratio of CO_2 at the site of carboxylation to atmospheric CO_2 partial pressure (p_c/p_a). Panels a and b represent droughted (○) and control (●) poplar plants; panels c and d represent droughted (■) and control (■) oak plants. Error bars in all panels represent one SE. Significant linear relationships existed between Δ_{obs} and both p_i/p_a and p_c/p_a (P <

0.0001) but slopes representing these relationships in drought and control treatments were not different (P > 0.05) in either poplar or oak plants.

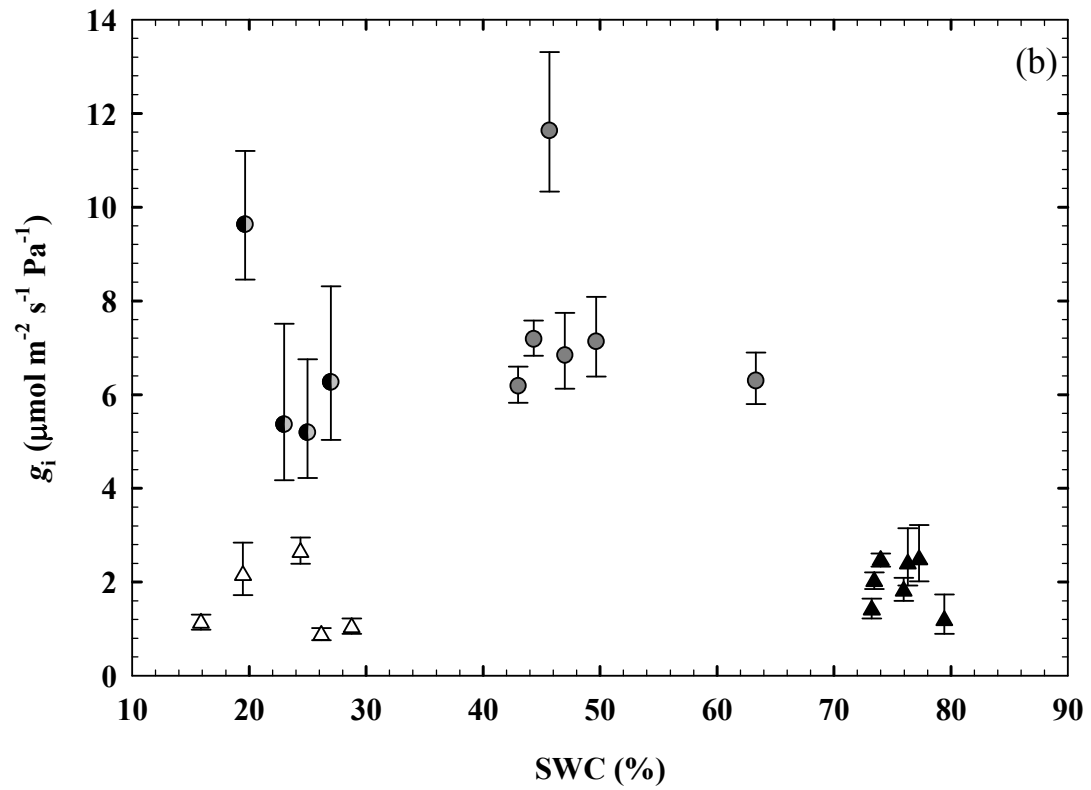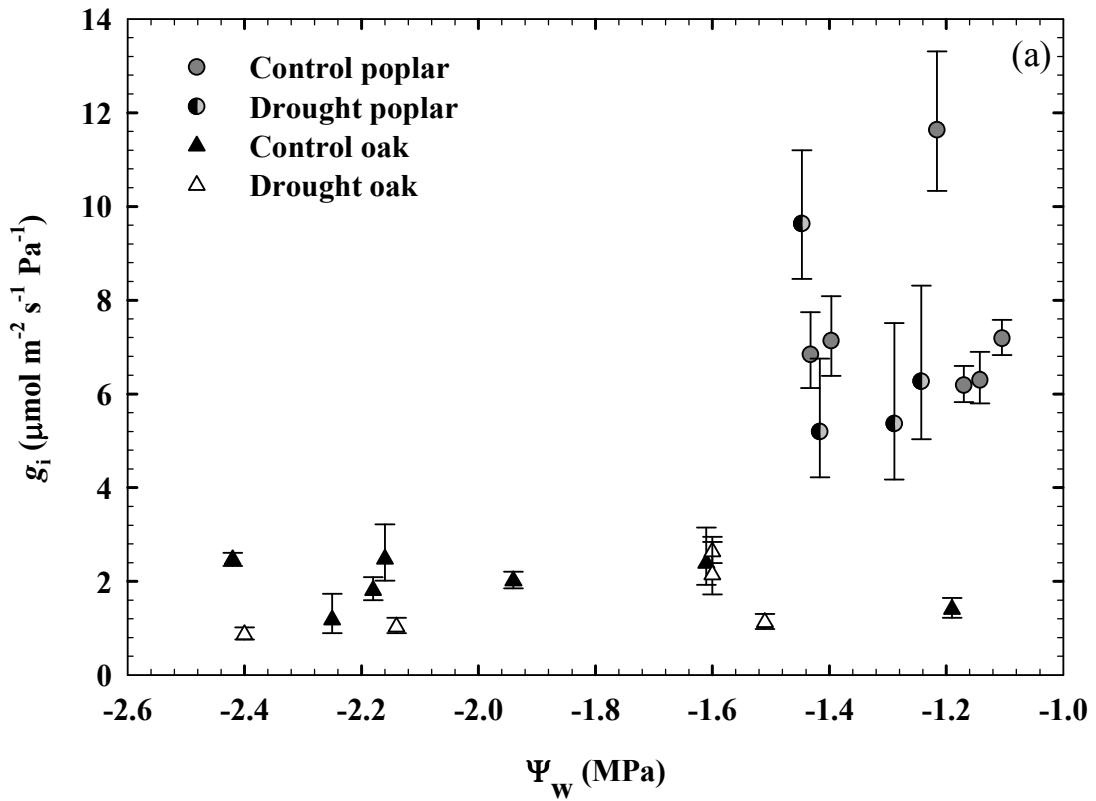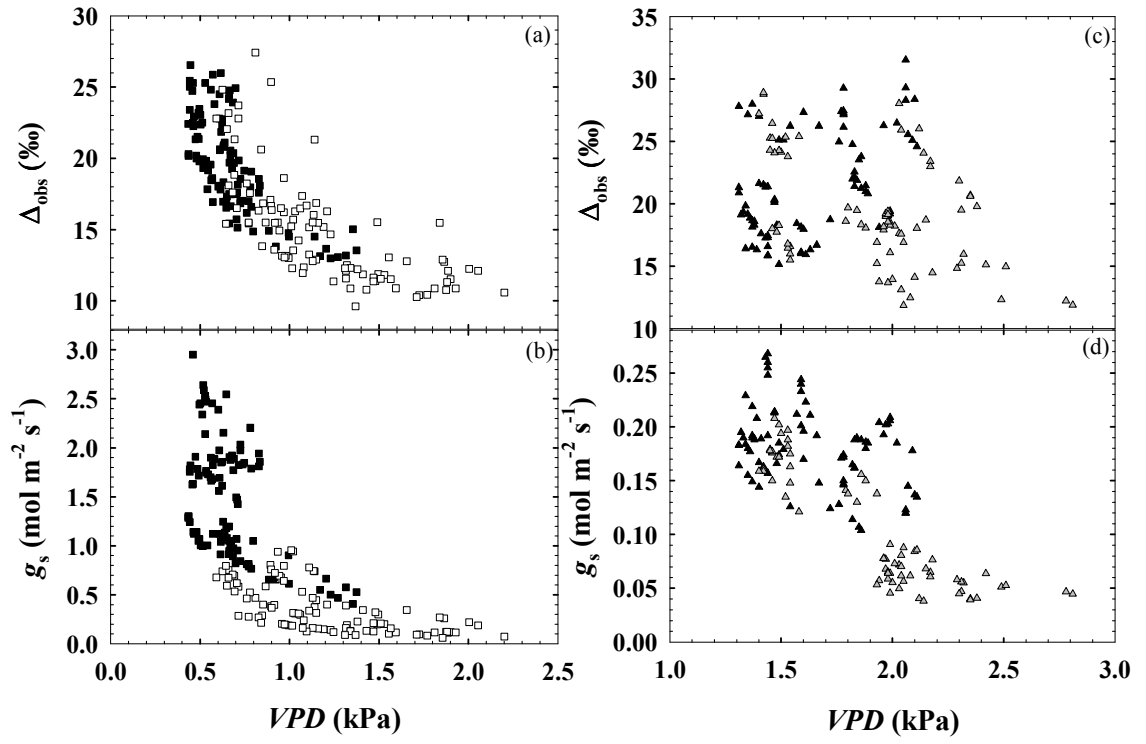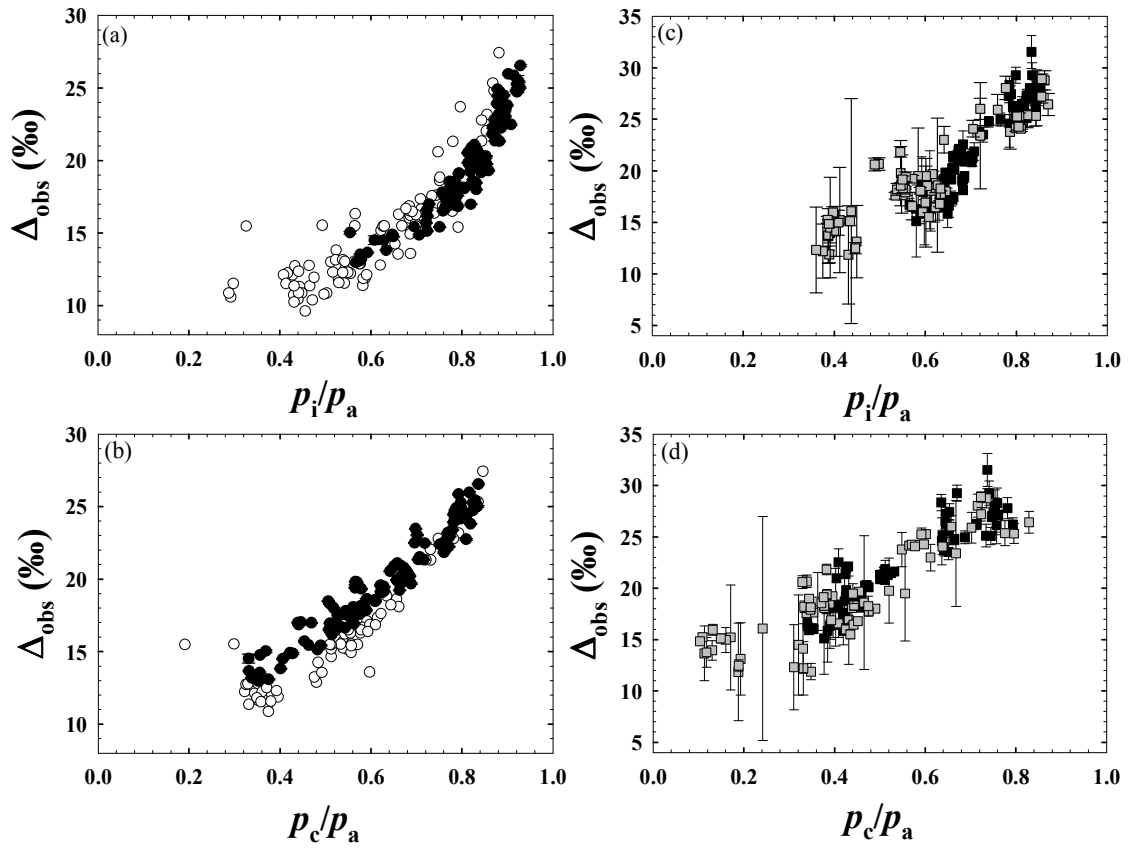**Figure 1.**

Figure 2.

Figure 3.

Chapter 5

Conclusions

The aims of this study were to utilize a novel gas exchange system to explore leaf

isotopic exchange at high frequency under field conditions, assess the importance internal

CO_2 conductance (g_i) in predicting carbon isotope discrimination (Δ), and explore

linkages between leaf water potential and g_i. Previous methods for measuring

instantaneous Δ in the field were cumbersome and expensive, involving flask collection

of gases and complex distillation processes followed by expensive analysis using mass

spectrometry. These burdens limited our understanding of the dynamic nature of Δ in

response to diurnal environmental shifts. In chapter two I detailed the first steps towards

measuring Δ in the field at high frequency, allowing us to better understand the

relationship between environmental drivers such as light, vapor pressure, and water

availability impact Δ process in a natural setting. Beyond these observations, however, in

chapters three and four I put forward an assessment of the importance of g_i in predicting

Δ using existing models. I found that, in juniper, accounting for g_i was important to

improve our predictions of Δ compared with simpler models that omit g_i and other

variables. This needs to be assessed in other species, and if verified as an important

component then further steps should be taken to account for g_i in large scale models of Δ,

possibly by utilizing mean g_i based on vegetation type. The current understanding of

environmental regulation of g_i is limited by a lacking mechanistic understanding of the

aquaporin regulation underlying the passage of CO_2 across cell walls. Linkages between

Ψ_w and g_i discussed in chapter 4 may provide insight into another aspect of coordinated

regulation of water and carbon relations and hopefully will provoke further study on the topic.

Field observations of Δ provided an opportunity to validate the most widely used models of leaf discrimination under both steady state and non-steady state conditions. As discussed in chapters 2 and 3, the widely used simple model of Δ performs well given its few components, however, with the increased use of isotopes to enhance understanding of ecosystem processes the discrepancies between measured and modeled Δ have substantial implications for prediction and interpretation and need to be recognized and improved upon. The variability in several of the components of the comprehensive model of Δ allow for just such improvements as we gain better understanding of large drivers like g_i, b, and decarboxylation components.

This research presented in chapter 4 provides yet another linkage in the intricate balance between carbon and water relations in leaves. We now have evidence that leaf water potential may be related to g_i, though the underlying mechanism is poorly understood. This phenomena needs to be explored in other isohydric species to determine if this is restricted to a limited group of plants, and if this contributes to the variability in g_i among anisohydric plants. In particular, does the water potential in cell walls or other cell subunits have regulatory influence over aquaporin activity? Future studies will be necessary to address this question.